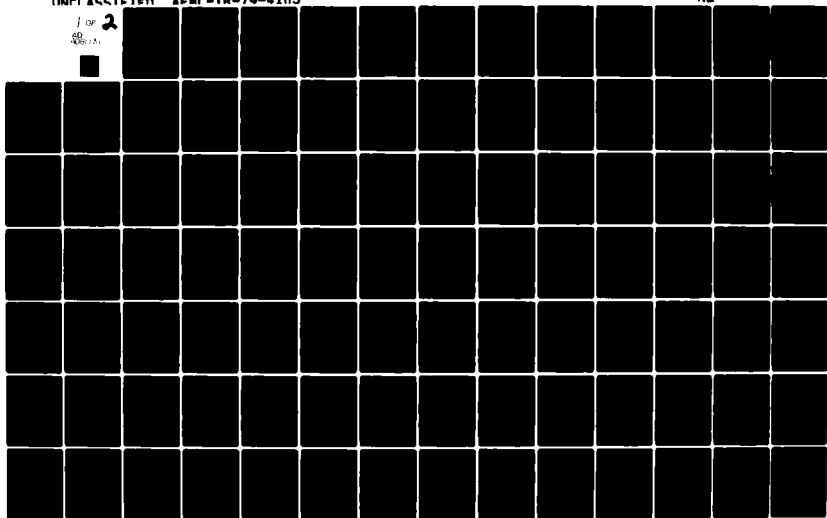


AD-A081 131

AIR FORCE MATERIALS LAB WRIGHT-PATTERSON AFB OH F/G 20/11
APPLICATIONS OF GENERALIZED DERIVATIVES TO VISCOELASTICITY.(U)
NOV 79 R L BAGLEY
AFML-TR-79-4103 NL

(UNCLASSIFIED)

1 of 2
AD-A081 131



AFML-TR-79-4103

ADA081131

APPLICATIONS OF GENERALIZED DERIVATIVES TO VISCOELASTICITY

Ronald L. Bagley, Capt., USAF

Metals Behavior Branch
Metals and Ceramics Division

November 1979

TECHNICAL REPORT AFML-TR-79-4103

DDC FILE COPY

Approved for public release; distribution unlimited

DDC
SERIALIZED
FEB 6 1980
A

AIR FORCE MATERIALS LABORATORY
AIR FORCE WRIGHT AERONAUTICAL LABORATORIES
AIR FORCE SYSTEMS COMMAND
WRIGHT-PATTERSON AIR FORCE BASE, OHIO 45433

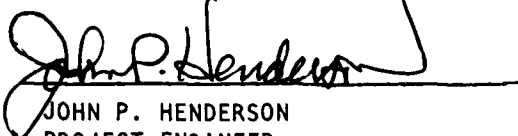
80 2 25 028

NOTICE

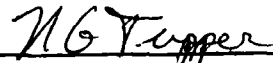
When Government drawings, specifications, or other data are used for any purpose other than in connection with a definitely related Government procurement operation, the United States Government thereby incurs no responsibility nor any obligation whatsoever; and the fact that the government may have formulated, furnished, or in any way supplied the said drawings, specifications, or other data, is not to be regarded by implication or otherwise as in any manner licensing the holder or any other person or corporation, or conveying any rights or permission to manufacture, use, or sell any patented invention that may in any way be related thereto.

This report has been reviewed by the Information Office (OI) and is releasable to the National Technical Information Service (NTIS). At NTIS, it will be available to the general public, including foreign nations.

This technical report has been reviewed and is approved for publication.



JOHN P. HENDERSON
PROJECT ENGINEER
METALS BEHAVIOR BRANCH
METALS AND CERAMICS DIVISION



NATHAN G. TUPPER, Chief
METALS BEHAVIOR BRANCH
METALS AND CERAMICS DIVISION

"If your address has changed, if you wish to be removed from our mailing list, or if the addressee is no longer employed by your organization please notify AFML/LLN, W-PAFB, OH 45433 to help us maintain a current mailing list".

Copies of this report should not be returned unless return is required by security considerations, contractual obligations, or notice on a specific document.

UNCLASSIFIED

SECURITY CLASSIFICATION OF THIS PAGE (When Data Entered)

REPORT DOCUMENTATION PAGE		READ INSTRUCTIONS BEFORE COMPLETING FORM
1. REPORT NUMBER AFML-TR-79-4103	2. GOVT ACCESSION NO.	3. RECIPIENT'S CATALOG NUMBER
4. TITLE (and Subtitle) APPLICATIONS OF GENERALIZED DERIVATIVES TO VISCOELASTICITY		5. TYPE OF REPORT & PERIOD COVERED Technical Report
7. AUTHOR(s) Ronald L. Bagley, Capt, USAF		6. PERFORMING ORG. REPORT NUMBER
9. PERFORMING ORGANIZATION NAME AND ADDRESS		8. CONTRACT OR GRANT NUMBER(s) 1.11.1
11. CONTROLLING OFFICE NAME AND ADDRESS		10. PROGRAM ELEMENT, PROJECT, TASK AREA & WORK UNIT NUMBERS 2418 03 02 01-1
14. MONITORING AGENCY NAME & ADDRESS (if different from Controlling Office)		12. REPORT DATE November 1979
		13. NUMBER OF PAGES 119
		15. SECURITY CLASS. (of this report)
		15a. DECLASSIFICATION/DOWNGRADING SCHEDULE
16. DISTRIBUTION STATEMENT (of this Report) Approved for public release; distribution unlimited.		
17. DISTRIBUTION STATEMENT (of the abstract entered in Block 20, if different from Report)		
18. SUPPLEMENTARY NOTES		
19. KEY WORDS (Continue on reverse side if necessary and identify by block number)		
20. ABSTRACT (Continue on reverse side if necessary and identify by block number) Generalized derivatives of fractional order are used to construct stress-strain constitutive relations for viscoelastic materials, based on the observed sinusoidal behavior of the materials. The non-periodic behavior of one material is observed in the laboratory and compares favorably with the non-periodic behavior of the material predicted by its generalized derivative constitutive relation. Having established that the generalized derivative constitutive relation is an appropriate mathematical model for the general motion of at least		

DD FORM 1 JAN 73 1473

EDITION OF 1 NOV 65 IS OBSOLETE

UNCLASSIFIED

SECURITY CLASSIFICATION OF THIS PAGE (When Data Entered)

01232

JLE

UNCLASSIFIED

SECURITY CLASSIFICATION OF THIS PAGE (When Data Entered)

20. (Cont'd)

one viscoelastic material, the tools for the analysis of structures of engineering interest are put forward. In particular, attention is focused on a finite element formulation of and solutions to the equations of motion for structures containing elastic and viscoelastic components.

UNCLASSIFIED

SECURITY CLASSIFICATION OF THIS PAGE (When Data Entered)

FOREWORD

This research, under project 24180302, was jointly sponsored by the U. S. Air Force Institute of Technology (AFIT) and the U. S. Air Force Materials Laboratory (AFML), both located at Wright-Patterson Air Force Base, Ohio.

AFML provided the properties of the viscoelastic materials considered in this investigation, as well as experimental testing support and funding for computer time. Drs. Jack Henderson and David I. G. Jones, both the AFML/LLN, were in large part responsible for this timely and generous support. I am also indebted to Mike Drake and Charles Cannon, both of the University of Dayton Research Institute under contract to AFML, and Dave Signor, AFML, for their help with the experimental testing.

I am indebted to the members of the AFIT faculty on my committee. Thanks to Professor Robert A. Calico and Captain John R. Shea, III for their encouragement in and constructive criticism of this work. Particular thanks are due to Professor Peter J. Torvik, the committee chairman, and Professor David A. Lee, head of the AFIT Department of Mathematics, for their guidance and good counsel.

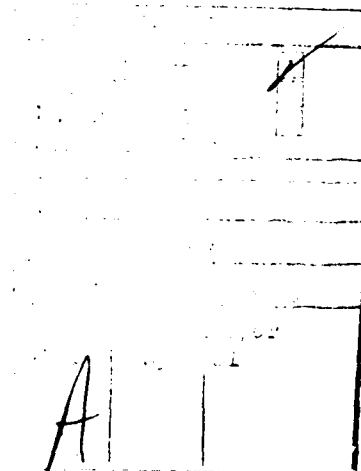


TABLE OF CONTENTS

SECTION	PAGE
I INTRODUCTION	1
II A BRIEF OVERVIEW OF GENERALIZED DERIVATIVES	6
III THE BASIC GENERALIZED CONSTITUTIVE RELATION	9
IV GENERALIZED DERIVATIVE CONSTITUTIVE RELATIONS FOR VISCOELASTIC MATERIALS	12
V THE RT MODEL FOR THE ELASTOMER 3M-467	26
VI A FINITE ELEMENT FORMULATION OF THE EQUATIONS OF MOTION	49
VII THE SOLUTION OF THE DISCRETE EQUATIONS OF MOTION	52
VIII CALCULATING THE LAPLACE TRANSFORM OF THE STRUCTURAL RESPONSE	63
IX THE EXISTENCE OF THE STRUCTURAL RESPONSE TO IMPULSIVE LOADING	73
X CALCULATING THE RESPONSE TO IMPULSIVE LOADING	77
XI SUMMARY AND CONCLUSIONS	87
APPENDIX A THE RT AND RTG MODELS AND THE SECOND LAW OF THERMODYNAMICS	89
APPENDIX B A GENERALIZED DERIVATIVE RELATION FOR A NEWTONIAN FLUID	95
APPENDIX C RT AND RTG MODELS FOR VISCOELASTIC MATERIALS	100
REFERENCES	106

LIST OF ILLUSTRATIONS

FIGURE	PAGE
1 Typical Mechanical Properties of a Viscoelastic Material	14
2 A Comparison of the Material Properties of 3M-467 and the Properties Predicted by its RT Model	28
3 A Schematic of the Oscillator and its Support Structure	30
4 Expanded Schematic of the Oscillator and Support Structure Not Displaying the Steel Foundation	31
5 The Magnitude of the Transfer Function for Case #1	34
6 The Phase of the Transfer Function for Case #1	35
7 The Magnitude of the Transfer Function for Case #2	36
8 The Phase of the Transfer Function for Case #2	37
9 The Magnitude of the Transfer Function for Case #3	38
10 The Phase of the Transfer Function for Case #3	39
11 The Magnitude of the Transfer Function for Case #4	40
12 The Phase of the Transfer Function for Case #4	41
13 The Magnitude of the Transfer Function for Case #5	42
14 The Phase of the Transfer Function for Case #5	43
15 A Comparison of the Material Properties of 3M-467 and the Properties Predicted by the Voigt Model	45
16 The Variations of Young's Modulus of 3M-467 with Changes in Relative Humidity	46
17 The Variations of Loss Factor of 3M-467 with Changes in Relative Humidity	47

LIST OF ILLUSTRATIONS (Cont'd)

FIGURE		PAGE
18	The Contour of Integration Used to Evaluate the Inverse Transform	78
B-1	Schematic of the Half-Space of Newtonian Fluid Bounded by a "Wetted" Surface	96
C-1	The Mechanical Properties of 3M-467 Compared to the RTG Model of 3M-467	103
C-2	The Mechanical Properties of Sylgard 188 Compared to the RT Model for Sylgard 188	104
C-3	The Mechanical Properties of BTR Compared to the RT Model for BTR	105

LIST OF TABLES

TABLE	PAGE
1 Parameters of the Five Oscillators	33
2 Homogeneous Solutions Obtained Using the Proposed Iterative Schemes for an Example Problem	71

LIST OF SYMBOLS

$[]$	a square matrix
$[]^T$	the transpose of a matrix
$[]^{-1}$	the inverse matrix
$\{ \}$	a column matrix
a_k	a parameter of the generalized derivative models
b_p	a parameter of the generalized derivative models
$D^\alpha []$	generalized derivative operator of order α
$E(t)$	the relaxation modulus
$E^*(\omega)$	the Fourier transform of the relaxation modulus
$E^*(s)$	the Laplace transform of the relaxation modulus
$F[]$	the Fourier transform operator
$\{f(t)\}$	a column vector of applied forces
$\{F(s)\}$	the Laplace transform of the column vector of applied forces
$G(t)$	the shear relaxation modulus
i	the imaginary coefficient
$[K(s)]$	a visco-stiffness matrix
$[K]$	the pseudo stiffness of the expanded equations of motion
$L[]$	the Laplace transform operator
$[M]$	a mass matrix
$[M]$	the pseudo mass matrix of the expanded equations of motion
s	the Laplace parameter
$\{x(t)\}$	a column vector of structural displacements
$\{X(s)\}$	the Laplace transform of the column vector of structural displacements
$\hat{\alpha}_j, \hat{\alpha}_l$	parameters of the generalized derivative models
$\hat{\beta}_k, \hat{\beta}_p$	parameters of the generalized derivative models

LIST OF SYMBOLS (Cont'd)

$\Gamma(\alpha)$	the gamma function of α
$\varepsilon_{mn}(t)$	a strain history
$\varepsilon_{mn}^*(s)$	the Laplace transform of the strain history
$\eta(\omega)$	the loss factor
$\tilde{\lambda}_n$	the eigenvalue associated with the expanded equations of motion
$\lambda^*(\omega)$	Fourier transform of the dilatation modulus
λ_0, λ_j	parameters of the generalized derivative models
$\mu^*(\omega)$	Fourier transform of the shear modulus
$\mu'(\omega), \mu''(\omega)$	the real and imaginary parts of $\mu^*(\omega)$, respectively
$\mu^*(s)$	the Laplace transform of the shear modulus
μ_0, μ_ℓ	parameters of the generalized derivative models
$\sigma_{mn}(t)$	a stress history
$\sigma_{mn}^*(s)$	the Laplace transform of the stress history
$\{\phi_n\}$	a mode shape of the structure
$\{\tilde{\phi}_n\}$	an eigenvector associated with the expanded equations of motion
ω	the Fourier parameter and the circular frequency of motion in radians per second

NOTE: Whenever a time history and its associated transform are expressed using the same symbol, e.g., $\sigma_{mn}(t)$ and $\sigma_{mn}^*(s)$, the asterisk denotes the transformed variable.

SECTION I

INTRODUCTION

The following investigation deals with constitutive relations employing generalized derivatives that relate stress and strain in viscoelastic materials, and the solution techniques for the resulting equations of motion for structures incorporating viscoelastic components to damp vibratory motion. The use of generalized derivatives of fractional order in stress-strain constitutive relations, first suggested by Caputo (Reference 1), may be viewed as an extension of the standard model for a linear, viscoelastic material.

The standard viscoelastic model for a uniaxial constitutive relation is (Reference 2)

$$\sigma(t) + \sum_{k=1}^K b_k \frac{d^k \sigma}{dt^k} = E_0 \epsilon(t) + \sum_{j=1}^J E_j \frac{d^j \epsilon}{dt^j} \quad (1)$$

The viscoelastic constitutive relation employing generalized derivatives of fractional order will be taken to be

$$\sigma(t) + \sum_{k=1}^K b_k D^{\alpha_k} [\sigma(t)] = E_0 \epsilon(t) + \sum_{j=1}^J E_j D^{\alpha_j} [\epsilon(t)] \quad (2)$$

where the generalized derivative operator of real order α is defined by

$$D^{\alpha} [x(t)] \equiv \frac{1}{\Gamma(1-\alpha)} \frac{d}{dt} \int_0^t \frac{x(\tau)}{(t-\tau)^{\alpha}} d\tau \quad 0 < \alpha < 1 \quad (3)$$

The generalized derivative constitutive relation (Equation 2) may be viewed as an extension of the standard model (Equation 1) in the sense that the derivatives are no longer limited to being of integer order.

The use of this generalized derivative constitutive relation in modeling the response of viscoelastic materials will be seen to have several advantages over present methods. The major drawback of the standard viscoelastic model (Equation 1) is that a large number of terms are often required to describe a material adequately. The use of derivatives of other than integer order in the constitutive relation will be seen to produce satisfactory models with very few parameters.*

Because of the large number of terms required, the standard model (Equation 1) often becomes too cumbersome to manipulate. Consequently, an alternative known as the "complex modulus method" has been developed. In the complex modulus method, measured values of $E^*(\omega)$ (Equation 4) are used as a discrete approximation of the function $E^*(\omega)$. In the transform domain, the general viscoelastic constitutive relation is

$$\sigma^*(\omega) = E^*(\omega) \epsilon^*(\omega) \quad (4)$$

$E^*(\omega)$ is measured for different frequencies of motion (Reference 4), ω_i , which produces a set of discrete values of the modulus, $E^*(\omega_i)$, over the frequency range of interest. These discrete values of $E^*(\omega)$ are substituted into the transformed equations of motion of a viscoelastic material to produce values of the transform of the response at discrete frequencies. The inverse transform of the response is evaluated numerically to produce the time history. The major drawback of this method is the arduous task of calculating the inverse transform for every point in time at which the value of the response is required. The use of the generalized derivative constitutive relation will do away with the need for numerical approximations in the frequency domain.

An elementary form of the "complex modulus" method, obtained by representing the transform of the modulus by

$$E^*(\omega) = E_0 (1 + i \text{ns} \text{gn}(\omega)) \quad (5)$$

*In Section V, a generalized derivative constitutive relation for the elastomer 3M-467 is presented. The relation characterizes the material's properties over four decades of frequency with three parameters.

$$\text{sgn}(\omega) = \begin{cases} 1, & \omega > 0 \\ 0, & \omega = 0 \\ -1, & \omega < 0 \end{cases} \quad (6)$$

and often known as "structural damping" (Reference 5), is valid only for sinusoidal stress and strain in the material. Crandall has shown that the response of a harmonic oscillator with "structural damping" for impulsive loading is non-causal (Reference 6); that is, the time response of the oscillator occurs before the loading.

Milne (Reference 7) has proposed several modifications of the imaginary part of the modulus given in Equation 7 to produce a causal response. Unfortunately, neither the modified modulus nor the one given in Equation 7 is particularly suitable for transient (broad-band) response of viscoelastic materials, because they do not account for the frequency-dependent stiffness typically encountered. Caputo (Reference 8) observed that a single term, generalized derivative, constitutive relation of the form

$$\sigma(t) = E_1 D^{\alpha_1} [\epsilon(t)] \quad 0 < \alpha_1 < 1 \quad (7)$$

produces frequency-dependent stiffness and damping and a loss factor*, η , that is frequency independent.

$$\eta = \tan \frac{\alpha_1 \pi}{2} \quad (8)$$

Caputo's work with generalized derivative constitutive relations focuses primarily on the propagation of waves in geological formations. One of Caputo's earliest papers (Reference 9) was on generalized independent loss factors or equivalently frequency-independent resonant qualities, Q . This work was followed by a book (Reference 10) in which Caputo dealt with the propagation of impulsive plane waves and the

*The loss factor in a linear material is the ratio of imaginary to the real part of the modulus.

free vibration of spherical strata using generalized derivatives in the constitutive relations of the media. In the last chapter of the book and in later papers with Minardi, Caputo compares the generalized derivative relations with experimental observations of the properties of some media: "some metals, glasses and the earth." (References 11, 12) In 1974 Caputo proposed a generalized derivatives viscoelastic constitutive relation of the form (Reference 13)

$$\sigma(t) = \eta D^{\alpha+n}[\epsilon(t)] , \quad 0 < \alpha < 1 ; n = 0, 1, 2, \dots \quad (9)$$

where the generalized derivative operator was defined by

$$D^{\alpha+n}[x(t)] \equiv \frac{1}{(1-\alpha)} \int_0^t \frac{d^n x(t)}{dt^n} \frac{1}{(t-\tau)^\alpha} dt \quad (10)$$

This definition differs slightly from the generalized derivative used in this investigation (Equation 3). Caputo used the relation (Equation 9) to determine the response of a uniformly driven infinite viscoelastic layer and investigated the hysteresis behavior of the constitutive relation (References 14, 15). Recently, Caputo suggested, but gave no application for, a constitutive relation of the form (Reference 16)

$$D^\beta[\sigma(t)] = \eta D^\alpha[\epsilon(t)] \quad (11)$$

which is the harbinger of the general constitutive relation (Equation 2) which is to be used in this study.

All of Caputo's work rests on a continuum formulation of the equations of motion. Unfortunately, a continuum formulation of the equations of motion for many structures of engineering interest is not practical. As a result, a discrete formulation of the equations of motion is adopted, based on assumed displacement, finite-element methods. A solution technique developed for the motion of structures incorporating viscoelastic materials modeled with generalized derivatives is developed as an extension of the solution technique developed by Foss for non-proportional viscous damping (Reference 17).

In the sections to follow, constitutive relations using generalized derivatives are developed, and their applications and limitations are considered. Some experimental results are presented and found to show that a constitutive relation, with parameters determined from the response to sinusoidal loading, predicts very well the response of one typical elastomeric material to an impact loading. Finally, the formulation of multi-degree of freedom systems, necessary for large-scale structural analysis, is considered. Special solution methods, necessary for such applications, are developed.

SECTION II

A BRIEF OVERVIEW OF GENERALIZED DERIVATIVES

Before construction of generalized derivative constitutive relations, it is appropriate to introduce the properties of generalized derivatives relevant to the following investigations. Of particular interest are the form of the Laplace and Fourier transforms of generalized derivatives, and the results of repeated differentiation of fractional order.

First and foremost, the generalized derivative is a linear operator.

$$D^{\alpha}[x_1(t) + x_2(t)] = D^{\alpha}[x_1(t)] + D^{\alpha}[x_2(t)] \quad (12)$$

This property follows directly from the definition (Equation 3)

$$D^{\alpha}[x(t)] \equiv \frac{1}{\Gamma(1-\alpha)} \frac{d}{dt} \int_0^t \frac{x(\tau)}{(t-\tau)^{\alpha}} dt \quad (3)$$

To put the definition into a form in which the calculation of its Laplace transform is straightforward, one first performs a change of variable

$$\tau = t - \eta \quad (13)$$

which results in

$$D^{\alpha}[x(t)] = \frac{1}{\Gamma(1-\alpha)} \frac{d}{dt} \int_0^t \frac{x(t-\eta)}{\eta^{\alpha}} d\eta \quad (14)$$

Using Leibnitz's rule to differentiate the integral produces

$$D^{\alpha}[x(t)] = \frac{1}{\Gamma(1-\alpha)} \int_0^t \frac{1}{\eta^{\alpha}} \frac{\partial}{\partial t} x(t-\eta) d\eta + \frac{x(0)}{\Gamma(1-\alpha)t^{\alpha}} \quad (15)$$

After taking the Laplace transform of Equation 14, the transform of the generalized derivative of order α of the function $x(t)$ is seen to be

$$L[D^\alpha[x(t)]] = \frac{1}{s^{1-\alpha}} \cdot (sL[x(t)] - x(0)) + \frac{x(0)}{s^{1-\alpha}} \quad (16)$$

which simplifies to

$$L[D^\alpha[x(t)]] = s^\alpha L[x(t)] \quad (17)$$

where

$$L[x(t)] = \int_0^\infty x(t)e^{-st} dt \quad (18)$$

Notice that the Laplace transform of a generalized derivative of order α of a function is equal to s^α times the transform of the function.

Under certain conditions a similar property of generalized derivatives is true for Fourier transforms.

$$F[D^\alpha[x(t)]] = (i\omega)^\alpha F[x(t)] \quad (19)$$

where

$$F[x(t)] \equiv \int_{-\infty}^\infty x(t)e^{-i\omega t} dt \quad (20)$$

The conditions are, first, that

$$x(t) = 0 \quad \text{for } t < 0 \quad (21)$$

in which case the Fourier transform becomes

$$F[x(t)] = \int_0^\infty x(t)e^{-i\omega t} dt \quad (22)$$

and, second, that the integral in Equation 22 exists. Note the parallel form of Equations 17 and 19. Both relations were used by Caputo (Reference 18).

A useful property of generalized derivatives is that the generalized derivative of order α_1 , of the generalized derivatives of order α_2 of a function is the generalized derivative of order $\alpha_1 + \alpha_2$ of the function. Again using operator notation, the property is

$$D^{\alpha_1}[D^{\alpha_2}[x(t)]] = D^{\alpha_1 + \alpha_2}[x(t)] \quad (23)$$

Notice that the definition of generalized differentiation given in Equation 3 is restricted to fractional order α less than one. If α is one or greater in Equation 3, the integral contains a non-integrable singularity*. The definition of a generalized derivative of order β , where $\beta > 1$ and $\beta = m + \alpha$ where m is the largest integer not exceeding β , is

$$D^{m+\alpha}[x(t)] = \frac{1}{\Gamma(1-\alpha)} \frac{d^{m+1}}{dt^{m+1}} \int_0^t \frac{x(\tau)}{(t-\tau)^\alpha} dt \quad (24)$$

*On the other hand, if α is zero in Equation 3, the relation is clearly valid and follows from the fundamental theorem of calculus.

SECTION III

THE BASIC GENERALIZED CONSTITUTIVE RELATION

In this section, the basic generalized derivative, viscoelastic constitutive relation is presented and some aspects of its behavior are established. The basic generalized derivative constitutive relation is

$$\sigma(t) = \lambda D^\alpha[\epsilon(t)] \quad 0 < \alpha < 1 \quad (25)$$

or

$$\sigma(t) = \frac{\lambda}{\Gamma(1-\alpha)} \frac{d}{dt} \int_0^t \frac{\epsilon(\eta)}{(t-\eta)^\alpha} d\eta \quad (26)$$

Since the generalized derivative is a linear operator, this relation is suitable only for the linear approximation of a material's properties. This linear constitutive relation satisfies many of the presently accepted constraints on viscoelastic constitutive relations.

In particular, it represents a material with fading memory. To demonstrate this claim, it is necessary to put the constitutive relation in a different form using a change in variable.

$$\eta = t - \tau \quad (27)$$

and again using Leibnitz's rule to differentiate the resulting integral produces

$$\sigma(t) = \frac{\lambda}{\Gamma(1-\alpha)} \int_0^t \frac{1}{\tau^\alpha} \frac{\partial}{\partial t} \epsilon(t-\tau) d\tau + \frac{\lambda \epsilon(0)}{\Gamma(1-\alpha)t^\alpha} \quad (28)$$

or

$$\sigma(t) = \int_0^t G(\tau) \dot{\epsilon}(t-\tau) d\tau + G(t)\epsilon(0) \quad (29)$$

where

$$G(t) = \frac{\lambda}{\Gamma(1-\alpha)t^\alpha} \quad (30)$$

The constitutive relation, (Equation 29), represents a viscoelastic material with a fading memory. A material is said to have a fading memory if its relaxation modulus, $G(t)$, goes to zero monotonically as t increases (Reference 20). Notice that $G(t)$ in Equation 30 does in fact go to zero monotonically.

Since the material has a memory, the value of the stress at time t is dependent on the entire strain history until time t . To ensure that the constitutive relation produces a stress that is dependent on the entire strain history until t , time zero must be chosen before or at the onset of the initial strain.

Consequently,

$$\epsilon(t) = 0 \quad \text{for } t < 0 \quad (31)$$

and the only way that

$$\epsilon(0) \neq 0 \quad (32)$$

is if the strain history is discontinuous at $t = 0$. According to Gurtin and Sternberg (Reference 21), the constitutive relation as shown in Equation 29 is in the correct form to handle discontinuous strain histories. Notice that a step discontinuity in the strain history at $t = 0$ produces a stress history* that is singular at $t = 0$.

When the strain history is a continuous function of time, and zero for negative times, the constitutive relation given in Equation 29 reduces to

$$\sigma(t) = \int_0^t G(\tau) \dot{\epsilon}(t-\tau) d\tau, \quad G(t) = \frac{\lambda}{\Gamma(1-\alpha)t^\alpha} \quad (33)$$

This relation satisfies three out of four of Pipkin's restrictions on viscoelastic constitutive relations (Reference 22). The first restriction, that the stress be an odd functional of strain rate, is satisfied.

*The Voigt viscoelastic model displays this same property.

AFML-TR-79-4103

The second restriction, that $G(t)$ go to zero as time increases, is also satisfied, which is in keeping with the fading memory property. The third restriction, also satisfied, is that the kernel, the relaxation modulus $G(t)$, be a function and not a distribution. Pipkin's fourth restriction, not satisfied by the generalized derivative constitutive relation, is that $G(t)$ be of negative exponential order.

SECTION IV

GENERALIZED DERIVATIVE CONSTITUTIVE
RELATIONS FOR VISCOELASTIC MATERIALS

The task at hand is to use the basic generalized derivative constitutive relation just presented as the building block for constitutive relations that model the frequency-dependent moduli of viscoelastic materials. The moduli of viscoelastic materials are complex numbers where the real and imaginary parts are functions of the frequency of motion.

$$\lambda^*(\omega) = \lambda'(\omega) + i\lambda''(\omega) \quad (34)$$

$$\mu^*(\omega) = \mu'(\omega) + i\mu''(\omega) \quad (35)$$

The moduli are defined as the transforms that relate the transforms of stress and strain

$$\sigma_{mn}^*(\omega) = \delta_{mn}\lambda^*(\omega)e^*(\omega) + 2\mu^*(\omega)\epsilon_{mn}^*(\omega) \quad (36)$$

where δ_{mn} is the Kronecker delta and $e^*(\omega)$ is the transform of the dilatation strain

$$e^*(\omega) = \epsilon_{11}^*(\omega) + \epsilon_{22}^*(\omega) + \epsilon_{33}^*(\omega) \quad (37)$$

A useful property of the moduli is that their values at frequency ω_0 relate sinusoidal stress and strain of frequency ω_0 in the material.

$$\sigma_{mn}(t) = \delta_{mn}\lambda^*(\omega_0)e_0 \exp[i\omega_0 t] + 2\mu^*(\omega_0)\epsilon_{mn_0} \exp[i\omega_0 t] \quad (38)$$

Consequently, one can measure the values of $\mu^*(\omega)$ and $\lambda^*(\omega)$ at discrete frequencies of sinusoidal motion. As a result, the frequency dependence of the moduli can be determined experimentally.

Typically, a viscoelastic material at constant, uniform temperature has moduli that vary with the frequency of motion as indicated in

Figure 1 (Reference 23). At low frequencies (the rubbery region) the real part of the modulus is relatively constant, while the imaginary part of the modulus increases with increasing frequency. At intermediate frequencies (the transition region) both the real and imaginary parts of the modulus increase with increasing frequency and the rate of increase of the real part slowly overtakes the rate of increase of the imaginary part. At high frequencies (the glassy region) the imaginary part of the modulus decreases with increasing frequency, and the real part of the modulus is relatively constant.

The generalized derivative constitutive relations presented here are of two types. The first type are those relations intended to model the viscoelastic behavior of the material in the rubbery and transition regions. For brevity, this type of model is referred to as the RT model. The second type are those relations intended to model the behavior of the material in the rubbery, transition and glassy regions. This type of relation is referred to as the RTG model. Since the RTG model may be viewed as a generalization of the RT model, the RT model is considered first.

The RT model for an isotropic, homogeneous, linear viscoelastic material is

$$\begin{aligned} \sigma_{mn}(t) = & \delta_{mn}(\lambda_0 + \sum_{j=1}^J \lambda_j D^{\alpha_j}) \epsilon(t) \\ & + 2(\mu_0 + \sum_{\ell=1}^L \mu_\ell D^{\hat{\alpha}_\ell}) \epsilon_{mn}(t) \end{aligned} \quad (39)$$

where

$$0 < \alpha_j < 1 \quad (40)$$

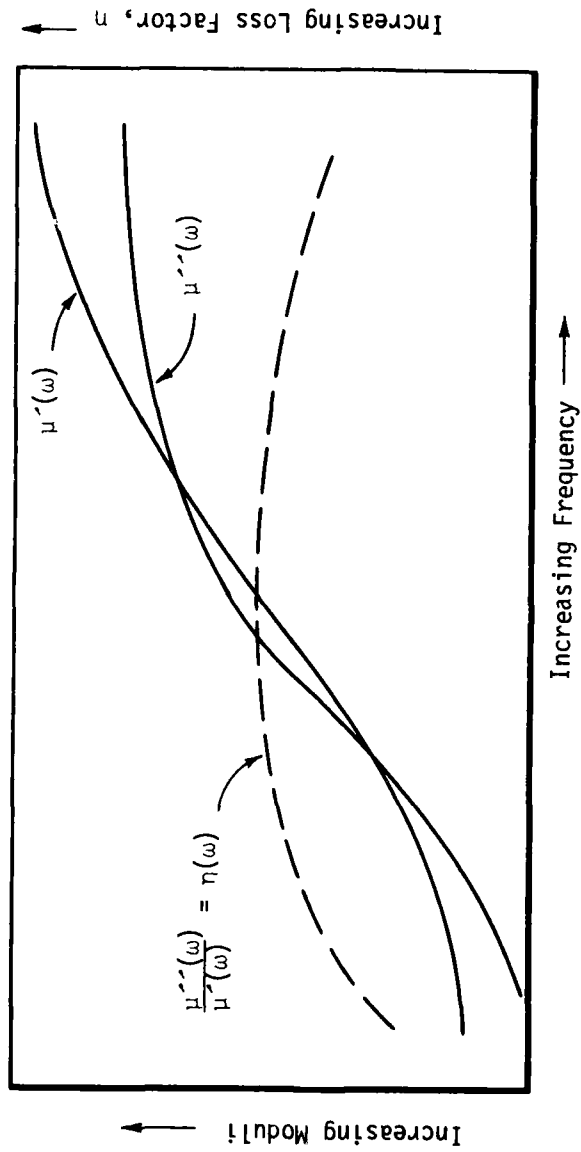


Figure 1. Typical Mechanical Properties of a Viscoelastic Material

$$0 < \hat{\alpha}_\ell < 1 \quad (41)$$

$$e(t) = \epsilon_{11}(t) + \epsilon_{22}(t) + \epsilon_{33}(t) \quad (42)$$

Note that the RT model portrays the stress as a combination of elastic stresses, proportional to the positive, real parameters λ_0 and μ_0 , and viscoelastic stresses, proportional to the positive, real parameters λ_j and μ_ℓ .

To establish the frequency dependence of the moduli in the RT model, one takes the Fourier transform of the constitutive relation.

$$\begin{aligned} \sigma_{mn}^*(\omega) &= \delta_{mn}(\lambda_0 + \sum_{j=1}^J \lambda_j (i\omega)^{\alpha_j}) e^*(\omega) \\ &+ 2(\mu_0 + \sum_{\ell=1}^L \mu_\ell (i\omega)^{\hat{\alpha}_\ell}) \epsilon_{mn}^*(\omega) \end{aligned} \quad (43)$$

Expressing the moduli in terms of their real and imaginary parts produces

$$\begin{aligned} \lambda^*(\omega) &= (\lambda_0 + \sum_{j=1}^J \lambda_j \omega^{\alpha_j} \cos \frac{\pi \alpha_j}{2}) \\ &+ i \sum_{j=1}^J \lambda_j \omega^{\alpha_j} \sin \frac{\pi \alpha_j}{2} \end{aligned} \quad (44)$$

$$\begin{aligned} \mu^*(\omega) &= (\mu_0 + \sum_{\ell=1}^L \mu_\ell \omega^{\hat{\alpha}_\ell} \cos \frac{\pi \hat{\alpha}_\ell}{2}) \\ &+ i \sum_{\ell=1}^L \mu_\ell \omega^{\hat{\alpha}_\ell} \sin \frac{\pi \hat{\alpha}_\ell}{2} \end{aligned} \quad (45)$$

Observe that for low frequencies of motion, defined by

$$\left| \frac{1}{\lambda_0} \sum_{j=1}^J \lambda_j \omega^{\alpha_j} \right| \ll 1 \quad (46)$$

and

$$\left| \frac{1}{\mu_0} \sum_{\ell=1}^L \mu_{\ell} \omega^{\hat{\alpha}_{\ell}} \right| \ll 1, \quad (47)$$

the moduli in the RT model, (Equations 44, 45), have essentially a constant real part and an imaginary part that increases with increasing frequency, similar to the properties of a viscoelastic material observed in the rubbery region (Figure 1).

At intermediate frequencies of motion, defined by

$$\left| \frac{1}{\lambda_0} \sum_{j=1}^J \lambda_j \omega^{\alpha_j} \right| \approx 1 \quad (48)$$

and

$$\left| \frac{1}{\mu_0} \sum_{\ell=1}^L \mu_{\ell} \omega^{\hat{\alpha}_{\ell}} \right| \approx 1, \quad (49)$$

the real and imaginary parts of the moduli in the RT model are increasing with frequency, similar to the properties of a viscoelastic material observed in the transition region.

It is evident that the RT model does not properly account for the properties of a viscoelastic material at high frequencies, defined by

$$\left| \frac{1}{\lambda_0} \sum_{j=1}^J \lambda_j \omega^{\alpha_j} \right| \gg 1 \quad (50)$$

and

$$\left| \frac{1}{\lambda_0} \sum_{\ell=1}^L \mu_{\ell} \omega^{\hat{\alpha}_{\ell}} \right| \gg 1 \quad (51)$$

The real and imaginary parts of the modulus are predicted by the RT model to increase indefinitely with frequency. In the glassy region, however, the real part of the modulus of viscoelastic materials is typically constant (Figure 1), and the imaginary part is decreasing with increasing frequency. This discrepancy motivates the construction of a more complex model which accounts for material properties in the glassy region, the RTG model.

The RTG model for an isotropic, homogeneous, linear, viscoelastic material is defined to be

$$\begin{aligned} & \left(1 + \sum_{k=1}^K a_k D^{\beta_k}\right) \left(1 + \sum_{p=1}^P b_p D^{\hat{\beta}_p}\right) \sigma_{mn}(t) \\ &= \delta_{mn} \left(1 + \sum_{p=1}^P b_p D^{\hat{\beta}_p}\right) \left(\lambda_0 + \sum_{j=1}^J \lambda_j D^{\alpha_j}\right) \epsilon(t) \\ &+ 2 \left(1 + \sum_{k=1}^K a_k D^{\beta_k}\right) \left(\mu_0 + \sum_{\ell=1}^L \mu_{\ell} D^{\hat{\alpha}_{\ell}}\right) \epsilon_{mn}(t) \end{aligned} \quad (52)$$

Again, the frequency dependence of the moduli in the model is observed by taking the Fourier transform of the constitutive relation. After some algebraic manipulation of the transformed relation, the result is

$$\sigma_{mn}^*(\omega) = \delta_{mn} \frac{\left(\lambda_0 + \sum_{j=1}^J \lambda_j (i\omega)^{\alpha_j}\right)}{\left(1 + \sum_{k=1}^K a_k (i\omega)^{\beta_k}\right)} \epsilon^*(\omega)$$

$$+ \frac{2 \left(\mu_0 + \sum_{\ell=1}^L \mu_{\ell} (i\omega)^{\hat{\alpha}_{\ell}} \right)}{\left(1 + \sum_{p=1}^P b_p (i\omega)^{\hat{\beta}_p} \right)} \epsilon_{mn}^*(\omega) \quad (53)$$

where

$$\lambda^*(\omega) = \frac{\left(\lambda_0 + \sum_{j=1}^J \lambda_j (i\omega)^{\alpha_j} \right)}{\left(1 + \sum_{p=1}^P b_p (i\omega)^{\beta_p} \right)} \quad (54)$$

$$\mu^*(\omega) = \frac{\left(\mu_0 + \sum_{\ell=1}^L \mu_{\ell} (i\omega)^{\hat{\alpha}_{\ell}} \right)}{\left(1 + \sum_{p=1}^P b_p (i\omega)^{\hat{\beta}_p} \right)} \quad (55)$$

$$0 < \alpha_j, \hat{\alpha}_{\ell}, \beta_k, \hat{\beta}_p < 1 \quad (56)$$

and

$$\lambda_0, \lambda_j, \mu_0, \mu_{\ell}, a_k, b_p > 0 \quad (57)$$

If the parameters a_k and b_p are chosen to be small, such that

$$\left| \sum_{k=1}^K a_k (i\omega)^{\beta_k} \right| \ll \left| \lambda_0 + \sum_{j=1}^J \lambda_j (i\omega)^{\alpha_j} \right| \quad (58)$$

and

$$\left| \sum_{p=1}^P b_p (i\omega)^{\hat{\beta}_p} \right| \ll \left| \mu_0 + \sum_{\ell=1}^L \mu_{\ell} (i\omega)^{\hat{\alpha}_{\ell}} \right| \quad (59)$$

for frequencies in the rubbery and transition regions of the material, the RTG model behaves like the RT model in the rubbery and transition regions of the material.

It is, however, the presence of the terms a_k and b_p which enables the RTG model to account for the properties of viscoelastic materials at high frequencies; i.e., in the glassy region. Note that, if the largest values of α_j and β_k are the same, and if the largest values $\hat{\alpha}_\ell$ and $\hat{\beta}_p$ are the same, then at high frequencies $\lambda^*(\omega)$ and $\mu^*(\omega)$ have real parts that become constant and imaginary parts that decrease with increasing frequencies, as is characteristic of a viscoelastic material in the glassy region.

An important property of the RT and RTG models is that they satisfy the "elastic-viscoelastic correspondence principle." (Reference 4) The correspondence principle states that the Laplace transform of the stress response of a viscoelastic material can be constructed from the Laplace transform of the response of an elastic material by replacing the elastic constants, λ and μ , in the elastic response by the Laplace transforms of viscoelastic moduli, $\lambda^*(s)$ and $\mu^*(s)$. The principle holds when the transform of the elastic stress-strain constitutive relation

$$\sigma_{mn}^*(s) = \delta_{mn} \lambda e^*(s) + 2\mu \epsilon_{mn}^*(s) \quad (60)$$

can be used to construct the transform of the viscoelastic stress-strain constitutive relation by replacing the elastic constants with the transforms of the viscoelastic moduli. Thus, the viscoelastic constitutive relation must be of the form

$$\sigma_{mn}^*(s) = \delta_{mn} \lambda^*(s) e^*(s) + 2\mu^*(s) \epsilon_{mn}^*(s) \quad (61)$$

The Laplace transforms of the RT and the RTG models are of the general form given in Equation 61. The Laplace transform of the RTG model is

$$\begin{aligned} \sigma_{mn}^*(s) = & \delta_{mn} \frac{(\lambda_0 + \sum_{j=1}^J \lambda_j s^{\alpha_j})}{(1 + \sum_{k=1}^K a_k s^{\beta_k})} e^*(s) \\ & + \frac{2(\mu_0 + \sum_{\ell=1}^L \mu_\ell s^{\hat{\alpha}_\ell})}{(1 + \sum_{p=1}^P b_p s^{\hat{\beta}_p})} \epsilon_{mn}^*(s) \end{aligned} \quad (62)$$

and the Laplace transform of the RT model is

$$\begin{aligned} \sigma_{mn}^*(s) = & \delta_{mn} (\lambda_0 + \sum_{j=1}^J \lambda_j s^{\alpha_j}) e^*(s) \\ & + 2 (\mu_0 + \sum_{\ell=1}^L \mu_\ell s^{\hat{\alpha}_\ell}) \epsilon_{mn}^*(s) \end{aligned} \quad (63)$$

Another important property of the RT and RTG models is that they can be constructed to be causal in the sense that the response (stress) does not occur before the input (strain). The stress response is zero for negative time if its Laplace transform is analytic in the right half s plane. This condition on the transform of the stress is met, for the class of strain histories having transforms that are analytic in the right half s plane, when the branch cuts of s^{α_j} , $s^{\hat{\alpha}_\ell}$, s^{β_k} and $s^{\hat{\beta}_p}$ are along the negative, real s axis, and $\mu^*(s)$ and $\lambda^*(s)$ have no zeros in the right half s plane. Since the stress is zero for negative time, the stress cannot anticipate the strain that begins at time zero.

Laplace transforms are also useful in determining the hysteresis predicted by the RT and RTG models. For a sinusoidal strain history

of frequency ω_0 starting at time zero, the transform of the stress history is

$$\epsilon_{mn}(t) = \epsilon_{mn_0} \sin \omega_0 t \quad (64)$$

$$\sigma_{mn}^*(s) = (\delta_{mn} \lambda^*(s) e_0 + 2\mu^*(s) \epsilon_{mn_0}) \cdot \frac{\omega_0}{s^2 + \omega_0^2} \quad (65)$$

Evaluating the inverse transform in the same manner as in Section X, the stress time history is found to be

$$\begin{aligned} \sigma_{mn}(t) = & \frac{1}{2i} \left[(\delta_{mn} \lambda^*(i\omega_0) e_0 + 2\mu^*(i\omega_0) \epsilon_{mn_0}) e^{i\omega_0 t} \right. \\ & - (\delta_{mn} \lambda^*(-i\omega_0) e_0 + 2\mu^*(-i\omega_0) \epsilon_{mn_0}) e^{-i\omega_0 t} \Big] \\ & + \operatorname{Im} \left[\frac{1}{\pi} \int_0^\infty (\delta_{mn} \lambda^*(re^{-i\pi}) e_0 + 2\mu^*(re^{-i\pi}) \epsilon_{mn_0}) \right. \\ & \left. \left. \frac{\omega_0 e^{-rt}}{\omega_0^2 + r^2} dr \right] \quad (66) \right] \end{aligned}$$

As time increases, the integral term in Equation 66 goes to zero and the sinusoidal terms dominate the stress time history. So, for a sinusoidal strain history, the stress eventually becomes sinusoidal as well.

Using Euler's formula, numerous trigonometric manipulations, and the observation that the two sinusoidal terms are conjugates, the stress for large time may be evaluated as components in-phase with the strain,

proportional to $\sin \omega_0 t$, and components out-of-phase, proportional to $\cos \omega_0 t$. The resulting expression for the stress using the RTG model is

$$\begin{aligned}
 \sigma_{mn}(t) \approx & \left\{ \delta_{mn} e_{o\Delta_1}(\omega_o) \left[\lambda_o + \sum_{j=1}^J \lambda_j \omega_o^{\alpha_j} \cos \frac{\pi \alpha_j}{2} \right. \right. \\
 & + \lambda_o \sum_{k=1}^K a_k \omega_o^{\beta_k} \cos \frac{\pi \beta_k}{2} + \sum_{j=1}^J \sum_{k=1}^K \lambda_j a_k \omega_o^{\alpha_j + \beta_k} \cos \frac{\pi}{2} (\alpha_j - \beta_k) \Big] \\
 & + 2 \epsilon_{mn o} \Delta_2(\omega_o) \left[\mu_o + \sum_{\ell=1}^L \mu_{\ell} \omega_o^{\hat{\alpha}_{\ell}} \cos \frac{\pi \hat{\alpha}_{\ell}}{2} + \mu_o \sum_{p=1}^P b_p \omega_o^{\hat{\beta}_p} \cos \frac{\pi \hat{\beta}_p}{2} \right. \\
 & + \left. \sum_{\ell=1}^L \sum_{p=1}^P \mu_{\ell} b_p \omega_o^{\hat{\alpha}_{\ell} + \hat{\beta}_p} \cos \frac{\pi}{2} (\hat{\alpha}_{\ell} - \hat{\beta}_p) \right] \Big\} \sin \omega_o t \\
 & + \left\{ \delta_{mn} e_{o\Delta_1}(\omega_o) \left[\lambda_o + \sum_{j=1}^J \lambda_j \omega_o^{\alpha_j} \sin \frac{\pi \alpha_j}{2} \right. \right. \\
 & + \lambda_o \sum_{k=1}^K a_k \omega_o^{\beta_k} \sin \frac{\pi \beta_k}{2} + \sum_{j=1}^J \sum_{k=1}^K \lambda_j a_k \omega_o^{\alpha_j + \beta_k} \sin \frac{\pi}{2} (\alpha_j - \beta_k) \Big] \\
 & + 2 \epsilon_{mn o} \Delta_2(\omega_o) \left[\mu_o + \sum_{\ell=1}^L \mu_{\ell} \omega_o^{\hat{\alpha}_{\ell}} \sin \frac{\pi \hat{\alpha}_{\ell}}{2} + \mu_o \sum_{p=1}^P b_p \omega_o^{\hat{\beta}_p} \sin \frac{\pi \hat{\beta}_p}{2} \right. \\
 & + \left. \sum_{\ell=1}^L \sum_{p=1}^P \mu_{\ell} b_p \omega_o^{\hat{\alpha}_{\ell} + \hat{\beta}_p} \sin \frac{\pi}{2} (\hat{\alpha}_{\ell} - \hat{\beta}_p) \right] \Big\} \cos \omega_o t
 \end{aligned} \tag{67}$$

where

$$\Delta_1(\omega_0) = \left| 1 + \sum_{k=1}^K a_k \cdot (i\omega_0)^{\beta_k} \right|^{-1} \quad (68)$$

and

$$\Delta_2(\omega_0) = \left| 1 + \sum_{p=1}^P b_p \cdot (i\omega_0)^{\hat{\beta}_p} \right|^{-1} \quad (69)$$

A more compact form of the expression for the stress is

$$\begin{aligned} \sigma_{mn}(t) \approx & \delta_{mn} F_1(\omega_0) e_0 \sin \omega_0 t + F_2(\omega_0) \epsilon_{mn_0} \sin \omega_0 t \\ & + \delta_{mn} F_3(\omega_0) e_0 \cos \omega_0 t + F_4(\omega_0) \epsilon_{mn_0} \cos \omega_0 t \end{aligned} \quad (70)$$

Under conditions of uniaxial stress and strain, Equations 64 and 70 may be recognized as the parametric equations of an ellipse; thus, it is clear that the RTG model predicts the existence of a hysteresis loop and the loop is elliptical.

The loss factor associated with the hysteresis loop, the ratio of the energy dissipated during a cycle, D , to the peak strain energy stored during a cycle, U_{\max} , is a parameter often used to characterize the ability of viscoelastic materials to damp vibratory motion.

$$\eta = \frac{D}{2\pi U_{\max}} \quad (71)$$

The energy dissipated per cycle is

$$D = \sum_{n=1}^3 \sum_{m=1}^3 \int_0^{2\pi/\omega_0} \sigma_{mn}(t) \dot{\epsilon}_{mn}(t) dt \quad (72)$$

where $\frac{2\pi}{\omega_0}$ is the period of the motion. Using Equations 64 and 70 to evaluate dissipated energy yields

$$D = \pi F_3(\omega_0) e_0^2 + \sum_{n=1}^3 \sum_{m=1}^3 F_4(\omega_0) \epsilon_{mn_0}^2 \quad (73)$$

The peak energy stored during a cycle is

$$U_{\max} = \sum_{n=1}^3 \sum_{m=1}^3 \int_{\epsilon_{mn}=0}^{\epsilon_{mn}=\epsilon_{mn}(\max)} \tilde{\sigma}_{mn} d\epsilon_{mn} = \sum_{n=1}^3 \sum_{m=1}^3 \int_0^{\frac{\pi}{2\omega_0}} \tilde{\sigma}_{mn} \dot{\epsilon}_{mn} dt \quad (74)$$

where $\tilde{\sigma}_{mn}$ are the stresses in-phase with their respective strains, $\epsilon_{mn_0} \sin \omega_0 t$. Again using Equations 65 and 66, the peak energy stored during a cycle is

$$U_{\max} = \frac{1}{2} F_1(\omega_0) e_0^2 + \sum_{n=1}^3 \sum_{m=1}^3 F_2(\omega_0) \epsilon_{mn_0}^2 \quad (75)$$

The resulting loss factor is seen to be

$$\eta = \frac{F_3(\omega_0) e_0^2 + \sum_{n=1}^3 \sum_{m=1}^3 F_4(\omega_0) \epsilon_{mn_0}^2}{F_1(\omega_0) e_0^2 + \sum_{n=1}^3 \sum_{m=1}^3 F_2(\omega_0) \epsilon_{mn_0}^2} \quad (76)$$

Notice that the form of the expressions for the hysteresis behavior and loss factor of the RT model is identical to that of the RTG model. This follows from the observation that the RT model is a special case of the RTG model for $b_k = 0$, $k = 1, 2, \dots, K$, and $b_p = 0$, $p = 1, 2, \dots, P$.

In summary, RT and RTG models satisfy the elastic viscoelastic correspondence principle. Conditions necessary to ensure that the stress does not anticipate the strain have been developed. In addition, both models predict the existence of stress-strain hysteresis effects and the resulting hysteresis loops are elliptical. Most significantly, the models predict moduli which have the same frequency dependence as is observed in frequency-dependent moduli in typical viscoelastic materials.*

The outstanding question is whether or not the parameters of the RT and RTG models can be chosen to describe accurately the properties of a particular viscoelastic material. The construction of the RT model for the elastomer 3M-467 is the topic of the following section.

*In addition, a generalized derivative constitutive relation occurs in Newtonian, viscous fluids as demonstrated in Appendix B.

SECTION V

THE RT MODEL FOR THE ELASTOMER 3M-467*

The first material examined for the possible application of generalized derivative constitutive relations was the adhesive tape 3M-467. The tape was chosen as a prime candidate because of its viscoelastic mechanical properties, its linear response in shear for engineering shear strains up to 1, its growing applications in mechanical damping, and the fact that sufficient data on its mechanical properties were available.

The proposed uniaxial shear RT model for 3M-467 is

$$\sigma_{mn}(t) = 2 (\mu_0 + \mu_1 D^{\hat{\alpha}_1}) \epsilon_{mn}(t), \quad m \neq n \quad (77)$$

where

$$\mu_0 = 1.0 \text{ lb/in}^2 \quad (78)$$

$$\mu_1 = 7.3 \text{ lb-sec}^{.56}/\text{in}^2 \quad (79)$$

and

$$\hat{\alpha}_1 = .56 \quad (80)$$

The parameters of the model, μ_0 , μ_1 , and $\hat{\alpha}_1$, are chosen so the sinusoidal, steady-state response of the model closely approximates the sinusoidal, steady-state response of the material observed experimentally. For sinusoidal strain

$$\epsilon_{mn}(t) = \begin{cases} \epsilon_{mn_0} e^{i\omega t} & t \geq 0. \\ 0. & t < 0. \end{cases} \quad (81)$$

*3M-467 is an adhesive produced by the Minnesota Mining and Manufacturing Co., Inc., Minneapolis, Minnesota.

the RT model generates stresses of the form

$$\sigma_{mn}(t) \approx 2 (\mu_0 + \mu_1 (i\omega)^{\hat{\alpha}_1}) \epsilon_{mn_0} e^{i\omega t} \quad (82)$$

$t \gg 0$

for t large enough for the transients to have died out. The frequency-dependent shear modulus, $\mu(\omega)$, is seen to be

$$\mu(\omega) = \mu_0 + \mu_1 (i\omega)^{\hat{\alpha}_1} \quad (83)$$

Figure 2 displays the good agreement between the experimentally observed mechanical properties of 3M-467 at 75°F and the RT model using the values of the parameters given above.*

The parameters of the RT model were determined in an iterative manner. Initial guesses of the parameters were made, and the resulting frequency dependent shear modulus was compared to the observed modulus. Successive guesses of the parameters were made to match the slopes and asymptotes of the model to those of the observed properties until an acceptable fit was obtained.

Although the parameters of the RT model are based on the sinusoidal response of the material at 75°F, the model can be used for non-periodic strain histories. To demonstrate the ability of the model to portray accurately the behavior of the material when undergoing non-periodic motion, the response of the material as predicted by the RT model is compared to the experimentally observed response of the material at 75°F.

In particular, the behavior of 3M-467 was observed when the material was used as a viscoelastic spring in a simple oscillator undergoing

*The mechanical properties of 3M-467 were provided by the U.S. Air Force Materials Laboratory, Wright-Patterson Air Force Base, Ohio.

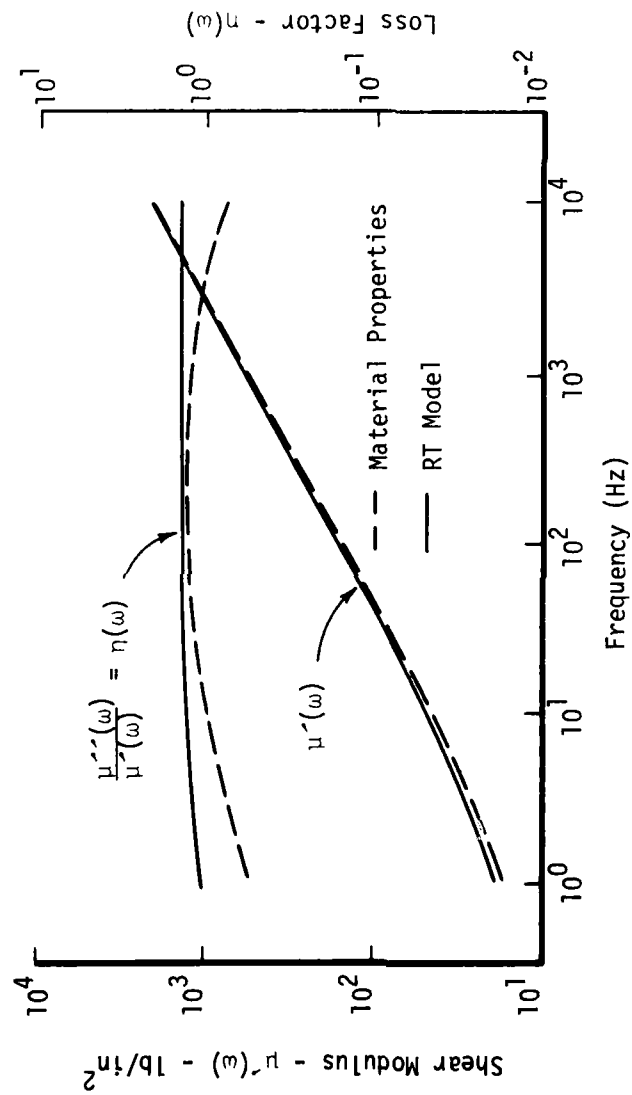


Figure 2. A Comparison of the Material Properties of 3M-467 and the Properties Predicted by its RT Model

non-periodic motion.* The viscoelastic spring was two pads of 3M-467 that underwent shear strain during the motion of the oscillator. Each pad of 3M-467 was made by laminating 2 mil layers of 3M-467. Air entrapped between the layers of the pad was removed by pressing the layers together with a 5 lb. weight for 48 hours.

The other two components of the oscillator are the mass and the support structure (Figure 3). The mass for the oscillator is a metal cube sandwiched between the two viscoelastic pads (Figure 4). Each pad is attached to an aluminum brace. Both braces are glued to an aluminum base which, in turn, is glued to a steel foundation as shown in Figure 3.

The specific objective of the experiment was to determine the acceleration transfer function of the oscillator. The acceleration transfer function is the ratio of the transform of the acceleration time history to the transform of the input force history. The force time history, measured by a Wilcoxon Z-11 impedance head, was sampled at 2×10^4 measurements per second and all frequencies above 8×10^3 Hz are filtered out. The mass of the oscillator was tapped with a Wilcoxon Z-11 impedance head to produce impulsive loading. The force time history measured by the impedance head and the resulting acceleration time history, measured by an Endevco accelerometer, Model 2217, were also sampled at 2×10^4 measurements per second where, as before, all frequencies above 8×10^3 Hz were filtered out. The transforms of the time histories were calculated using the "fast Fourier transform" routines of the Hewlett Packard System 5451B.

This experimentally determined transfer function is compared to the analytically predicted transfer function based on the equations of motion of the oscillator and the RT model for the viscoelastic pads. The force-displacement relation for the two pads based on the RT model (Equation 77) is

$$f_p(t) = \frac{2A}{\delta} (\mu_0 + \mu_1 D^{\hat{a}_1}) x(t) \quad (84)$$

*A schematic of the viscoelastic spring appears in Figure 4.

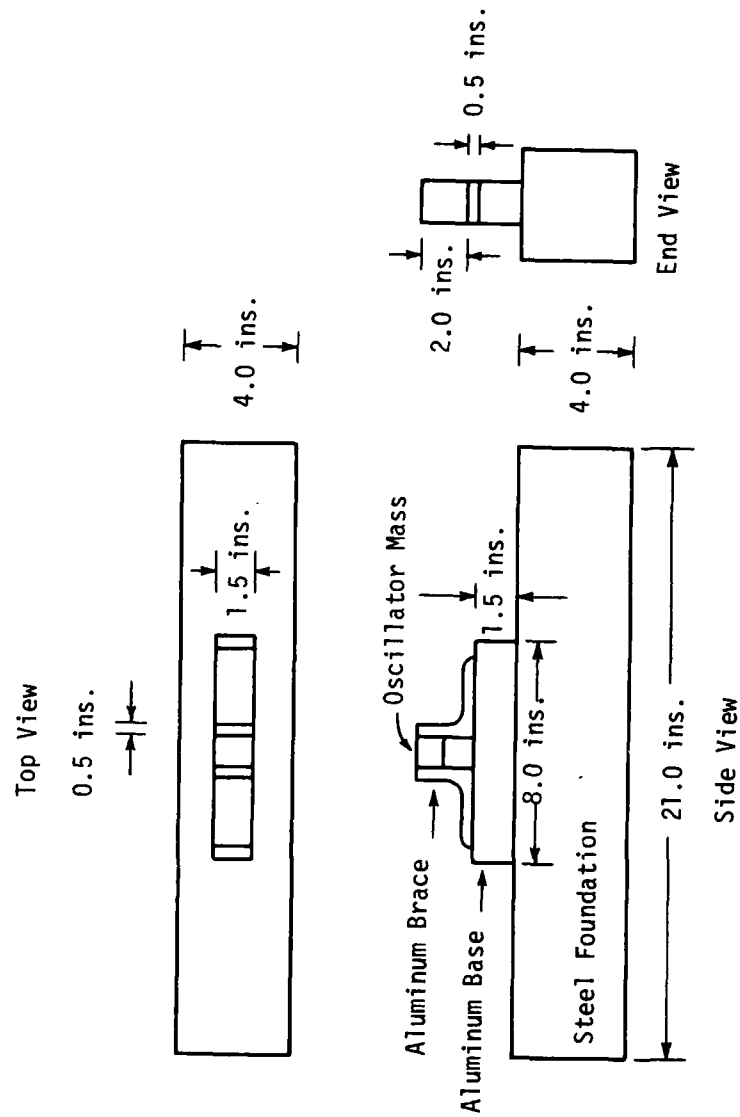


Figure 3. A Schematic of the Oscillator and its Support Structure

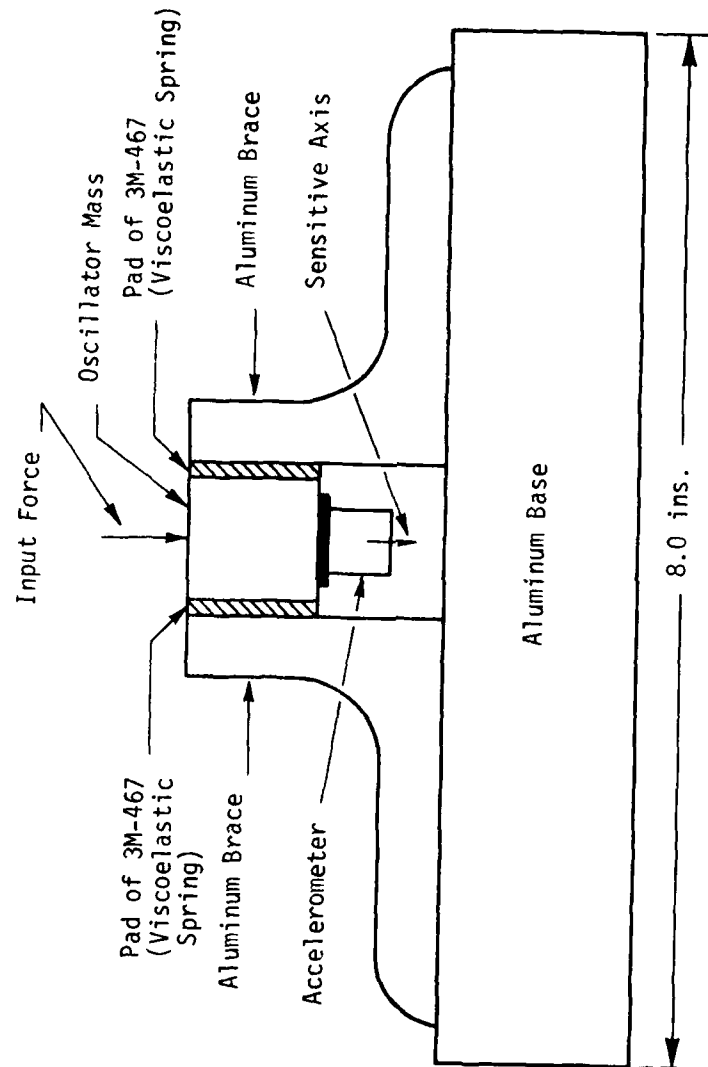


Figure 4. Expanded Schematic of the Oscillator and Support Structure
Not Displaying the Steel Foundation

where A is an area of contact with the mass for each pad, δ is the thickness of the pad, $f_p(t)$ is the total force acting on the faces of the pads in contact with the mass, and $x(t)$ is the displacement of the face of the pad in contact with the mass. This force displacement relation is based on the assumption that the displacement in the pad varies linearly between the support wall and the mass of the oscillator.*

The resulting equation of motion for the oscillator is

$$f(t) = m\ddot{x}(t) + \frac{2A}{\delta} (\mu_0 + \mu_1 D^{\hat{\alpha}_1}) x(t) \quad (85)$$

Taking the Fourier transform of the equations of motion and determining the acceleration transfer function produces

$$\frac{(i\omega)^2 X(\omega)}{F(\omega)} = \frac{1}{\left(m + \frac{2A}{\delta} \frac{(\mu_0 + \mu_1 (i\omega)^{\hat{\alpha}_1})}{(i\omega)^2} \right)} \quad (86)$$

A comparison of the experimentally determined and analytically predicted transfer functions for five oscillators with various masses and viscoelastic spring stiffnesses is presented in Figures 5 through 14.** Each transfer function is displayed in terms of its magnitude and phase. The agreement between the observed and predicted transfer functions is very good.

For comparison, the calculated transfer function based on a Voigt viscoelastic model of 3M-467

$$\sigma_{mn}(t) = 2 (\mu_0 \epsilon_{mn}(t) + \mu_1 \dot{\epsilon}_{mn}(t)) , \quad m \neq n \quad (87)$$

*A finite element analysis of the viscoelastic pad verifies this assumption to be valid for the frequency range of the tests, 0 to 5×10^3 Hz.

**The relevant parameters for each of the five oscillators are given in Table 1.

TABLE 1
PARAMETERS OF THE FIVE OSCILLATORS

<u>Case Number</u>	<u>Mass* (m)</u>	<u>Pad Thickness (δ)</u>	<u>Pad Area (A)</u>
1	1.57×10^{-3} slug	2.2×10^{-2} in	1.55 in^2
2	8.9×10^{-4} slug	3.2×10^{-2} in	$.968 \text{ in}^2$
3	4.8×10^{-4} slug	2.0×10^{-2} in	$.555 \text{ in}^2$
4	4.4×10^{-4} slug	3.2×10^{-2} in	$.968 \text{ in}^2$
5	2.9×10^{-4} slug	2.0×10^{-2} in	$.555 \text{ in}^2$

* Includes the mass of the accelerometer.

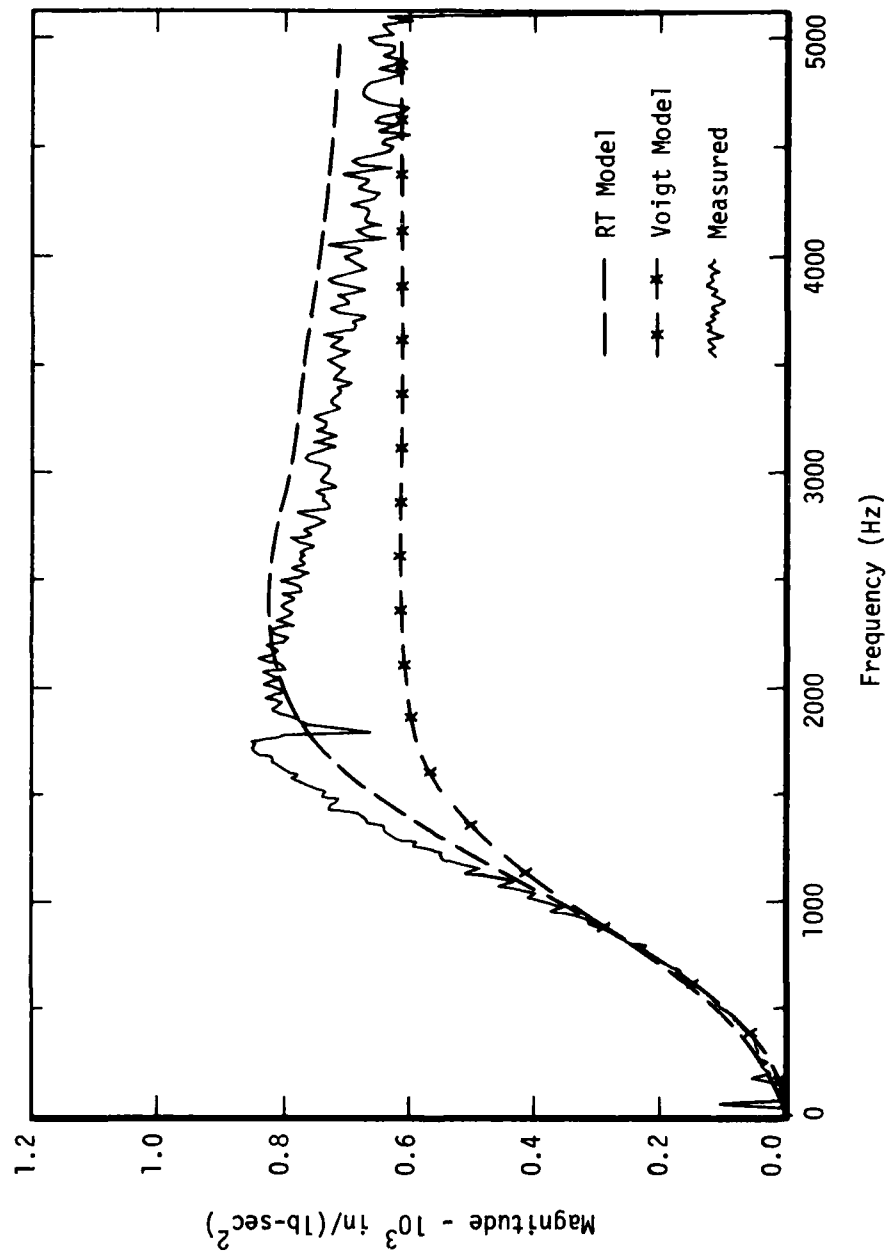


Figure 5. The Magnitude of the Transfer Function for Case #1

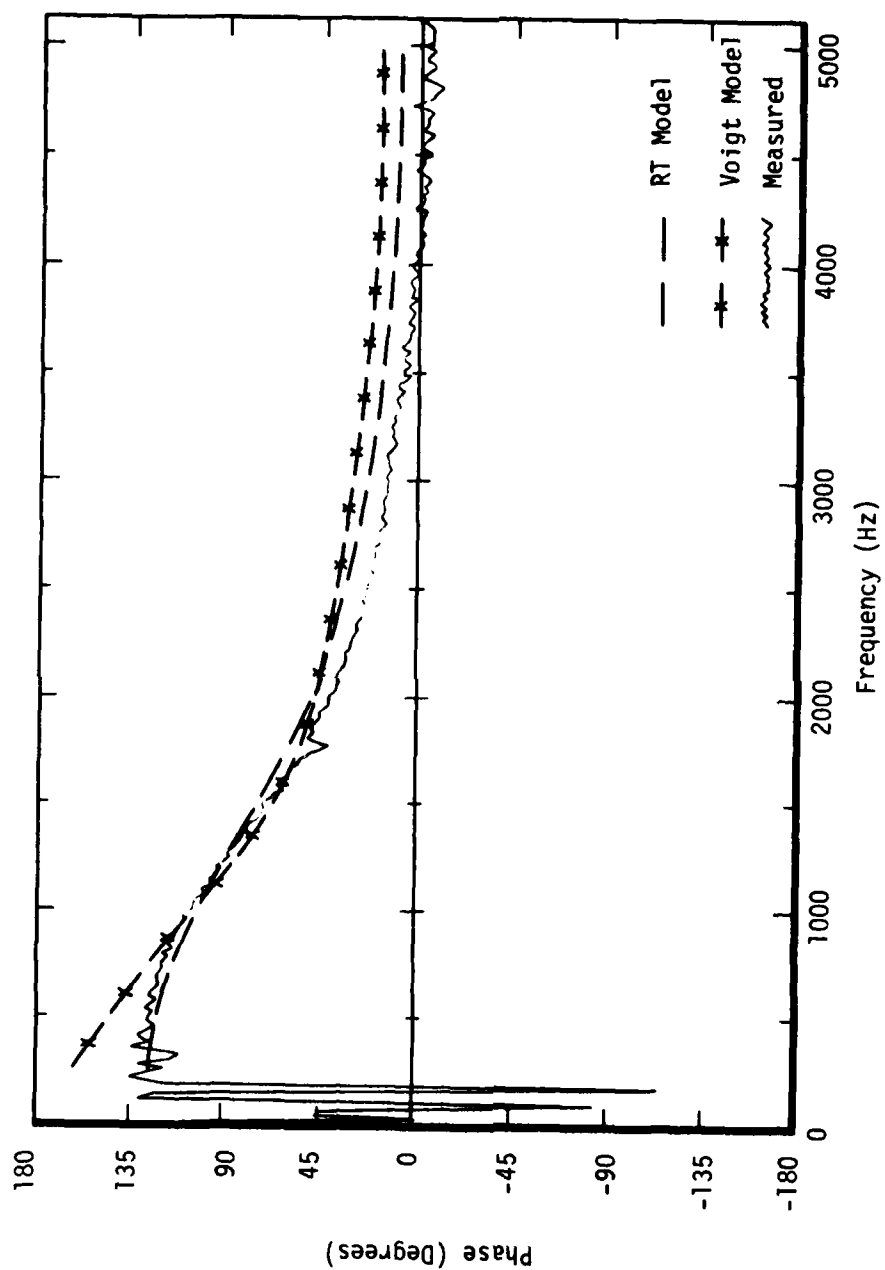


Figure 6. The Phase of the Transfer Function for Case #1

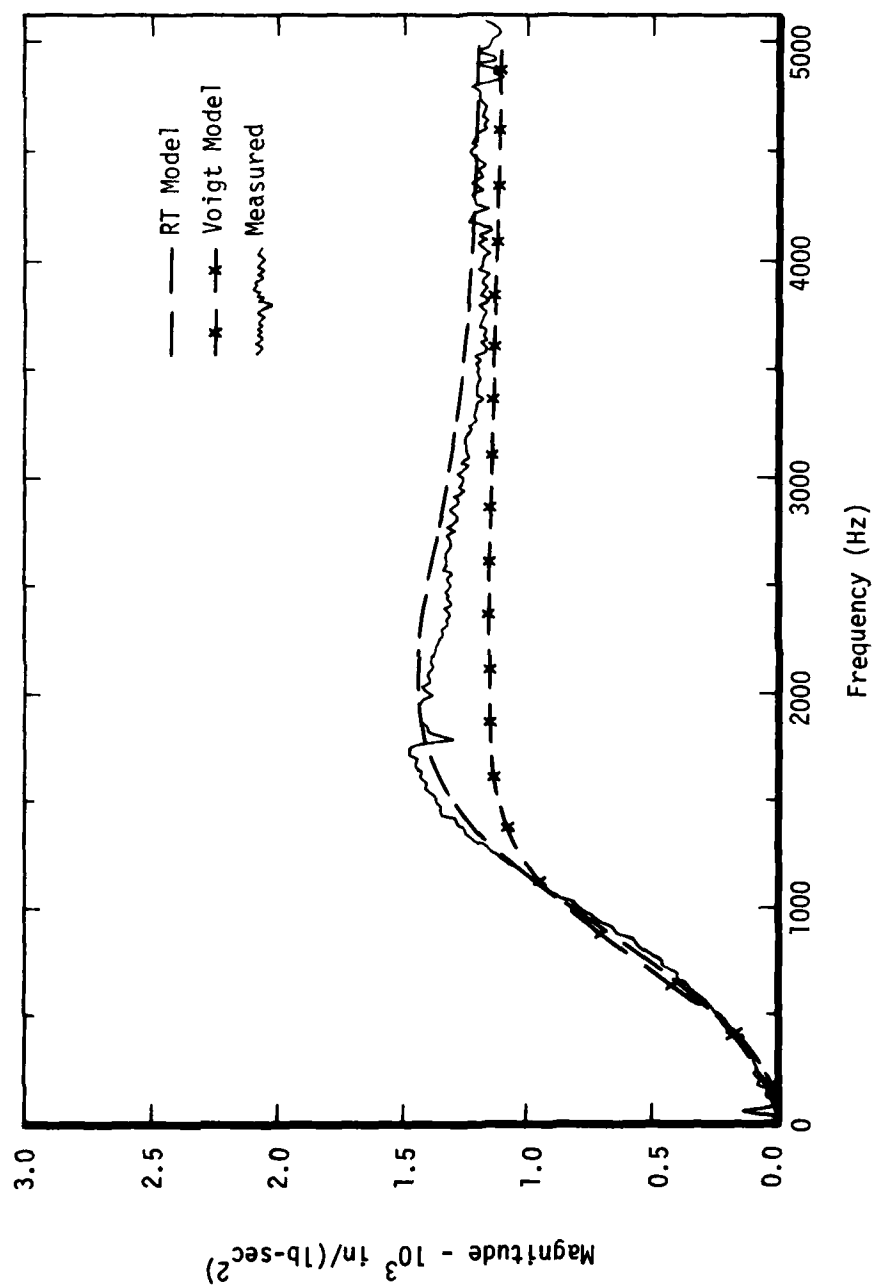


Figure 7. The Magnitude of the Transfer Function for Case #2

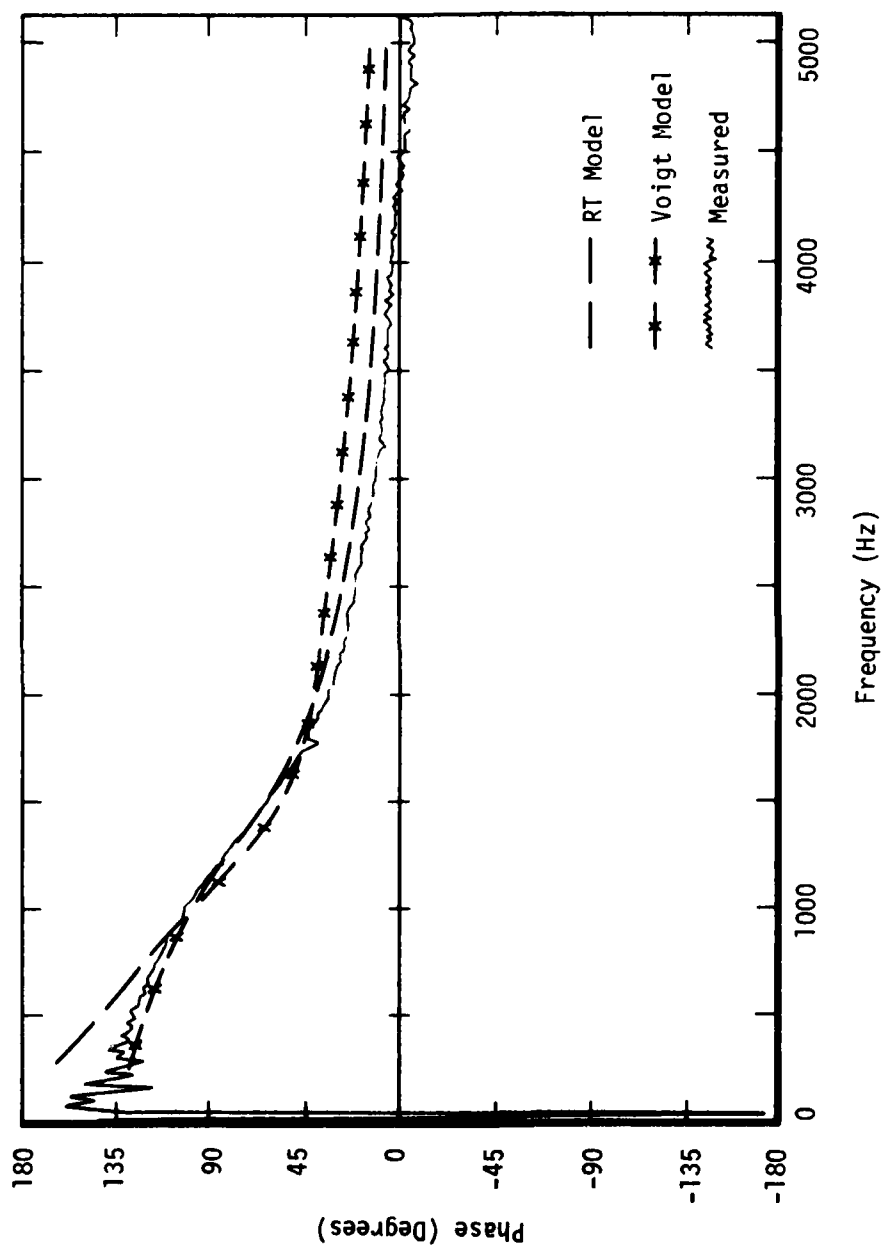


Figure 8. The Phase of the Transfer Function for Case #2

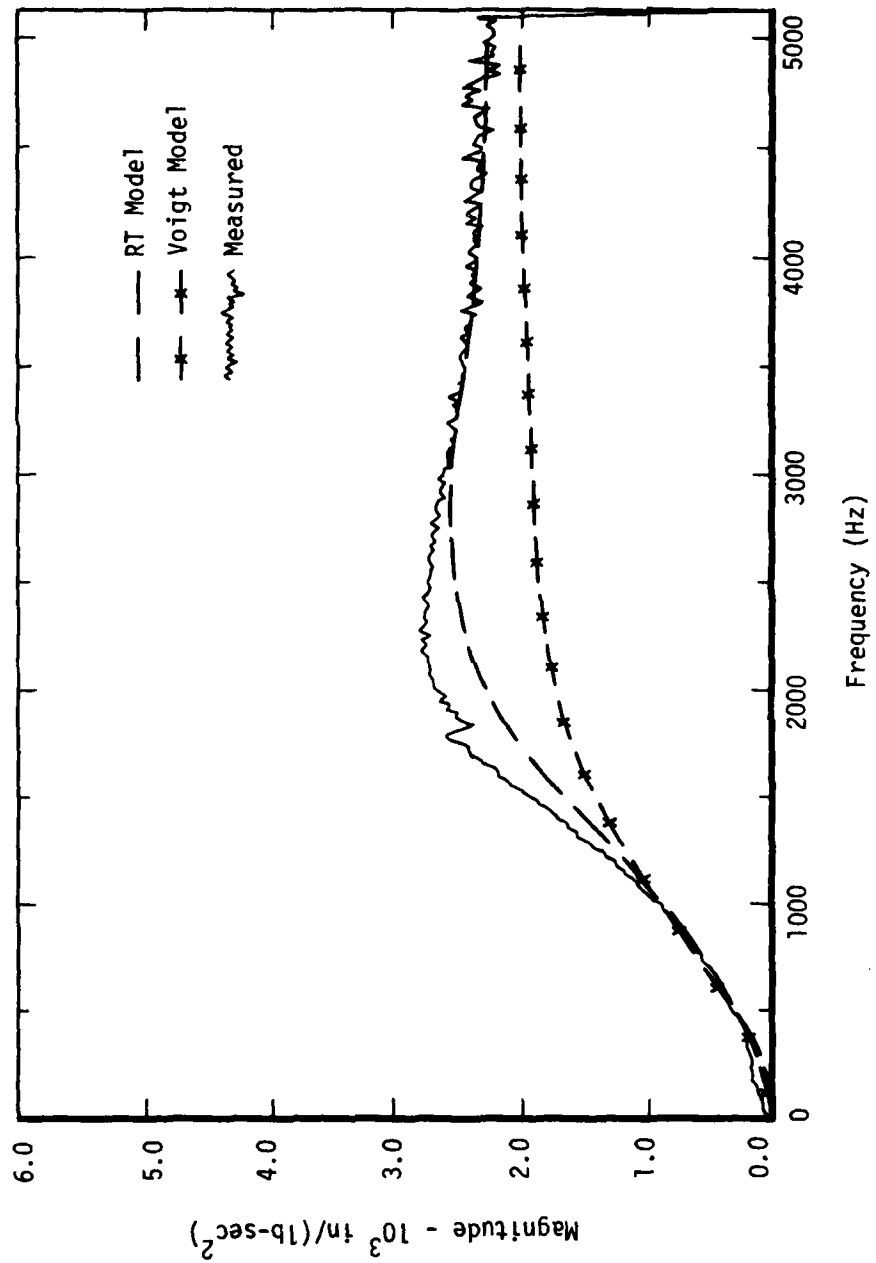


Figure 9. The Magnitude of the Transfer Function for Case #3

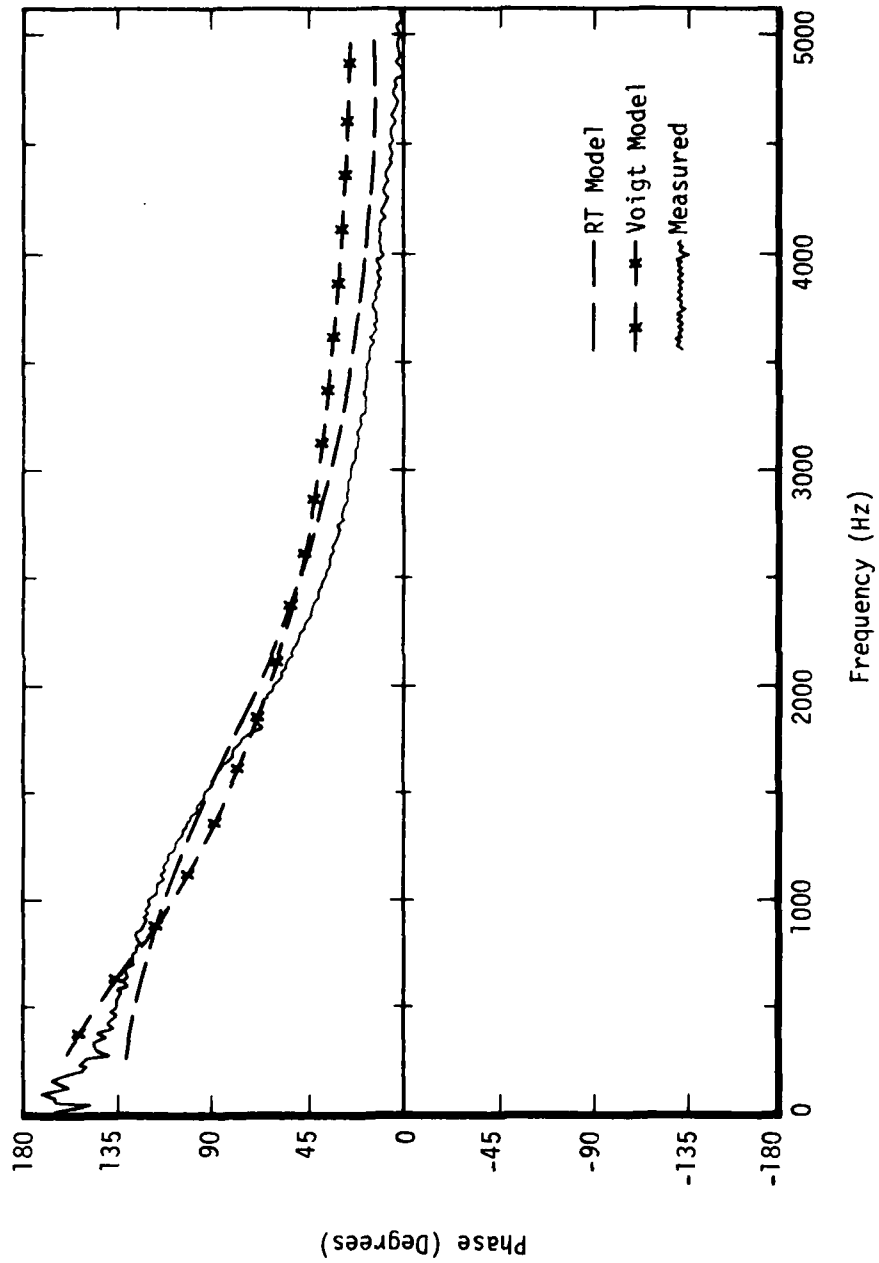


Figure 10. The Phase of the Transfer Function for Case #3

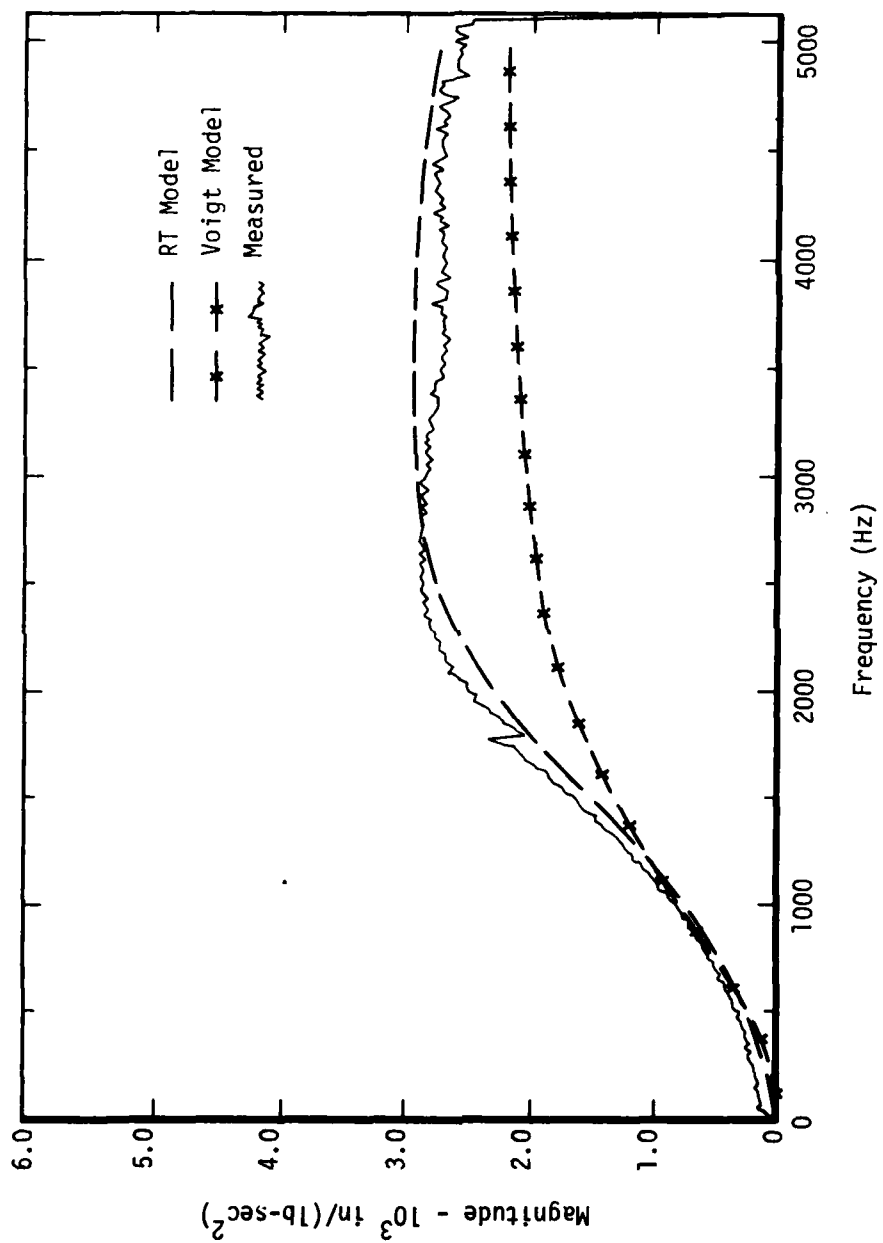


Figure 11. The Magnitude of the Transfer Function for Case #4

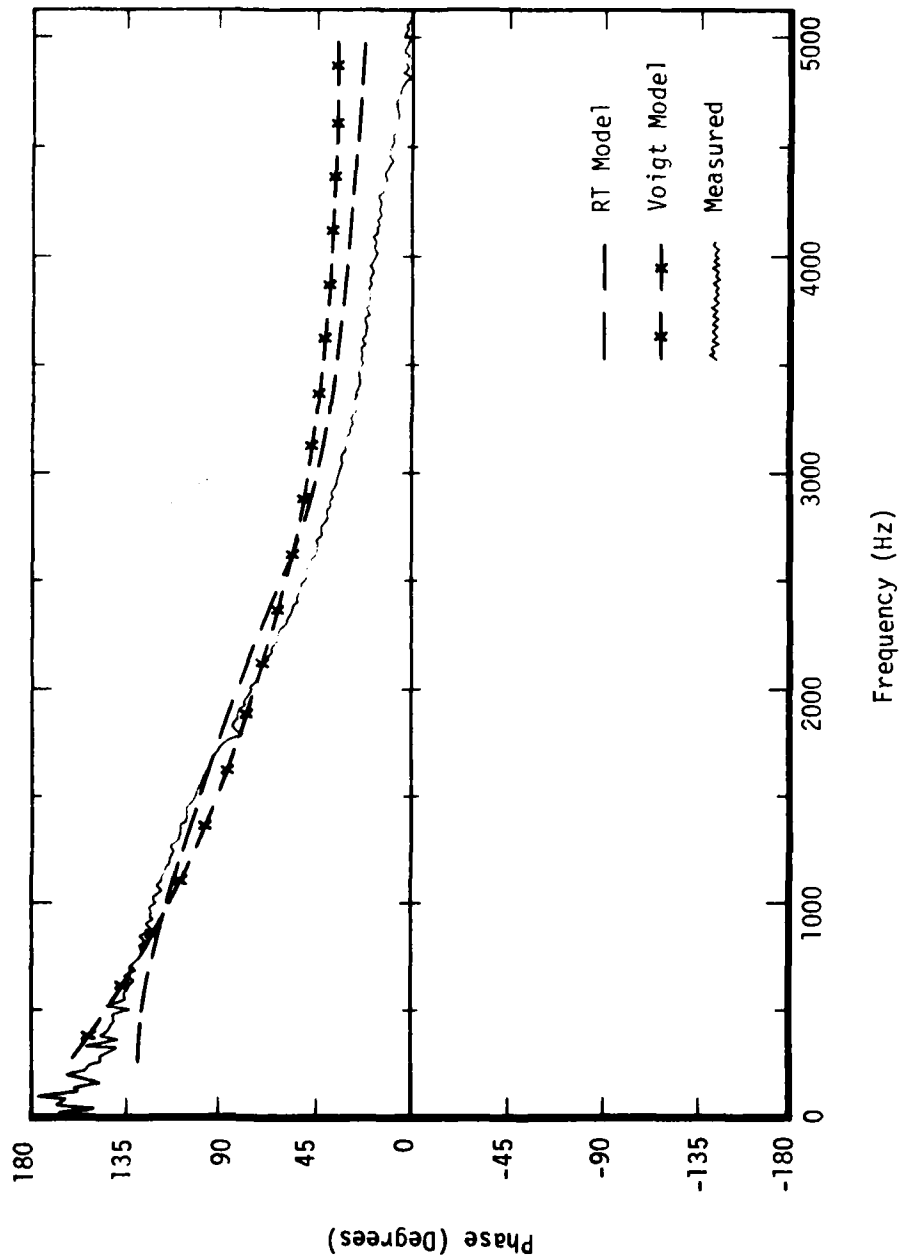


Figure 12. The Phase of the Transfer Function for Case #4

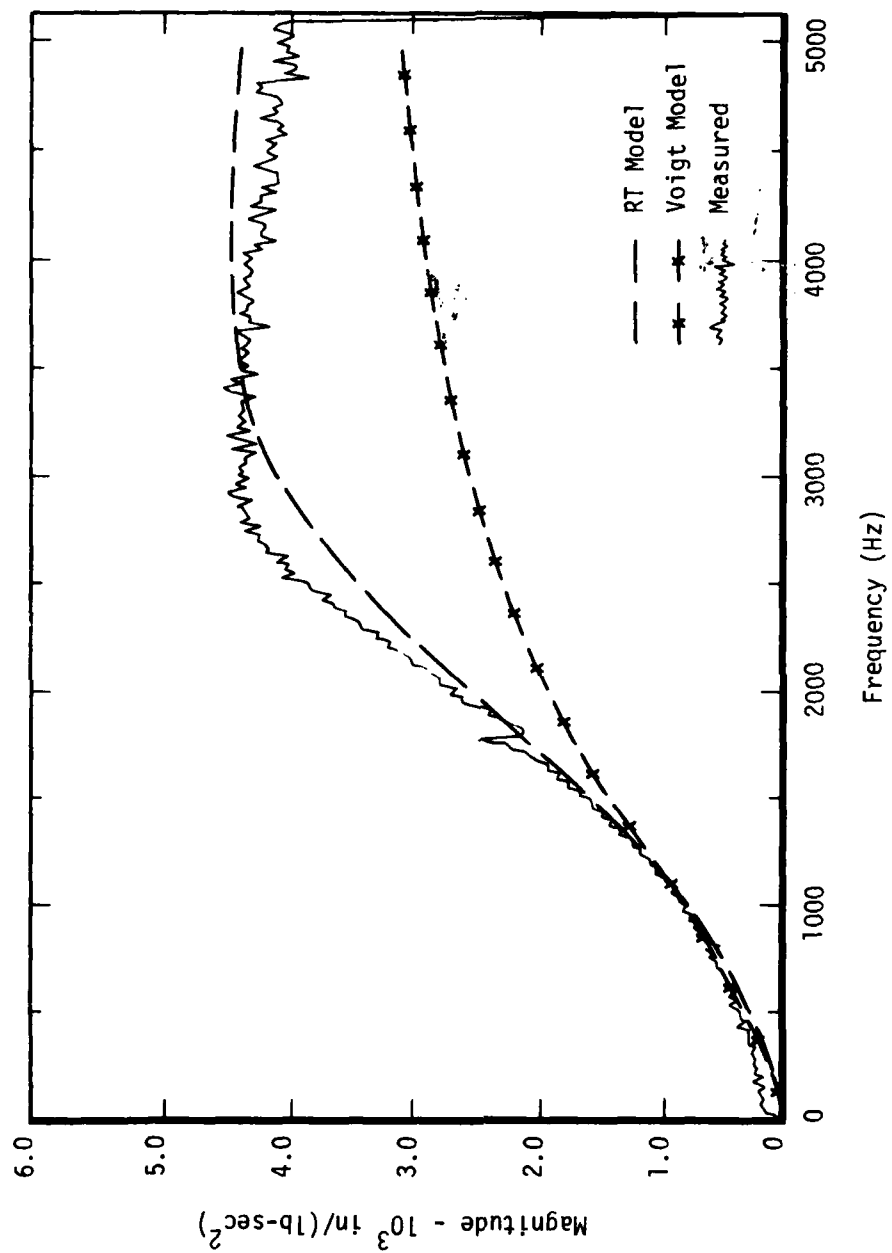


Figure 13. The Magnitude of the Transfer Function for Case #5

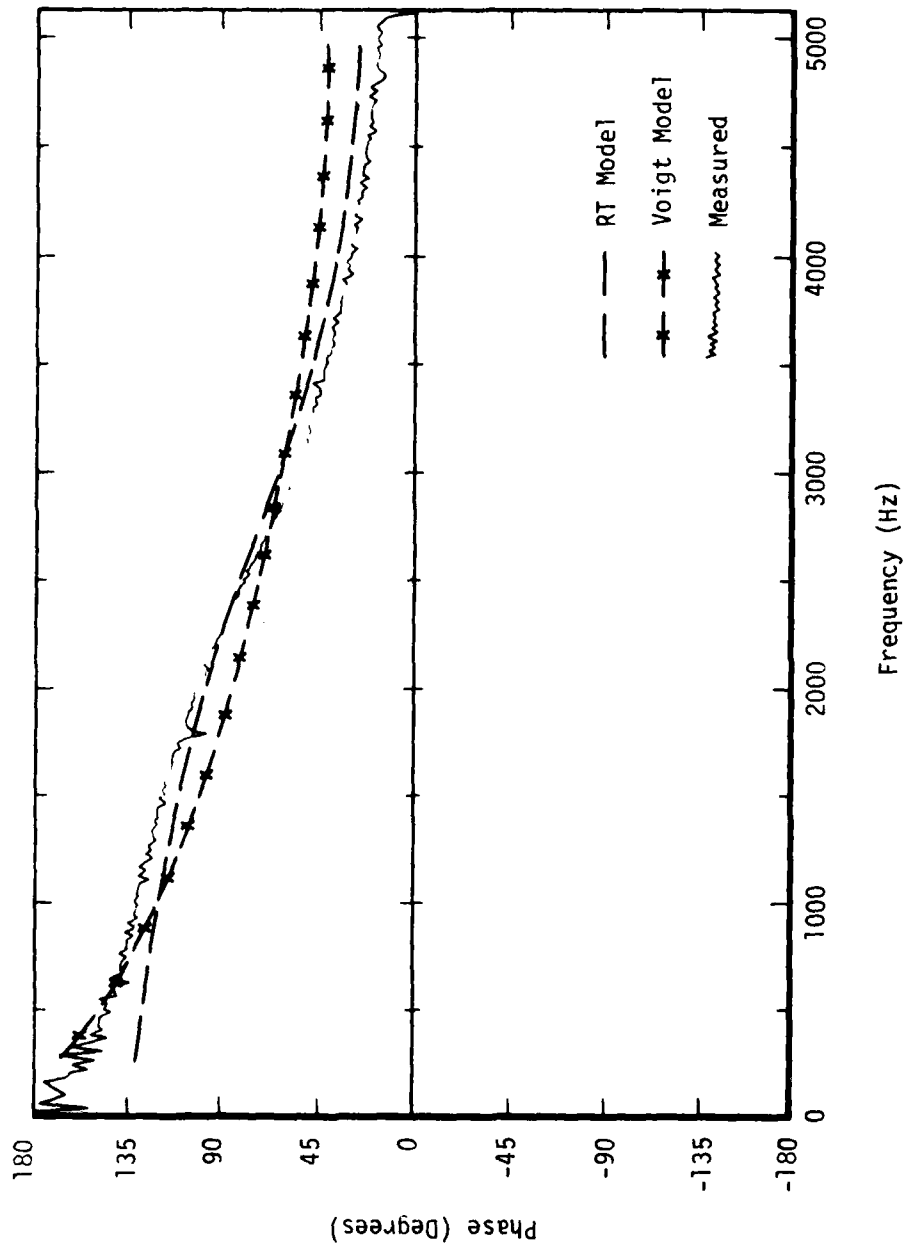


Figure 14. The Phase of the Transfer Function for Case #5

is also given in Figures 5 through 14. The parameters of the Voigt model, μ_0 and μ_1 , are chosen to match the properties of 3M-467 at 10^3 Hz.

$$\mu_0 = 630 \text{ lb/in}^2 \quad (88)$$

$$\mu_1 = .113 \text{ lb-sec/in}^2 \quad (89)$$

Note that for some of the oscillators, the Voigt model and the RT model both generate transfer functions that agree reasonably well with the observed transfer functions. However, for those oscillators having the peak magnitude of acceleration response at higher frequencies, (Figure 13 for example) the transfer function based on the RT model is clearly in better agreement with the measured transfer function than the transfer function based on the Voigt model. In addition, the phase of the observed transfer functions is consistently modeled more accurately by the phase of the transfer functions calculated using the RT model. These results follow directly from the fact that the RT model accounts for the observed properties of 3M-467 over the entire frequency range of interest, 10^2 Hz to 5×10^3 , whereas the Voigt model accounts for the observed properties of 3M-467 only in the neighborhood of 10^3 Hz. This is clearly seen by comparing Figures 2 and 15.

If one attempts to duplicate the results presented here, one should be aware that the mechanical properties of 3M-467 are strongly dependent on the water present in the material. Figure 16 shows the variation of the real part of the modulus with relative humidity. Changes in the imaginary part of the modulus with relative humidity are roughly proportional to changes in the real part. Hence, the loss factor, the ratio of imaginary part to real part of the modulus, is relatively insensitive to changes in relative humidity, as seen in Figure 17.

The pads of 3M-467 used in this experiment were fabricated under conditions of 40% relative humidity at room temperature. However, the pads were kept covered during the time between fabrication and installation into the test setup.

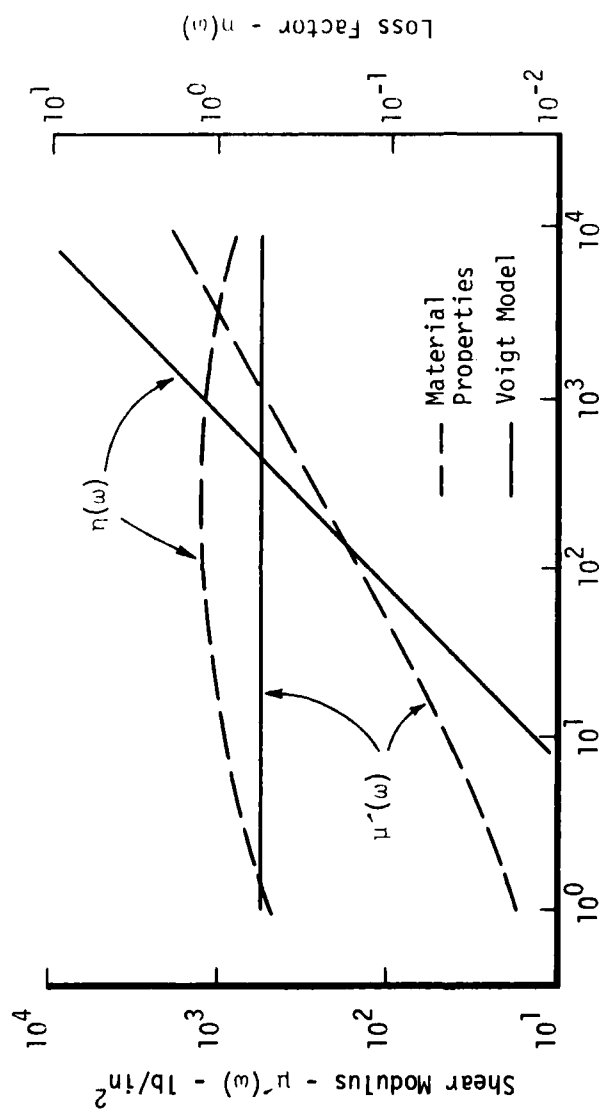


Figure 15. A Comparison of the Material Response of 3M-467 and the Properties Predicted by a Voigt Model.

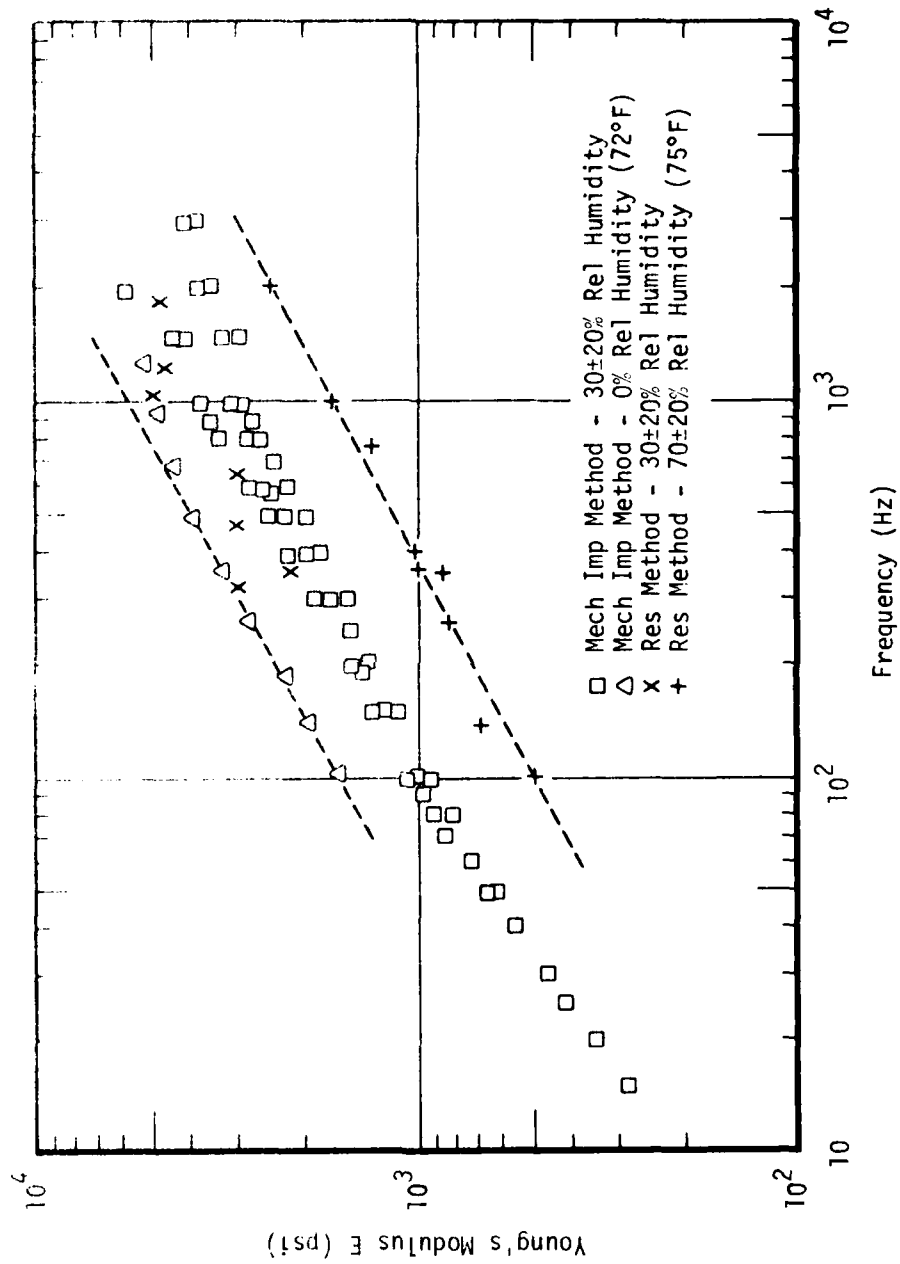


Figure 16. The Variations of Young's Modulus of 3M-467 with Changes in Relative Humidity

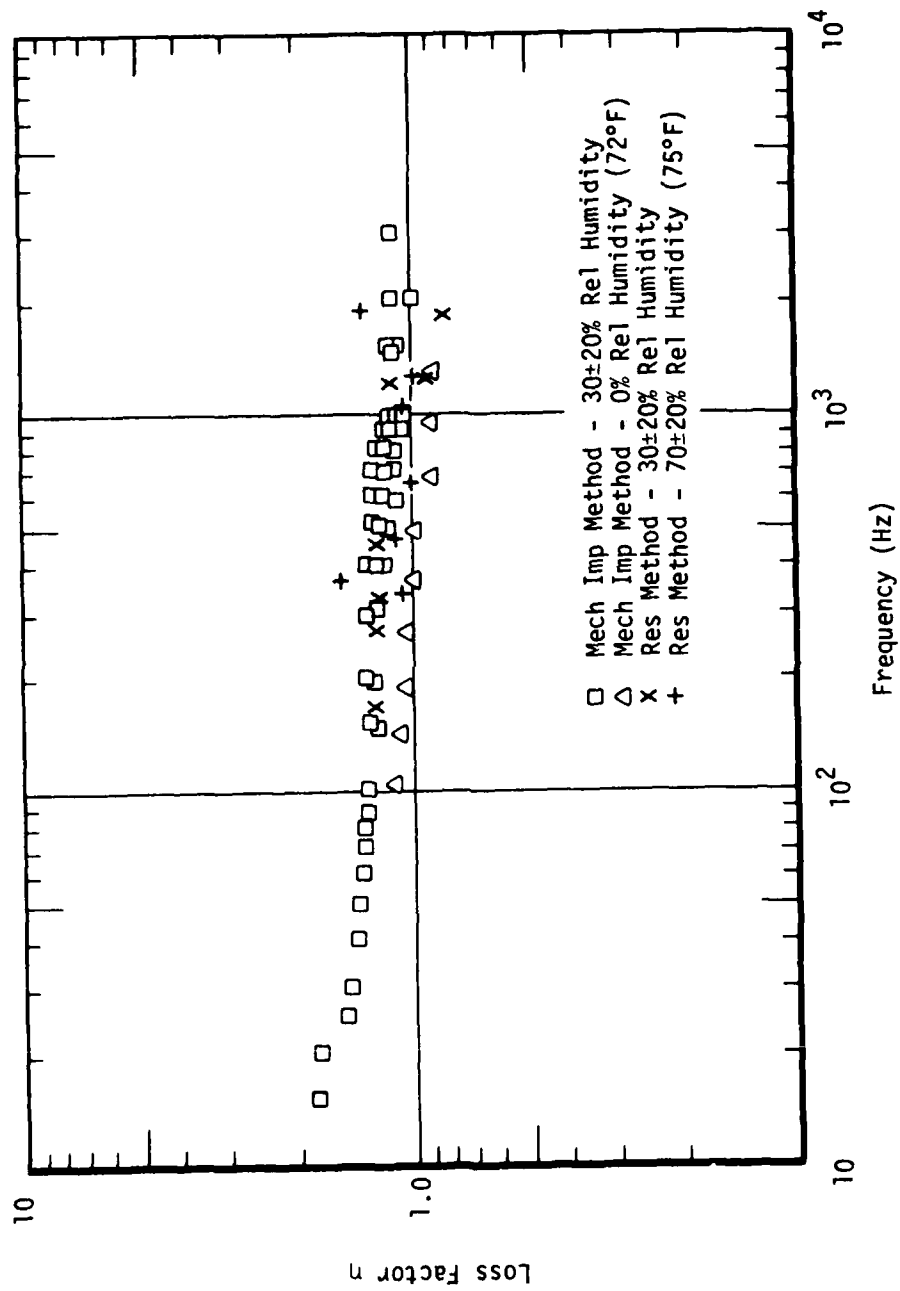


Figure 17. The Variations of Loss Factor of 3M-467 with Changes in Relative Humidity

In summary, the RT model for 3M-467 is capable of accurately predicting the non-periodic response of the material over several decades of frequency, and is superior to a Voigt model of the material. Consequently, the RI model having parameters based on the sinusoidal steady motion of the material at numerous frequencies is capable of predicting the response of the material to impulse-like, short duration loading. Therefore, one can conclude that the RT model can accurately predict the general response of the material within the frequency range of the model.

SECTION VI

A FINITE ELEMENT FORMULATION OF THE EQUATIONS OF MOTION

Having established that a very elementary formulation of the equation of motion for an elastomer-damped oscillator produced excellent agreement with experimental observation, it is appropriate at this point to put forward the tools required in the analysis of more complicated structures of engineering interest. In particular, the development focuses on the analysis of structures having both elastic and viscoelastic components.

A continuum formulation of the equations of motion for such structures is impractical because of the resulting complexity of the formulation for most structures with complex geometry and varying material properties. As a result, a finite element formulation of the equations of motion is adopted.

The cornerstone of the finite element approach is the construction of the stiffness matrices for each of the finite elements in the structure. The stiffness matrices for the elastic finite elements of structure are constructed in the normal fashion using assumed displacement methods or assumed stress methods, etc.

The formulation of the stiffness matrices for the finite elements in the viscoelastic components, however, is limited to those methods that do not constrain the stresses in each finite element to be in equilibrium with the forces at the nodes the element. The assumed stress method, in particular, is based on this constraint (Reference 24). As a result, the time dependence of the stresses in the element is predicated on time dependence of the nodal forces. However, this contradicts the fundamental nature of the generalized derivative models in which the time dependence of the stresses is predicated on the time dependence of the strain histories.

Consequently, the assumed displacement method is adopted to formulate the stiffness matrix of the viscoelastic finite element (Reference 2b). In an assumed displacement element, the displacements within the element are assumed functions of the nodal displacements.

The stiffness matrix of the viscoelastic finite element is constructed using the elastic viscoelastic correspondence principle. The stiffness matrix is first formulated as though the material were elastic. The stiffness matrix is then separated into two matrices, one matrix containing those elements proportional to the elastic constant λ , and the other matrix containing those elements proportional to the elastic constant μ .

$$[K_e] = \lambda[K'_e] + \mu[K''_e] \quad (90)$$

At this point the transforms of the moduli, $\mu^*(s)$ and $\lambda^*(s)$, from either the RT or the RTG models, are substituted in place of the elastic constants, μ and λ . The result is the viscostiffness matrix of the finite element, $[K_e(s)]$.

$$[K_e(s)] = \lambda^*(s)[K'_e] + \mu^*(s)[K''_e] \quad (91)$$

Specifically, the viscostiffness matrix for a finite element in which the RTG constitutive relation is used to model the material is

$$[K_e(s)] = \frac{(\lambda_0 + \sum_{j=1}^J \lambda_j s^{\alpha_j})}{(1 + \sum_{k=1}^K a_k s^{\beta_k})} [K'_e] + \frac{(\mu_0 + \sum_{l=1}^L \mu_l s^{\hat{\alpha}_l})}{(1 + \sum_{p=1}^P b_p s^{\hat{\beta}_p})} [K''_e] \quad (92)$$

The viscostiffness matrix of the finite element relates the nodal forces, $\{F(s)\}$, and nodal displacements, $\{X(s)\}$, as shown below

$$\{F(s)\} = [K_e(s)] \{X(s)\} \quad (93)$$

and the viscostiffness matrix of a viscoelastic structural component is constructed from the viscostiffness matrices of the elements within the component in the normal manner. The viscostiffness matrices of the R viscoelastic structural components

$$\{F(s)\}_r = [K(s)]_r \{X(s)\}_r \quad r = 1, 2, 3, \dots, R \quad (94)$$

and the stiffness matrices of the Q elastic structural components

$$\{F(s)\}_q = [K]_q \{X(s)\}_q \quad q = 1, 2, 3, \dots, Q \quad (95)$$

are used to construct the stiffness matrix of the total structure, again in the normal manner.

The stiffness matrix of the total structures, $[K(s)]$, and the mass matrix of the total structure are now used to construct the Laplace transform of the equations of motion of the structure

$$s^2[M] \{X(s)\} + [K(s)] \{X(s)\} = \{F(s)\} \quad (96)$$

Since some of the elements in $[K(s)]$ are functions of s , decoupling the equations of motion, (Equation 96) to obtain solutions is more complicated than decoupling the equations of motion of a completely elastic structure where the stiffness matrix has constant elements. Finding solutions to Equation 96 is the topic of the next section.

SECTION VII

THE SOLUTION OF THE DISCRETE EQUATIONS OF MOTION

The task at hand is the solution of the equations of motion which resulted from the finite element formulation (Equation 96). A form of modal analysis is adopted where the mode shapes, eigenvectors, of the equations of motion are used to construct an orthogonal transformation of the variables that decouple the equations of motion. The decoupled equations of motion are then used to determine the components of the structure's response and a general form of the solution to the equations of motion is derived.

Throughout this development, the viscoelastic components of the structure are described by their respective RTG models. Since the RT model is a simplified version of the RTG model, the method of solving the equations of motion of a structure with viscoelastic components described by RT models will be seen to be a special case of the following solution technique.

The reason for developing a special solution technique for the equations of motion

$$s^2[M] \{X(s)\} + [K(s)] \{X(s)\} = \{F(s)\} \quad (97)$$

is that the normal method of decoupling the equations of motion, using modal analysis to construct an orthogonal transformation that diagonalizes the mass and stiffness matrices, is not applicable because the stiffness matrix of the structure, $[K(s)]$, contains terms that are dependent on the Laplace parameter, s .

The method of solution for Equation 97 is an extension of the method proposed by Foss to decouple the equations of motion for a structure with non-proportional viscous damping (Reference 26).

$$[M] \{\ddot{x}(t)\} + [C] \{\dot{x}(t)\} + [K] \{x(t)\} = \{f(t)\} \quad (98)$$

Non-proportional damping occurs when the damping matrix $[C]$ is not a linear combination of the mass and stiffness matrices of the structure.

$$[C] \neq a_1[M] + a_2[K] \quad (99)$$

At present there is no general method of constructing an orthogonal transformation for three, real, square, symmetric matrices when each of the matrices is not a linear combination of the remaining two. Consequently, Foss posed the equations of motion for non-proportional damping in terms of two real, symmetric matrices.

$$\frac{d}{dt} \begin{bmatrix} 0 & M \\ \text{---} & \text{---} \\ M & C \end{bmatrix} \begin{bmatrix} \dot{x} \\ x \end{bmatrix} + \begin{bmatrix} -M & 0 \\ \text{---} & \text{---} \\ 0 & K \end{bmatrix} \begin{bmatrix} \dot{x} \\ x \end{bmatrix} = \begin{bmatrix} 0 \\ \text{---} \\ f(t) \end{bmatrix} \quad (100)$$

The lower set of the partitioned matrix equations is the equations of motion of the structure and the upper set of matrix equations is satisfied identically. The equations of motion as posed in Equation 100 are readily decoupled and solved.

To solve the equations of motion of the structure containing elastic and viscoelastic components (Equation 96) the equations are posed in terms of two real, square, symmetric matrices. To begin, one multiplies the equations of motion by each distinct term appearing in the denominators of the elements of the stiffness matrix, $[K(s)]$,

$$[D(s)s^2[M] + D(s)[K(s)]] \{X(s)\} = D(s) \{F(s)\} \quad (101)$$

where

$$D(s) = \prod_{n=1}^N (1 + \sum_{k=1}^{K_n} a_{nk} s^{\beta_{nk}}) \cdot \prod_{n=1}^N (1 + \sum_{p=1}^{P_n} b_{np} s^{\hat{\beta}_{np}}) \quad (102)$$

assuming that there are N different viscoelastic materials in the structure. Multiplying $D(s)$ times $[K(s)]$, the stiffness matrix, produces a matrix, $[K_D(s)]$, that has no terms in s appearing in the denominators of its elements.

$$D(s) [K(s)] = [K_D(s)] \quad (103)$$

In fact, all of the elements of $[K_D(s)]$ are constant terms plus terms containing s raised to real, positive powers. Also note that the matrix $D(s)s^2[M]$ has elements which are sums of terms containing s raised to real, positive powers.

The equations of motion are now expressed as

$$[Z(s)] \{X(s)\} = D(s)\{F(s)\} \quad (104)$$

where

$$[Z(s)] = [D(s)s^2[M] + [K_D(s)]] \quad (105)$$

At this point in the development, the real, positive exponents of s appearing in the matrix $[Z(s)]$ are taken to be rational as well. Had any of the exponents been initially irrational, they are replaced by their rational approximations to as many significant digits as desired. Since all of the exponents in $[Z(s)]$ are rational, the matrix may be expressed as

$$[Z(s)] = [[M] \sum_{j=2m}^J c_j s^{j/m} + \sum_{\ell=1}^L [K_\ell] s^{\ell/m}] \quad (106)$$

where m is the smallest common denominator of the exponents of s in $[Z(s)]$ and

$$s^2 D(s) = \sum_{j=2m}^J c_j s^{j/m} \quad (107)$$

$$[K_D(s)] = \sum_{\ell=0}^L [K_{\ell}] s^{\ell/m} \quad (108)$$

where $[K_{\ell}]$ is symmetric and some of the $[K_{\ell}]$ and c_j appearing above may be zero.

Using Equation 106, the equations of motion of the structure become

$$[[M] \sum_{j=2m}^J c_j s^{j/m} + \sum_{\ell=0}^L [K_{\ell}] s^{\ell/m}] \{X(s)\} = D(s)\{F(s)\} \quad (109)$$

and expressed in terms of one index of summation, they are

$$\sum_{j=0}^J [[M]c_j + [K_j]] s^{j/m} \{X(s)\} = D(s)\{F(s)\} \quad (110)$$

or

$$\sum_{j=0}^J [A_j] s^{j/m} \{X(s)\} = D(s)\{F(s)\} \quad (111)$$

where

$$[A_j] = [[M]c_j + [K_j]] \quad (112)$$

and again recognizing that some of the c_j and $[K_j]$ are zero.

The equations of motion as given in Equation 111 are now posed in terms of two real, square, symmetric matrices.

$$s^{1/m} \begin{pmatrix} & & & A_J \\ ZERO & & A_J & A_{J-1} \\ & & A_J & A_{J-1} & A_{J-2} \\ & . & . & . & . & . \\ & & A_J & . & . & A_5 & A_4 & A_3 \\ A_J & A_{J-1} & . & . & . & A_4 & A_3 & A_2 \\ A_J & A_{J-1} & A_{J-2} & . & . & . & A_3 & A_2 & A_1 \end{pmatrix} \sim \begin{pmatrix} s^{\frac{J-1}{m}} X(s) \\ s^{\frac{J-2}{m}} X(s) \\ s^{\frac{J-3}{m}} X(s) \\ . \\ . \\ s^{2/m} X(s) \\ s^{1/m} X(s) \\ X(s) \end{pmatrix}$$

$$+ \begin{bmatrix} & & & & -A_J & 0. \\ & & & & -A_J & -A_{J-1} & 0. \\ & & & . & -A_{J-1} & -A_{J-2} & 0. \\ & & . & . & . & . & . \\ & . & . & . & . & . & . \\ & -A_J & -A_{J-1} & . & . & -A_4 & -A_3 & 0. \\ -A_J & -A_{J-1} & -A_{J-2} & . & . & -A_3 & -A_2 & 0. \\ 0. & 0. & 0. & . & . & 0. & 0. & A_0 \end{bmatrix} \begin{bmatrix} s^{\frac{J-1}{m}} \{X(s)\} \\ s^{\frac{J-2}{m}} \{X(s)\} \\ s^{\frac{J-3}{m}} \{X(s)\} \\ . \\ . \\ s^{2/m} \{X(s)\} \\ s^{1/m} \{X(s)\} \\ \{X(s)\} \end{bmatrix}$$

$$= \begin{bmatrix} \{0.\} \\ \{0.\} \\ \{0.\} \\ \cdot \\ \cdot \\ \cdot \\ \{0.\} \\ \{0.\} \\ D(s)\{F(s)\} \end{bmatrix} \quad (113)$$

Note that each matrix $[A_j]$, $j = 0, 1, 2, \dots, J$, is real, square, and symmetric because they are linear combinations of $[M]$ and $[K_j]$. It follows that the two matrices containing $[A_j]$ in Equation 113 are also real, square, and symmetric. Also notice that the lowest set of partitioned matrix equations in Equation 113 are the equations of motion of the structure as given by Equation 111, and that all of the upper sets of matrix equations in Equation 113 are satisfied identically.

The equations of motion as posed in Equation 113, referred to as the expanded equations of motion, can be decoupled using an orthogonal transformation. The general form of the expanded equations of motion is

$$s^2[\tilde{M}]\{\tilde{X}(s)\} + [\tilde{K}]\{\tilde{X}(s)\} = \{\tilde{F}(s)\} \quad (114)$$

which is Equation 113 expressed in more compact notation. The orthogonal transformation is constructed from the eigenvectors associated with the eigenvalue problem for the expanded equations of motion.

$$\bar{\lambda}_n[\tilde{M}]\{\tilde{\phi}_n\} + [\tilde{K}]\{\tilde{\phi}_n\} = \{0.\} \quad (115)$$

The eigenvectors $\{\tilde{\phi}_n\}$ are used to construct the orthogonal transformation matrix $[\tilde{\phi}]$ in the normal fashion, and the resulting transformation of variables is

$$\{\tilde{X}(s)\} = [\tilde{\phi}]\{a(s)\} \quad (116)$$

Substituting this transformation into Equation 14 and premultiplying the equation by $[\tilde{\phi}]^T$ produces

$$s^{1/m}[\tilde{\phi}]^T[\tilde{M}][\tilde{\phi}]\{a(s)\} + [\tilde{\phi}]^T[\tilde{K}][\tilde{\phi}]\{a(s)\} = [\tilde{\phi}]^T\{\tilde{F}(s)\} \quad (117)$$

To demonstrate that Equation 117 is, in fact, the decoupled expanded equations of motion, one uses the fact that eigenvectors of the expanded equations of motion are orthogonal with respect to $[\tilde{M}]$ and $[\tilde{K}]$.

$$\{\tilde{\phi}_j\}^T[\tilde{M}]\{\tilde{\phi}_n\} = 0. \quad j \neq n \quad (118)$$

$$\{\tilde{\phi}_j\}^T[\tilde{K}]\{\tilde{\phi}_n\} = 0. \quad j \neq n \quad (119)$$

Equation 117 then reduces to

$$s^{1/m}[\tilde{m}_n]\{a(s)\} + [\tilde{k}_n]\{a(s)\} = [\tilde{\phi}]^T\{\tilde{F}(s)\} \quad (120)$$

where $[\tilde{m}_n]$ and $[\tilde{k}_n]$ are diagonal matrices of the modal constants m_n and k_n , respectively.

$$m_n = \{\tilde{\phi}_n\}^T[\tilde{M}]\{\tilde{\phi}_n\} \quad (121)$$

$$k_n = \{\tilde{\phi}_n\}^T[\tilde{K}]\{\tilde{\phi}_n\} \quad (122)$$

Premultiplying Equation 120 by $[\tilde{m}_n]^{-1}$ or equivalently $[\tilde{m}_n^{-1}]$ yields

$$s^{1/m}[\tilde{I}]\{a(s)\} + [\tilde{m}_n^{-1}]\{a(s)\} = [\tilde{m}_n^{-1}][\tilde{\phi}]^T\{\tilde{F}(s)\} \quad (123)$$

The ratio of the n^{th} modal parameters, k_n/m_n , is minus the n^{th} eigenvalue of the expanded equations of motion.

$$k_n/m_n = -\tilde{\lambda}_n \quad (124)$$

Premultiplying Equation 115 by $\{\phi_n\}^T$ produces

$$\tilde{\lambda}_n \{\tilde{\phi}_n\}^T [\tilde{M}] \{\phi_n\} + \{\tilde{\phi}_n\}^T [\tilde{K}] \{\phi_n\} = 0 \quad (125)$$

$$\tilde{\lambda}_n m_n + k_n = 0 \quad (126)$$

from which Equation 124 follows. As a result, the equations of motion can be further simplified to

$$s^{1/m} [-I] \{a(s)\} - [\tilde{\lambda}_n] \{a(s)\} = [-\frac{1}{m_n}] [\tilde{\phi}]^T \{\tilde{F}(s)\} \quad (127)$$

From Equation 127 it follows that the expression for the Laplace transform of the n^{th} modal coefficient, $a_n(s)$, is

$$a_n(s) = \frac{\{\tilde{\phi}_n\}^T \{\tilde{F}(s)\}}{m_n (s^{1/m} - \tilde{\lambda}_n)} \quad (128)$$

This expression for the modal coefficient can be further simplified by noting the general form of the eigenvector $\{\tilde{\phi}_n\}$ associated with the expanded equations of motion

$$\{\tilde{\phi}_n\} = \begin{bmatrix} \tilde{\lambda}_n^{J-1} \{\phi_n\} \\ \tilde{\lambda}_n^{J-2} \{\phi_n\} \\ \tilde{\lambda}_n^{J-3} \{\phi_n\} \\ \vdots \\ \lambda_n^2 \{\phi_n\} \\ \lambda_n \{\phi_n\} \\ \{\phi_n\} \end{bmatrix} \quad (129)$$

where $\{\phi_n\}$ and $\tilde{\lambda}_n$ are the solutions of the eigenvalue problem associated with the original equations of motion in the form of Equation 111.

$$\left[\sum_{j=0}^J [A_j] \tilde{\lambda}_n^j \right] \{\phi_n\} = \{0.\} \quad n = 1, 2, 3, \dots, N \quad (130)$$

The general form of the n^{th} eigenvector, $\{\phi_n\}$, can be verified by direct substitution in Equation 115 when $[\tilde{M}]$ and $[\tilde{K}]$ are expressed in terms of the matrices $[A_j]$ as indicated in Equation 113. The lowest set of resulting partitioned matrix equations produces Equation 130, and the upper sets of the partitioned matrix equations are satisfied identically. Consequently, the numerator of the n^{th} modal coefficient, $\{\phi_n\}^T \{\tilde{F}(s)\}$, is

$$\{\tilde{\phi}_n\}^T \{\tilde{F}(s)\} = \begin{matrix} \sim \\ \sim \end{matrix} \begin{bmatrix} \tilde{\lambda}_n^{J-1} \{\phi_n\} \\ \tilde{\lambda}_n^{J-2} \{\phi_n\} \\ \tilde{\lambda}_n^{J-3} \{\phi_n\} \\ \vdots \\ \tilde{\lambda}_n \{\phi_n\} \\ \tilde{\lambda}_n \{\phi_n\} \\ \{\phi_n\} \end{bmatrix}^T \begin{matrix} \sim \\ \sim \end{matrix} \begin{bmatrix} \{0.\} \\ \{0.\} \\ \{0.\} \\ \vdots \\ \{0.\} \\ \{0.\} \\ D(s)\{F(s)\} \end{bmatrix} \quad (131)$$

or

$$\{\tilde{\phi}_n\}^T \{\tilde{F}(s)\} = \{\phi_n\}^T \{F(s)\} D(s) \quad (132)$$

and the n^{th} modal coefficient reduces to

$$a_n(s) = \frac{\{\phi_n\}^T \{F(s)\} D(s)}{m_n(s)^{1/m-\lambda_n}} \quad (133)$$

The Laplace transform of the displacement response of the structures follows from Equation 116 and takes the form

$$\{X(s)\} = \sum_{n=1}^N a_n(s) \{\phi_n\} \quad (134)$$

or

$$\{X(s)\} = \sum_{n=1}^N \frac{\{\phi_n\}^T \{F(s)\} D(s)}{m_n(s)^{1/m-\lambda_n}} \{\phi_n\} \quad (135)$$

where N is the order of the matrices $[\tilde{M}]$ and $[\tilde{K}]$ in the expanded equations of motion.

The order of the expanded equations, N , can be very large. From Equation 113 it is clear that the order of the expanded equations of motion is equal to δ , the order of the matrices $[A_j]$, times J where J is defined in Equation 107.

$$N = \delta \cdot J \quad (136)$$

From Equation 107, it is clear that J/m is the largest exponent in the expression $s^2 D(s)$ which is $2 + \beta$, where β is the largest exponent in $D(s)$. Therefore,

$$J = m(2+\beta) \quad (137)$$

and the order of the expanded equations is seen to be

$$N = \delta m(2+\beta) \quad (138)$$

Note that if m , the smallest common denominator of the rational exponents of s , in the original equations of motion is large, the order of the expanded equations is quite large for a structure with anything more than a very modest number of degrees of freedom. However, the solutions to the

expanded equations of motion can be obtained by using numerical methods that do not involve the manipulation of the expanded equations, as will be shown in the following section.

Before proceeding, it should be pointed out that the equations of motion of a structure containing both elastic and viscoelastic components can be solved given that a finite element formulation of the equations of motion is possible and that an RT or RTG model exists for each viscoelastic material in the structure. The general form of the solution technique for the equations of motion containing only RT models for the viscoelastic components is identical to the above development except that $D(s)$ is set equal to one.

SECTION VIII

CALCULATING THE LAPLACE TRANSFORM
OF THE STRUCTURAL RESPONSE

At this point, it is clear that solutions to the equations of motion for the structure containing elastic and viscoelastic components

$$\{X(s)\} = \sum_{n=1}^N \frac{\{\phi_n\}^T \{F(s)\} D(s)}{m_n (s^{1/m} - \tilde{\lambda}_n)} \{\phi_n\} \quad (135)$$

are difficult to calculate from the expanded equations of motion, because of the large order of the matrices in the expanded equations. As a result, an alternative method of obtaining the solutions is required if the finite element formulation of the equations of motion using generalized derivative models is to be a useful tool to the engineer.

The alternative method adopted here is a combination of iterative schemes used to obtain the eigenvalues, $\tilde{\lambda}_n$, and eigenvectors, $\{\phi_n\}$, associated with the original equations of motion.

$$\left[\sum_{j=0}^J [A_j] \tilde{\lambda}_n^j \right] \{\phi_n\} = \{0\} \quad , \quad n = 1, 2, 3, \dots, N \quad (130)$$

Recall that the number of distinct homogeneous solutions to the equations of motion, N , is dependent on the smallest common denominator of the exponents in the equations of motion, m ; the largest exponent in the product of the denominators terms of the Laplace transform of the RTG models in the equations of motion, β ; and the number of degrees of freedom of the structure, δ .

$$N = \delta m (2 + \beta) = 2m\delta + \beta m\delta \quad (138)$$

Using an iterative scheme based on the homogeneous form of the equations of motion in Equation 96, $2\delta m$ of the homogeneous solutions are obtained.

$$[\tilde{\lambda}_n^{2m}[M] + [K(\tilde{\lambda}_n)]\{\phi_n\}] = \{0.\} \quad (139)$$

The iteration for the solutions centers on calculating successive estimates of $\tilde{\lambda}_n$ and $\{\phi_n\}$ using the scheme

$$[\tilde{\lambda}_n^{2m(p+1)}[M] + [K(\tilde{\lambda}_n^{(p)})]]\{\phi_n\}^{(p+1)} = \{0.\} \quad (140)$$

$\tilde{\lambda}_n^{(p)}$ is the p^{th} estimate of $\tilde{\lambda}_n$. $\tilde{\lambda}_n^{2m(p+1)}$ is the $(p+1)^{\text{th}}$ estimate of $\tilde{\lambda}_n^{2m}$ and $\{\phi_n\}^{(p+1)}$ is the $(p+1)^{\text{th}}$ estimate of $\{\phi_n\}$.

Given a value of $\tilde{\lambda}_n^{(p)}$, the $(p+1)^{\text{th}}$ estimates of $\tilde{\lambda}_n^{2m}$ and $\{\phi_n\}$ may be calculated using matrix iteration or any other method that is appropriate to obtain the solution to the eigenvalue problem

$$[B]\{\phi\} = \mu\{\phi\} \quad (141)$$

where B is complex. Note that Equation 140 can be expressed as

$$[K(\tilde{\lambda}_n^{(p)})]^{-1}[M]\{\phi_n\}^{(p+1)} = -\frac{1}{\tilde{\lambda}_n^{2m(p+1)}}\{\phi_n\}^{(p+1)} \quad (142)$$

which is of the same general form as Equation 141.

The iterative scheme as it appears in Equation 142 is only useful in obtaining the eigenvalue with the smallest magnitude, $\tilde{\lambda}_1$, and the associated eigenvector, $\{\phi_1\}$. To obtain the other eigenvalues and eigenvectors, the iteration scheme is modified to allow the scheme to converge on the larger eigenvalues and associated eigenvectors. For instance, the scheme used to obtain the L^{th} eigenvalue, $\tilde{\lambda}_L$, and the L^{th} eigenvector, $\{\phi_L\}$, is (Reference 27)

$$\begin{aligned}
 & \left[[K(\tilde{\lambda}_L^{(P)})]^{-1} + \sum_{\ell=1}^L \frac{\{\psi_\ell\}^{(P)} \{\psi_\ell\}^{(P)T}}{\Lambda_\ell^{2m(P)}} \right] [M] \{\phi_L\}^{(P+1)} \\
 & = - \frac{1}{\tilde{\lambda}_L^{2m(P+1)}} \{\phi_L\}^{(P+1)} \quad (143)
 \end{aligned}$$

The terms in the summation on the index ℓ subtract the components of the first $L - 1$ eigenvectors, associated with eigenvalue problem,

$$[K(\tilde{\lambda}_L^{(P)})]^{-1} [M] \{\psi_\ell\}^{(P)} = - \frac{1}{\Lambda_\ell^{2m(P)}} \{\psi_\ell\}^{(P)} \quad \ell=1, 2, 3, \dots, L-1 \quad (144)$$

from the successive approximations of $\{\phi_L\}^{(P+1)}$ calculated when matrix iteration is used to solve Equation 143.

Given that matrix iteration has successfully produced $\tilde{\lambda}_L^{2m}$ and $\{\phi_L\}^{(P+1)}$, one can take advantage of the orthogonality of the mode shapes

$$\{\psi_\ell\}^{(P)T} [M] \{\phi_L\}^{(P+1)} = 0. \quad \ell=1, 2, \dots, L-1 \quad (145)$$

to demonstrate that

$$\sum_{\ell=1}^L \frac{\{\psi_\ell\}^{(P)}}{\Lambda_\ell^{2m(P)}} \{\psi_\ell\}^{(P)T} [M] \{\phi_L\}^{(P+1)} = \{0.\} \quad (146)$$

and Equation 143 reduces to

$$[K(\tilde{\lambda}_L^{(P)})]^{-1} [M] \{\phi_L\}^{(P+1)} = - \frac{1}{\tilde{\lambda}_L^{2m(P+1)}} \{\phi_L\}^{(P+1)} \quad (147)$$

Thus, $\{\phi_L\}^{(P+1)}$ and $\tilde{\lambda}_L^{2m(P+1)}$ are in fact the $(p + 1)^{th}$ approximation of the solution to the equations of motion.

On the other hand, $\{\psi_\ell\}^{(P)}$ and $\Lambda_\ell^{(P)}$, $\ell = 1, 2, \dots, L-1$, are not in any sense approximations of the solutions to the equations of motion. However, they are the first $L-1$ eigenvalues and eigenvectors associated with Equation 147. This can be seen by comparing Equation 144 with Equation 147. $\{\psi_\ell\}^{(P)}$ and $\Lambda_\ell^{(P)}$ can be calculated using matrix iteration.

Notice that in continuing the iterative processes in Equation 140 or 143 the $(P+2)^{\text{th}}$ approximations of the solution, $\tilde{\lambda}_n^{2m(P+2)}$ and $\{\phi_n\}^{(P+2)}$, are based on the value of $\tilde{\lambda}_n^{(P+1)}$. However, the function $Z^{1/2m}$ has $2m$ branches. Given a value of $\tilde{\lambda}_n^{2m(P+1)}$, one can calculate $2m$ values of $\tilde{\lambda}_n^{(P+1)}$, one value for each branch of $Z^{1/2m}$.

So, when using Equations 140 and 143 to obtain solutions of the equations of motion, it is necessary to choose one branch of $Z^{1/2m}$ to calculate the δ eigenvalues and δ eigenvectors. Then another branch of $Z^{1/2m}$ is chosen and δ other solutions are obtained. This process is continued until all $2m$ branches have each been used to calculate δ solutions producing a total of $2m\delta$ homogeneous solutions to the equations of motion. The general form of the equations that has these $2m\delta$ homogeneous solutions is

$$[\tilde{\lambda}_j^{2m}(k)[M] + [K(\tilde{\lambda}_j(k))]]\{\phi_j(k)\} = \{0\} \quad \begin{matrix} j=1, 2, \dots, \delta \\ k=1, 2, \dots, 2m \end{matrix} \quad (148)$$

where the subscript k denotes the branch of $Z^{1/2m}$ on which the relation

$$(\tilde{\lambda}_j^{2m}(k))^{1/2m} = \tilde{\lambda}_j(k) \quad (149)$$

is valid.

The remaining $\beta m \delta$ of the N homogeneous solutions to the equations of motion are determined using Equation 138, an iterative scheme based on the homogeneous form of Equation 109.*

$$[[M] \sum_{j=2m}^J c_j \tilde{\lambda}_n^j + \sum_{\ell=0}^L [K_\ell] \tilde{\lambda}_k^\ell] \{\phi_n\} = \{0.\} \quad (150)$$

The iterative scheme is

$$[[M] (c_J \tilde{\lambda}_n^{(P+1)} \tilde{\lambda}_n^{J-1(P)} + \sum_{j=2m}^{J-1} \tilde{\lambda}_n c_j \tilde{\lambda}_n^j)^{(P)} + \sum_{\ell=0}^L [K_\ell] \tilde{\lambda}_n^\ell] \{\phi_n\}^{(P+1)} = \{0.\} \quad (151)$$

or, in more compact form

$$[[M] Q(\tilde{\lambda}_n^{(P+1)}, \tilde{\lambda}_n^{(P)}) + [K_D(\tilde{\lambda}_n^{(P)})]] \{\phi_n\}^{(P+1)} = \{0.\} \quad (152)$$

where, as before, $\tilde{\lambda}_n^{(P)}$ is the P^{th} estimate of the eigenvalue, $\tilde{\lambda}_n^{(P+1)}$ is the $(P+1)^{\text{th}}$ estimate of the eigenvalue and $\{\phi_n\}^{(P+1)}$ is the $(P+1)^{\text{th}}$ estimate of the eigenvector. Given a value for $\tilde{\lambda}_n^{(P)}$, one can calculate $\{\phi_n\}^{(P+1)}$ and $Q(\tilde{\lambda}_n^{(P+1)}, \tilde{\lambda}_n^{(P)})$ using matrix iteration or any other method suitable for the solution of Equation 141. Equation 152, expressed in the form of Equation 141, is

$$[K_D(\tilde{\lambda}_n^{(P)})]^{-1} [M] \{\phi_n\}^{(P+1)} = - \frac{1}{Q(\tilde{\lambda}_n^{(P+1)}, \tilde{\lambda}_n^{(P)})} \{\phi_n\}^{(P+1)} \quad (153)$$

*Note that, if the equations of motion contain only RT models for the viscoelastic materials, that $D(s)$ is one and β , the largest exponent of s in $D(s)$, is zero. Hence, the total number of homogeneous solution, N , is $2m\delta$ as seen by Equation 138. Since Equations 140 and 143 provided $2m\delta$ solutions, one can return to Equation 136 and calculate structural responses.

At this point, the numerical value of $Q(\tilde{\lambda}_n^{(P+1)}, \lambda_n^{(P)})$ from Equation 153 is used to calculate $\tilde{\lambda}_n^{(P+1)}$ with the relation

$$Q(\tilde{\lambda}_n^{(P+1)}, \tilde{\lambda}_n^{(P)}) = c_J \tilde{\lambda}_n^{(P+1)} \tilde{\lambda}_n^{J-1(P)} + \sum_{j=2m}^J c_j \tilde{\lambda}_n^{(P)} \quad (154)$$

which follows from Equation 151 and 152. However, this method of calculating $\tilde{\lambda}_n^{(P+1)}$ assumes that $\tilde{\lambda}_n^{(P+1)}$ are both on the principal branch of $(\tilde{\lambda}_n^{\beta m})^{1/\beta m}$. The method of calculating $\tilde{\lambda}_n^{(P+1)}$ assuming that $\tilde{\lambda}_n^{(P+1)}$ and $\tilde{\lambda}_n^{(P)}$ are both on the k^{th} branch of $(\tilde{\lambda}_n^{\beta m})^{1/\beta m}$ is

$$\left(\left(\frac{Q(\tilde{\lambda}_{n(k)}^{(P+1)}, \tilde{\lambda}_{n(k)}^{(P)}) - \sum_{j=1}^J c_j \tilde{\lambda}_{n(k)}^{(P)}}{c_J \tilde{\lambda}_{n(k)}^{J-1(P+1)}} \right)^{\beta m} \right)^{1/\beta m} = \tilde{\lambda}_{n(k)}^{(P+1)} \quad (155)$$

where the k^{th} branch of $Z^{1/\beta m}$ is used to calculate $\tilde{\lambda}_{n(k)}^{(P+1)}$.

The resulting form of the iteration process is

$$\begin{aligned} [K_D(\tilde{\lambda}_{n(k)}^{(P)})]^{-1} [M] \{\phi_{n(k)}\}^{(P+1)} \\ = - \frac{1}{Q(\tilde{\lambda}_{n(k)}^{(P+1)}, \tilde{\lambda}_{n(k)}^{(P)})} \{\phi_{n(k)}\}^{(P+1)} \end{aligned} \quad (156)$$

where successive estimates of $\tilde{\lambda}_{n(k)}$ are calculated using $Q(\tilde{\lambda}_{n(k)}^{(P+1)}, \tilde{\lambda}_{n(k)}^{(P)})$ from Equation 156 and then using Equation 155 to calculate $\tilde{\lambda}_{n(k)}^{(P+1)}$. When using matrix iteration to solve for $Q(\tilde{\lambda}_{n(k)}^{(P+1)}, \tilde{\lambda}_{n(k)}^{(P)})$ and $\{\phi_{n(k)}\}^{(P+1)}$ in Equation 156, one usually obtains only the Q with the smallest magnitude and its associated eigenvector, $\{\phi_1(k)\}$.

To obtain successive estimates of the other Q 's with larger magnitudes and their associated eigenvectors, the iteration scheme

is modified as before. The iterative scheme that yields $Q(\tilde{\lambda}_{L(k)}^{(P+1)}, \tilde{\lambda}_{L(k)}^{(P)})$ and $\{\phi_{L(k)}\}$ is

$$\left[[K_D(\tilde{\lambda}_{L(k)}^{(P)})]^{-1} + \sum_{\ell=1}^{L-1} \frac{\{\psi_{\ell(k)}\}^{(P)} \{\psi_{\ell(k)}\}^{(P)T}}{Q(\Lambda_{\ell(k)}^{(P+1)}, \Lambda_{\ell(k)}^{(P)})} \right] [M] \{\phi_{L(k)}\}^{(P+1)} \\ = - \frac{1}{Q(\tilde{\lambda}_{L(k)}^{(P+1)}, \tilde{\lambda}_{L(k)}^{(P)})} \{\phi_{L(k)}\}^{(P+1)} \quad (157)$$

where $Q(\Lambda_{\ell(k)}^{(P+1)}, \Lambda_{\ell(k)}^{(P)})$ and $\{\psi_{\ell(k)}\}^{(P)}$ are the solutions to

$$[K_D(\tilde{\lambda}_{L(k)}^{(P)})]^{-1} [M] \{\psi_{\ell(k)}\}^{(P)} = - \frac{1}{Q(\Lambda_{\ell(k)}^{(P+1)}, \Lambda_{\ell(k)}^{(P)})} \{\psi_{\ell(k)}\}^{(P)} \quad (158)$$

having the $L-1$ smallest values of Q . The values of $Q(\Lambda_{\ell(k)}^{(P+1)}, \Lambda_{\ell(k)}^{(P)})$ and $\{\psi_{\ell(k)}\}^{(P)}$ can be obtained using matrix iteration.

Using Equations 155, 156, and 157, $\beta\delta m$ homogeneous solutions to the equations of motion are obtained for each branch of $Z^{1/\beta m}$. Since there are βm branches of $Z^{1/\beta m}$, the iteration process should produce $\beta m \delta$ homogeneous solutions. These homogeneous solutions satisfy the homogeneous equations of motion.

$$[[M] \sum_{j=2m}^J c_j \tilde{\lambda}_P^j(k) + \sum_{\ell=0}^L [K_{\ell}] \tilde{\lambda}_P^{\ell}(k)] \{\phi_P(k)\} = \{0.\} \quad \begin{matrix} p=1,2,\dots,\delta \\ k=1,2,\dots,\beta m \end{matrix} \quad (159)$$

The two iterative schemes used to obtain the N solutions to the homogeneous equations are considered to have converged when successive approximations of $\tilde{\lambda}_{n(k)}^{(P)}$ and $\tilde{\lambda}_{n(k)}^{(P+1)}$ are approximately the same complex number.

$$\frac{\tilde{\lambda}_{n(k)}^{(P+1)}}{\tilde{\lambda}_{n(k)}^{(P)}} = 1.0 \quad (160)$$

The general convergence criteria of the iterative schemes are considered beyond the scope of this investigation; however, the schemes have converged for numerous structures considered by the author. Homogeneous solutions for an example problem, calculated using the iterative scheme given above appear in Table 2.

Note that all of the parameters of the Laplace transform of the structure's response are determined, except the modal constant m_n defined by Equation 121.

$$m_n = \{\tilde{\phi}_n\}^T [M] \{\tilde{\phi}_n\} \quad (121)$$

The eigenvector of the expanded equations of motion, $\{\tilde{\phi}_n\}$, can be constructed from the n^{th} eigenvalue and associated eigenvector of the original equations of motion, $\tilde{\lambda}_n$ and $\{\phi_n\}$, using the relation given in Equation 129. This, coupled with the general form of $[M]$ given in Equation 113, produces an expression for m_n which takes the form

$$m_n = \{\phi_n\}^T \left[\sum_{j=1}^J j \cdot \tilde{\lambda}_n^{j-1} [A_j] \right] \{\phi_n\} \quad (60)$$

The modal constant of the expanded equations of motion, m_n , can be calculated without manipulating the expanded equations of motion.

In conclusion, all of the parameters in the general form of the Laplace transform of the structure's response can be calculated without manipulating the expanded equations of motion, given that the iterative schemes outlined above converge.

TABLE 2
HOMOGENEOUS SOLUTIONS OBTAINED USING
THE PROPOSED ITERATIVE SCHEMES FOR AN EXAMPLE PROBLEM

$$[M] = \begin{bmatrix} .3300 & .0825 \\ .0825 & .3300 \end{bmatrix}$$

$$[K(s)] = \begin{bmatrix} 4.0 + \frac{0.2 + 0.2s^2}{1.0 + 0.1s^2} & -2.0 \\ -2.0 & 4.0 + \frac{0.01 + 0.01s^2}{1.0 + 0.1s^2} \end{bmatrix}$$

Using Equations 140 and 143

$$\tilde{\lambda}_{1(1)} = 1.071768 + i 1.099794 \quad \{\phi_{1(1)}\} = \begin{Bmatrix} 1.000 + i 0.0 \\ 1.040 + i 0.0165 \end{Bmatrix}$$

$$\tilde{\lambda}_{1(2)} = 1.073498 + i 1.028611 \quad \{\phi_{1(2)}\} = \begin{Bmatrix} 1.000 + i 0.0 \\ 1.001 + i 0.0238 \end{Bmatrix}$$

$$\tilde{\lambda}_{1(4)} = 1.073498 - i 1.028611 \quad \{\phi_{1(3)}\} = \begin{Bmatrix} 1.000 + i 0.0 \\ 1.001 - i 0.0238 \end{Bmatrix}$$

$$\tilde{\lambda}_{1(5)} = 1.071768 - i 1.099794 \quad \{\phi_{1(4)}\} = \begin{Bmatrix} 1.000 + i 0.0 \\ 1.040 - i 0.0165 \end{Bmatrix}$$

$$\tilde{\lambda}_{2(1)} = 1.581998 + i 1.601989 \quad \{\phi_{2(1)}\} = \begin{Bmatrix} 1.000 + i 0.0 \\ -.9713 + i 0.0120 \end{Bmatrix}$$

$$\tilde{\lambda}_{2(2)} = -1.584631 + i 1.547150 \quad \{\phi_{2(2)}\} = \begin{Bmatrix} 1.000 + i 0.0 \\ -1.002 + i 0.0240 \end{Bmatrix}$$

TABLE 2 (Continued)

$$\tilde{\lambda}_{2(4)} = -1.584631 - i 1.547150 \quad \{\phi_{2(3)}\} = \begin{Bmatrix} 1.000 + i 0.0 \\ -1.003 - i 0.0240 \end{Bmatrix}$$

$$\tilde{\lambda}_{2(5)} = 1.581998 - i 1.601989 \quad \{\phi_{2(4)}\} = \begin{Bmatrix} 1.000 + i 0.0 \\ -.971 - i 0.0120 \end{Bmatrix}$$

Using Equations 156, 157, and 158

$$\tilde{\lambda}_{1(3)} = -9.997418 + i 0.0 \quad \{\phi_{1(3)}\} = \begin{Bmatrix} 1.000 + i 0.0 \\ 4.462 + i 0.0 \end{Bmatrix}$$

$$\tilde{\lambda}_{2(3)} = -9.99385 + i 0.0 \quad \{\phi_{2(3)}\} = \begin{Bmatrix} 1.000 + i 0.0 \\ -0.448 + i 0.0 \end{Bmatrix}$$

SECTION IX

THE EXISTENCE OF THE STRUCTURAL
RESPONSE TO IMPULSIVE LOADING

Of particular interest at this juncture is whether or not the inverse transform of the Laplace transform of the structure's displacement response for impulsive loading exists. In fact, the inverse transform always exists and is real, continuous, and causal.

To demonstrate this, one starts with the general form of the transform of the structural response.

$$\{X(s)\} = \sum_{n=1}^N \frac{\{\phi_n\}^T \{F(s)\} D(s)}{m_n(s^{1/m_n - \tilde{\lambda}_n})} \{\phi_n\} \quad (135)$$

For simultaneous unit, impulsive loading at the structure's degrees of freedom, the column vector of applied forces is

$$\{f(t)\} = \delta(t)\{1.\} \quad (161)$$

where $\{1.\}$ is a column vector of ones. The Laplace transform of the column vector of forces is

$$\{F(s)\} = \{1.\} \quad (162)$$

and the transform of the response for the impulsive loading is

$$\{\hat{X}(s)\} = \sum_{n=1}^N \frac{\{\phi_n\}^T \{1.\} D(s)}{m_n(s^{1/m_n - \tilde{\lambda}_n})} \{\phi_n\} \quad (163)$$

The inverse transform of this expression always exists, which follows from a theorem on the existence of the inverse transform (Reference 28). Paraphrasing the theorem in terms of the notation used above; it states that the inverse transform of $\{\hat{X}(s)\}$ exists and is real, continuous, and causal when

1. $\{\hat{X}(s)\}$ is analytic for $\text{Re}[s] > 0$,

2. $\{\hat{X}(s)\}$ is real for s real and positive, and
3. $\{\hat{X}(s)\}$ is order $s^{-\gamma}$, where $\gamma > 1$, for s large in the right half s plane.

$\{\hat{X}(s)\}$ is analytic for $\text{Re}[s] > 0$ when the branch cut of $s^{1/m}$ is chosen to lie along the negative, real axis in the s plane and the poles of $\{\hat{X}(s)\}$, which occur at

$$s = \tilde{\lambda}_n^m \quad (164)$$

and do not appear in the right half s plane.*

$\{\hat{X}(s)\}$ is real for s real and positive. The only quantities appearing in Equation 163 that can be complex are $\{\phi_n\}$, $\tilde{\lambda}_n$ and m_n , because $D(s)$ and $s^{1/m}$ are real for s real and positive. When $\{\phi_n\}$, $\tilde{\lambda}_n$ and m_n are complex, they occur in conjugate pairs. Note if $\tilde{\lambda}_n$ and $\{\phi_n\}$ are a homogeneous solution to the equations of motion

$$\left[\sum_{j=1}^J [A_j] \tilde{\lambda}_n^j \right] \{\phi_n\} = \{0.\} \quad (130)$$

where $\tilde{\lambda}_n$ and $\{\phi_n\}$ are complex, that their conjugates are homogeneous solutions to the equations of motion.

$$\left[\sum_{j=1}^J [A_j] \overline{\tilde{\lambda}_n^j} \right] \overline{\{\phi_n\}} = \{0.\} \quad (165)$$

Equation 165 follows directly from the complex conjugate of Equation 130. Since homogeneous solutions occur in conjugate pairs, the modal constant m_n occurs in conjugate pairs.

$$m_n = \{\phi_n\}^T \left[\sum_{j=1}^J j \cdot \tilde{\lambda}_n^{j-1} [A_j] \right] \{\phi_n\} \quad (160)$$

*A pole in the right half s plane indicates that an RT or RTG model in the equations of motion characterizes the viscoelastic material as generating energy instead of dissipating energy.

$$\bar{m}_n = \{\bar{\phi}_n\}^T \left[\sum_{j=1}^J j \cdot \bar{\lambda}_n^{j-1} [A_j] \right] \{\bar{\phi}_n\} \quad (166)$$

It follows directly that when the terms in Equation 163 are complex, they occur in complex conjugate pairs and $\{\hat{X}(s)\}$ is real for s real and positive.

$\{\hat{X}(s)\}$ also satisfies the third and last condition placed on the transform. To show that $\{\hat{X}(s)\}$ is order s^{-2} for s large in the right half s plane, one uses the transformed equations of motion as they appear in Equation 97.

$$s^2[M]\{X(s)\} + [K(s)]\{X(s)\} = \{F(s)\} \quad (97)$$

The transformed equations of motion for simultaneous, unit impulsive loading is

$$[s^2[M] + [K(s)]]\{X(s)\} = \{1.\} \quad (167)$$

The only terms in $[K(s)]$, other than the constant terms, are those terms proportional to $\mu^*(s)$ and $\lambda^*(s)$ from the RT and/or RTG models of the viscoelastic materials. The general forms of $\mu^*(s)$ and $\lambda^*(s)$ appear in Equation 62 for the RTG model and Equation 63 for the RT model. As a direct result of the general forms of $\mu^*(s)$ and $\lambda^*(s)$, Equation 167 reduces to

$$s^2[M]\{X(s)\} \approx \{1.\} \quad (168)$$

for s large. Since the elements in the mass matrix are constant, $\{\hat{X}(s)\}$ must be order s^{-2} . Therefore, $\{\hat{X}(s)\}$ is order s^{-2} for s large in the right half s plane.

Having now established that response of the structure to impulsive loading, $\{\hat{x}(t)\}$,

$$\{\hat{x}(t)\} = L^{-1}\{\hat{X}(s)\} \quad (169)$$

AFML-TR-79-4103

exists and is real, continuous, and causal, the next issue to be addressed is the calculation of the inverse transform, the topic of the next section.

SECTION X

CALCULATING THE RESPONSE TO IMPULSIVE LOADING

The final step in determining the impulse response of the structure is to calculate the inverse transform of the Laplace transform of the response to impulsive loading.

$$\{\hat{X}(t)\} = L^{-1}\{\hat{X}(s)\} = L^{-1} \sum_{n=1}^N \frac{\{\phi_n\}^T \{1.\} D(s)}{m_n (s^{1/m} - \tilde{\lambda}_n)} \{\phi_n\} \quad (170)$$

The inverse transform integral

$$L^{-1}\{\hat{X}(s)\} = \frac{1}{2\pi i} \int_{\gamma-i\infty}^{\gamma+i\infty} e^{st} \{\hat{X}(s)\} ds \quad (171)$$

is evaluated using the residue theorem from the calculus of a complex variable.

The closed contour of integration, used in conjunction with the residue theorem, is given in Figure 18. The contour is divided into six segments and the direction of integration along each segment is indicated by the arrows. Segments 3, 4, and 5 of the contour are required, because the branch cut and branch point of the function $s^{1/m}$ are taken to be along the negative real axis and at the origin of the s plane, respectively.

The residue theorem states that the integral along the closed contour, divided by $2\pi i$, is equal to the sum of the residues of the poles of the poles of the integrand. In this case, the statement of the residue theorem translates into

$$\frac{1}{2\pi i} \int_1 \{\hat{X}(s)\} e^{st} ds = - \frac{1}{2\pi i} \sum_{k=2}^6 \int_k \{\hat{X}(s)\} e^{st} ds + \sum_j b_j \quad (172)$$

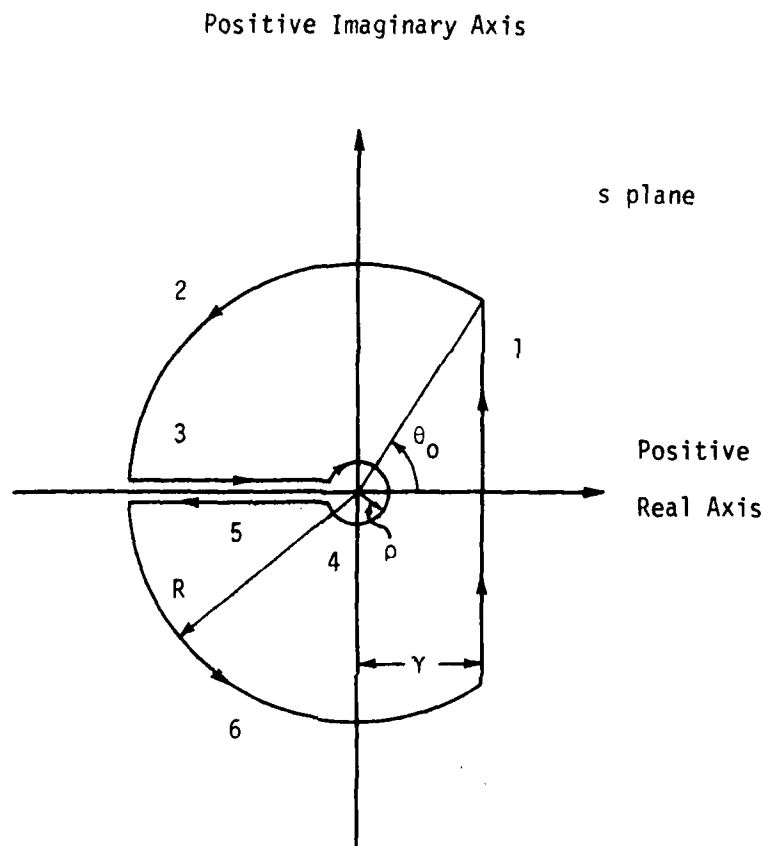


Figure 18. The Contour of Integration Used to Evaluate the Inverse Transform

where the circled index indicates the contour over which the integration is to be performed, and b_j are the residues of the poles of $\{\hat{X}(s)\}$ enclosed by the contour.

The integrals on the segments of the closed contour are evaluated for the case where the length of segment 1 is extended indefinitely in the positive and negative imaginary directions.

$$\int_1 \{\hat{X}(s)\} e^{st} ds = \int_{\gamma-i\infty}^{\gamma+i\infty} \{\hat{X}(s)\} e^{st} ds \quad (173)$$

and, as a result, Equation 171 becomes

$$\frac{1}{2\pi i} \int_{\gamma-i\infty}^{\gamma+i\infty} \{\hat{X}(s)\} e^{st} ds = - \frac{1}{2\pi i} \sum_{k=2}^6 \int \{\hat{X}(s)\} e^{st} ds + \sum_j b_j \quad (174)$$

showing that one need evaluate the right side of Equation 174 to obtain the inverse transform.

To maintain the continuity of the closed contour, the radii of segments 2 and 6 are increased indefinitely, and segments 3 and 5 are extended indefinitely in the negative real direction. When the radii of contours 2 and 6 are increased indefinitely, it can be demonstrated that the resulting value of the integrals along these two segments is zero. This follows directly from the fact that, for large s , $\{\hat{X}(s)\}$ is order s^{-2} . Hence, the l^{th} component of $\{\hat{X}(s)\}$ is order s^{-2}

$$\hat{X}_l(s) \sim \frac{c_l}{s^2} \quad |s| \gg 1 \quad (175)$$

Therefore, the asymptotic expression the integral on segment 2 as its radius increases is

$$\int_2 \hat{X}_l(s) e^{st} ds \sim \int_{\text{Re } i\theta_0}^{\text{Re } i\pi} c_l \frac{e^{st}}{s^2} ds \quad (176)$$

Expressing s in polar notation, the relation is

$$\int_2 \hat{X}_\ell(s) e^{st} ds \sim \int_{\theta_0}^{\pi} c_\ell \frac{e^{Re^{i\theta}t}}{R^2 e^{i2\theta}} R i e^{i\theta} d\theta \quad (177)$$

$$|s| \gg 1$$

The magnitude of an integral is less than or equal to the maximum value of the magnitude of the integrands, M , times the length of the path of integration, L .

$$\left| \int_{\theta_0}^{\pi} c_\ell \frac{e^{Re^{i\theta}t}}{R^2 e^{i2\theta}} R i e^{i\theta} d\theta \right| \leq M \cdot L \quad (178)$$

The maximum value of the magnitude of the integral is

$$M = \frac{|c_\ell| e^{\gamma t}}{R} \quad (179)$$

and the length of the path of integration in radians is

$$L = \pi - \theta_0 \quad (180)$$

The resulting bound for the magnitude of the integral is

$$M \cdot L = \frac{|c_\ell| e^{\gamma t}}{R} \quad (181)$$

which is clearly zero for finite time in the limit as R becomes large or equivalently, in the limit as s becomes large. Since the magnitude of the integral is zero, both the real and imaginary parts of the integral are zero.

$$\lim_{R \rightarrow \infty} \int_2 \hat{X}(s) e^{st} ds = 0. + i0. \quad (182)$$

The expression for the magnitude of the integral along segment 6 is

$$\left| \int_{-\pi}^{-\theta_0} c_\ell \frac{e^{Re^{i\theta}t}}{R^2 e^{i2\theta}} Re^{i\theta} i d\theta \right| \leq M \cdot L \quad (183)$$

and the proof that

$$\lim_{R \rightarrow \infty} \int_6 \hat{X}_\ell(s) e^{st} ds = 0. + i0. \quad (184)$$

follows the steps given in Equations 179 through 181.

The integral along segment 4 of the contour is evaluated for the case where the radius of the contour shrinks to zero. The asymptotic expression for the integrand, the ℓ^{th} component of Equation 163, for small s is

$$\hat{X}_\ell(s) \sim \sum_{n=1}^N \frac{\{\phi_n\}^T \{1.\}}{m_n(-\tilde{\lambda}_n)} \phi_{n\ell}$$

$$|s| \ll 1$$

$$|1| \ll |\tilde{\lambda}_n| \quad (185)$$

where $\phi_{n\ell}$ is the ℓ^{th} component of $\{\phi_n\}$, and

$$D(s) \sim 1.$$

$$|s| \ll 1 \quad (186)$$

and

$$\frac{1}{s^{1/m-\tilde{\lambda}_n}} \frac{1}{(-\tilde{\lambda}_n)}$$

$$|s| \ll |\tilde{\lambda}_n| \quad (187)$$

The asymptotic expression for the integral on segment 4 is

$$\int_4 \hat{X}(s) e^{st} ds \sim \int_4 \sum_{n=1}^N \frac{\{\phi_n\}^T \{1.\}}{m_n(-\tilde{\lambda}_n)} \phi_{nl} e^{st} ds$$

$$|s| \ll 1$$

$$|s| \ll |\tilde{\lambda}_n| \quad (188)$$

In polar notation, where

$$s = \rho e^{i\theta} \quad (189)$$

the expression the integral on segment 4 is

$$\int_4 \hat{X}_\ell(s) e^{st} ds \sim \int_{\pi}^{-\pi} \sum_{n=1}^N \frac{\{\phi_n\}^T \{1.\}}{m_n(-\tilde{\lambda}_n)} e^{\rho e^{i\theta} t} i \rho e^{i\theta} d\theta \quad (190)$$

Again, the magnitude of the integral on segment 4 is less than or equal to the maximum magnitude of the integrand, M , times the length of the path of integration, L .

$$\left| \int_{\pi}^{-\pi} \sum_{n=1}^N \frac{\{\phi_n\}^T \{1.\}}{m_n(-\tilde{\lambda}_n)} e^{\rho e^{i\theta} t} i \rho e^{i\theta} d\theta \right| \leq M \cdot L \quad (191)$$

The maximum magnitude of the integrand is

$$M = \left| \sum_{n=1}^N \frac{\{\phi_n\}^T \{1.\}}{m_n(-\tilde{\lambda}_n)} \right| e^{\rho |t| \cdot \rho} \quad (192)$$

and the length of the path of integration is

$$L = 2\pi \quad (193)$$

The resulting expression for the upper bound on the magnitude of the integral on segment 4 is

$$\left| \int_4 \hat{X}_\ell(s) e^{st} ds \right| \leq \left| \sum_{n=1}^N \frac{\{\phi_n\}^T \{1.\}}{m_n(-\lambda_n)} \right| e^{\rho t} 2\pi\rho$$

$$|s| \ll 1$$

$$|s| \ll |\tilde{\lambda}_n| \quad (194)$$

and clearly as ρ goes to zero, or equivalently as s goes to zero, the upper bound on the magnitude of the integral goes to zero. Therefore,

$$\lim_{\rho \rightarrow 0} \int_4 \hat{X}_\ell(s) e^{st} ds = 0. + i0. \quad (195)$$

It has been demonstrated that the integrals on segments 2, 4, and 6 are zero, which reduces the expression for the inverse transform given in Equation 174 to

$$\frac{1}{2\pi i} \int_{\gamma-i\infty}^{\gamma+i\infty} \{\hat{X}(s)\} e^{st} ds = -\frac{1}{2\pi i} \sum_{k=3,5} \int_5 \{\hat{X}(s)\} e^{st} ds + \sum_j b_j \quad (196)$$

The inverse transform is seen to be the integrals along the branch cuts, segments 3 and 5, plus the sum of the residues of the poles, b_j .

The expression for the integral along segment 3 is

$$\int_3 \hat{X}_\ell(s) e^{st} ds = \int_R^\rho X_\ell(re^{i\pi}) e^{re^{i\pi}t} e^{i\pi} dr \quad (197)$$

where

$$s = re^{i\pi} \quad (198)$$

This expression simplifies to

$$\int_3 \hat{X}_\ell(s) e^{st} ds = \int_\rho^R \hat{X}_\ell(re^{i\pi}) e^{-rt} dr \quad (199)$$

In the limit as the radius of contour 2, R , goes to infinity and as the radius of contour 4, ρ , goes to zero, the integral along segment 3 becomes

$$\lim_{\substack{\rho \rightarrow 0 \\ R \rightarrow \infty}} \int_3 \hat{X}_\ell(s) e^{st} ds = \int_0^\infty \hat{X}_\ell(re^{i\pi}) e^{-rt} dr \quad (200)$$

Similarly, the expression for the integral along segment 5 in the limit as the radius of contour 6 goes to infinity and the radius of contour 4 goes to zero is

$$\lim_{\substack{\rho \rightarrow 0 \\ R \rightarrow \infty}} \int_5 \hat{X}_\ell(s) e^{st} ds = - \int_0^\infty \hat{X}_\ell(re^{-i\pi}) e^{-rt} dr \quad (201)$$

The sum of the integrals along segment 3 and segment 5 is

$$\sum_{k=3,5} \int_k \hat{X}_\ell(s) e^{st} ds = \int_0^\infty (\hat{X}_\ell(re^{i\pi}) - \hat{X}_\ell(re^{-i\pi})) e^{-rt} dr \quad (202)$$

Noting that $\hat{X}_\ell(re^{i\pi})$ and $\hat{X}_\ell(re^{-i\pi})$ are complex conjugates of each other, the expression simplifies to

$$\sum_{k=3,5} \int_k \hat{X}_\ell(s) e^{st} ds = -2i \operatorname{Im} \int_0^\infty \hat{X}_\ell(re^{-i\pi}) e^{-rt} dr \quad (203)$$

The only terms in the inverse transform, (Equation 195), remaining to be evaluated are the residues of the poles of $\hat{X}_\ell(s) e^{st}$. By definition, the residues of the poles of $\hat{X}_\ell(s) e^{st}$ are

$$b_j = \lim_{s \rightarrow \tilde{\lambda}_j^m} (s - \tilde{\lambda}_j^m) \hat{X}_\ell(s) e^{st} \quad (204)$$

or

$$b_j = \lim_{s \rightarrow \tilde{\lambda}_j^m} (s - \tilde{\lambda}_j^m) \sum_{n=1}^N \frac{\{\phi_n\}^T \{1.\} D(s)}{m_n (s^{1/m} - \tilde{\lambda}_n)} \phi_n e^{st} \quad (205)$$

which reduces to

$$b_j = \lim_{s \rightarrow \tilde{\lambda}_j^m} \frac{(s - \tilde{\lambda}_j^m)}{(s^{1/m} - \tilde{\lambda}_j)} \frac{\{\phi_j\}^T \{1.\} D(s)}{m_j} \phi_{j\ell} e^{st} \quad (206)$$

Before taking the limit to evaluate the residue, it should be pointed out that

$$\frac{(s - \tilde{\lambda}_j^m)}{(s^{1/m} - \tilde{\lambda}_j)} = \sum_{r=1}^m \tilde{\lambda}_j^{r-1} s^{1-r/m} \quad (207)$$

which simplifies the expression for the residue to

$$b_j = \lim_{s \rightarrow \tilde{\lambda}_j^m} \left(\sum_{r=1}^m \tilde{\lambda}_j^{r-1} s^{1-r/m} \right) \cdot \frac{\{\phi_j\}^T \{1.\} D(s)}{m_j} \phi_{j\ell} e^{st} \quad (208)$$

Evaluating the limit produces

$$b_j = m \tilde{\lambda}_j^{m-1} \frac{\{\phi_j\}^T \{1.\} D(\tilde{\lambda}_j^m)}{m_j} \phi_{j\ell} e^{\tilde{\lambda}_j^m t} \quad (209)$$

Having evaluated the residues of the poles of the integrand in the inversion integral, the evaluation of the inverse transform

AD-A081 131

AIR FORCE MATERIALS LAB WRIGHT-PATTERSON AFB OH F/G 20/11
APPLICATIONS OF GENERALIZED DERIVATIVES TO VISCOELASTICITY.(U)
NOV 79 R L BAGLEY
AFML-TR-79-4103

UNCLASSIFIED

NL

2 of 2

850-101

END

DATE

FILED

3-80

DDC

is complete. The general expression for the displacement response of the structure for simultaneous, unit, impulsive loading at all its degrees of freedom is

$$\begin{aligned} \hat{x}_\ell(t) = & \frac{1}{\pi} \operatorname{Im} \left[\int_0^\infty \hat{X}_\ell(re^{-i\pi}) e^{-rt} dr \right] \\ & + \sum_j \frac{m \tilde{\lambda}_j^{m-1} \{\phi_j\}^T \{1.\} D(\tilde{\lambda}_j^m)}{m_j} \phi_{j\ell} e^{\tilde{\lambda}_j^m t} \end{aligned} \quad (210)$$

This expression is based on Equation 195, using Equations 181, 203, and 209 for the appropriate substitutions.

Note that the response of the structure has two parts, one part being a sum of decaying sinusoids and the other part an integral that decreases with increasing time. The integral does not decrease exponentially, because it is asymptotic to $t^{-\alpha}$ for large t , where α is greater than one. Therefore, the integral dominates the response for a time long after the loading. This component of the response describes the non-oscillatory return of the structure to its unloaded equilibrium position.

In summary, the response of the structure to impulsive loading can be calculated using contour integration to evaluate the inverse transform. Having obtained the response to impulsive loading as a function of time makes possible determination of the response of the structure to general loading conditions using convolution. In essence, the calculation of the response of the structure is no longer tied to the use of Laplace or Fourier transforms. In other words, the response of the structure to loading time histories for which transforms do not exist can be calculated using the response to impulsive loading and the convolution integral.

SECTION XI

SUMMARY AND CONCLUSIONS

The generalized derivative of fractional order is a mathematical operator well-suited for describing the frequency-dependent mechanical properties of viscoelastic materials. As shown in Section V and Appendix C, the generalized derivative constitutive relations for the materials are capable of describing the frequency-dependent stiffness and damping of the materials over several decades of frequency, as observed under conditions of sinusoidal motion.

Moreover, as demonstrated in Section V, the constitutive relation for 3M-467 predicts accurately the non-periodic (transient) response of the material as observed in the laboratory. In addition, the generalized derivative model for 3M-467 performed remarkably better than the Voigt model.

The generalized derivative RT and RTG viscoelastic models enabled the formulation of the viscostiffness matrix of the viscoelastic finite element. This led to the successful formation of the equations of motion, for a structure containing both elastic and viscoelastic components, which can be decoupled and solutions obtained using modal analysis. As demonstrated in Section VIII, the parameters of the solutions can be determined using the iterative numerical schemes presented.

Finally, it was demonstrated that the response of the structure to impulsive loading always exists and is continuous, real, and causal. The general form of the response to impulsive loading was evaluated using contour integration.

In conclusion, the approach to viscoelasticity resulting from this investigation is particularly powerful, in that the general motion of a structure having both elastic and viscoelastic components can be determined given that two conditions are met. First, the RT and/or RTG models for the viscoelastic materials in the structure must exist and comply with the second law of thermodynamics as indicated in Appendix A. Second, every component of the structure must have a suitable finite element approximation.

2000

APPENDIX A

THE RT AND RTG MODELS AND THE SECOND LAW
OF THERMODYNAMICS

The focus of the thermodynamic considerations centers on the ability of the RT and RTG models of viscoelastic materials to satisfy the second law of thermodynamics. In particular, the objective is to derive constraints on the parameters of the RT and RTG models to ensure that the state of stress and strain in the material predicted by the models is consistent with the second law. The considerations are limited to the case where the material is at a constant, uniform temperature and the deformations and resulting stresses in the material are sinusoidal.

The assumption of constant, uniform temperature is motivated by the observation that the moduli of viscoelastic materials are usually strongly dependent on temperature. Allowing the temperature of the material to vary, due to the energy dissipated during the deformation process, implies that the parameters of the RT and/or RTG model should be modified to account for the resulting changes in material properties. However, the RT and RTG models are employed where the parameters of the models are not changed during the deformation process, which is in essence a statement that the temperature of material does not change during deformation.

To implement the assumption of constant, uniform temperature, energy sinks are assumed to be present at every point in the material. The energy sinks instantaneously absorb all the dissipated energy, preventing the temperature from changing.

The energy sinks are represented in the first law of thermodynamics

$$\rho \dot{\epsilon} = p + \bar{\nabla} \cdot \bar{h} + \rho q \quad (A.1)$$

by q , the local rate of change of energy density through non-mechanical effects. In this local form of the first law, $\bar{\nabla} \cdot \bar{h}$ is the divergence of the energy flux vector, p is the local rate at which internal work is

done by mechanical means, ϵ is the internal energy per unit mass of the material, and ρ is the mass density.

The following development, based solely on the first and second laws, is an adaptation of the work of Coleman and Truesdell on the thermodynamics of deformations for the specific case at hand (Reference 29). In notation identical to Truesdell's, the second law for a material at constant, uniform temperature is

$$\rho \theta \dot{\eta} - \bar{\nabla} \cdot \bar{h} - \rho q \geq 0 \quad (\text{A.2})$$

where η is the entropy per unit mass and θ is temperature. This local form of the second law is based on the Clausius-Planck inequality.

Two other entities relevant to the following discussion are the free energy of the material, ψ ,

$$\psi = \epsilon - \eta \theta \quad (\text{A.3})$$

and the internal dissipation rate, δ ,

$$\delta \equiv p - \rho(\eta \dot{\theta} - \dot{\psi}) \quad (\text{A.4})$$

where the dots indicate first time derivatives. Substituting the expression for the dissipation rate produces

$$\delta = \rho \theta \dot{\eta} + (p - \rho \dot{\epsilon}) \quad (\text{A.5})$$

Using the first law to substitute for $p - \rho \dot{\epsilon}$ in Equation A.5 yields

$$\delta = \rho \theta \dot{\eta} - \bar{\nabla} \cdot \bar{h} - \rho q \quad (\text{A.6})$$

From the second law and the above expression for the dissipation rate, it is clear that the second law is always satisfied when

$$\delta \geq 0 \quad (\text{A.7})$$

In other words, when the local internal dissipation rate of a material is non-negative, the behavior of the material is consistent with the second law.*

*This result is contained in Coleman's general theorem on the non-equilibrium thermodynamics of deformation (References 30, 32).

The task remaining is to express the dissipation rate in terms of the stresses and strains in the material. To that end, recall that the energy sinks absorb all the dissipated energy.

$$\delta = -\rho q \quad (\text{A.8})$$

In light of the expression for the dissipation rate given in Equation A.6,

$$-\bar{\nabla} \cdot \bar{h} + \rho \theta \dot{\eta} = 0 \quad (\text{A.9})$$

Since the absorption of the energy by the sinks prevents the opportunity for energy conduction,

$$\bar{h} = \bar{0} \quad (\text{A.10})$$

and, as a result

$$\bar{\nabla} \cdot \bar{h} = 0 \quad (\text{A.11})$$

and consequently

$$\dot{\eta} = 0. \quad (\text{A.12})$$

Since the rate of change of the entropy, $\dot{\eta}$, is zero, Equation A.5 reduces to

$$\delta = (p - \rho \dot{\epsilon}) \quad (\text{A.13})$$

The internal dissipation rate can now be expressed in terms of stress and strain, provided the internal energy per unit volume, $\rho \dot{\epsilon}$, can be expressed in terms of the rate of change of strain energy, \dot{u} . The internal energy per unit mass, ϵ , is taken to be a function of temperature plus the strain energy per unit mass, u/ρ .

$$\epsilon = f(\theta) + u/\rho \quad (\text{A.14})$$

For small strain the expression for one over density is

$$1/\rho(t) \approx (1 + e(t))/\rho_0 \quad (\text{A.15})$$

where ρ_0 is the unstrained density and $e(t)$ is the dilatation strain, defined in Equation 38. The resulting expression for the internal energy is

$$\epsilon \approx f(\theta) + u \cdot (1 + e(t))/\rho_0 \quad (\text{A.16})$$

which simplifies to

$$\epsilon \approx f(\theta) + u/\rho_0 \quad (\text{A.17})$$

for small strain. Since the temperature is constant, the expression for the strain energy rate is

$$\dot{\epsilon} \approx \dot{u}/\rho_0 \quad (\text{A.18})$$

and the resulting expression for the dissipation rate is

$$\delta = (p - \dot{u}) \quad (\text{A.19})$$

again, for the small strain.

The dissipation rate in terms of the stresses and strains is

$$\delta = \{\sigma(t)\}^T \{\dot{\epsilon}(t)\} - \{\sigma'(t)\}^T \{\dot{\epsilon}(t)\} \quad (\text{A.20})$$

or

$$\delta = \{\{\sigma(t)\} - \{\sigma'(t)\}\}^T \{\dot{\epsilon}(t)\} \quad (\text{A.21})$$

where $\{\dot{\epsilon}(t)\}$ is the column vector of the strain rates, $\{\sigma(t)\}$ is the column vector of the stresses and $\{\sigma'(t)\}$ is the column vector of those components of the stress acting to store and retrieve strain energy in the material. As indicated in Section IV, the stresses storing and retrieving strain energy for steady-state, sinusoidal motion were those stresses in-phase with the strains. Consequently, the total stresses, $\{\sigma(t)\}$, minus the in-phase stresses, $\{\sigma'(t)\}$, leaves the out-of-phase stresses, $\{\sigma''(t)\}$.

$$\delta = \{\sigma''(t)\}^T \{\dot{\epsilon}(t)\} \quad (\text{A.22})$$

The stress out-of-phase with the strains

$$\epsilon_{mn}(t) = \epsilon_{mn_0} \sin \omega_0 t \quad (64)$$

are those stresses proportional to $\cos \omega_0 t$ in Equation 65

$$\sigma_{mn}(t) = \delta_{mn} F_3(\omega_0) e_0 \cos \omega_0 t + F_4(\omega_0) \epsilon_{mn_0} \cos \omega_0 t \quad (A.23^*)$$

The dissipation rate in terms of the stresses and strains given above is

$$\delta = \omega_0 F_3(\omega_0) e_0^2 \cos^2 \omega_0 t + \sum_{n=1}^3 \sum_{m=1}^3 \omega_0 F_4(\omega_0) \epsilon_{mn_0}^2 \cos^2 \omega_0 t \quad (A.24)$$

If the parameters of the RT and/or RTG models are chosen such that

$$\omega_0 F_3(\omega_0) \geq 0 \quad (A.25)$$

$$\omega_0 F_4(\omega_0) \geq 0 \quad (A.26)$$

for all positive ω_0 , the state of stress and strain in the material predicted by the models is consistent with the second law.

Although the above development is for sinusoidal motion of the material, its application extends to periodic strain histories. Consider the case where the material undergoes prescribed, piece-wise continuous and bounded strain history of finite duration and the material is allowed sufficient time for the stresses to relax to their unloaded equilibrium value of zero. Assume that at some later time the same strain history is imposed on the material and the material again allowed to fully relax, and this process of loading and relaxation is repeated continuously at a specified interval. The stress and strain histories of the material are periodic and can be broken into their respective frequency components using Fourier analysis. The internal dissipation of each frequency component of the strain is given by Equation A.24 and satisfies the second law, given that Equations A.25 and A.26 hold.

* $F_3(\omega_0)$ and $F_4(\omega_0)$ are functions of the parameters of the RT and RTG models and are defined by Equations 67 and 70.

Consequently, the periodic stress and strain histories of the material comply with the second law. As a result, satisfying Equations A.25 and A.26 is sufficient to ensure that the response of the material to a piece-wise continuous and bounded strain history of finite duration satisfies the second law. This follows from the observation that each loading and relaxation cycle of the material can be viewed as an independent response sequence.

APPENDIX B
A GENERALIZED DERIVATIVE RELATION FOR A
NEWTONIAN FLUID

By way of motivation toward describing the motion of physical systems with generalized derivative equations, it is interesting to note that a Newtonian fluid, defined by the stress-strain rate constitutive relation

$$\sigma = \mu \frac{\partial v}{\partial z} \quad (B.1)$$

where μ is the bulk viscosity, can undergo dynamic motion which lends itself to description using a generalized derivative. When the Newtonian constitutive relation is introduced into the one-dimensional momentum equation for a homogeneous, incompressible fluid at uniform, constant temperature

$$\rho \frac{\partial v}{\partial t} = \frac{\partial \sigma}{\partial z} \quad (B.2)$$

the resulting differential equation is

$$\rho \frac{\partial v}{\partial t} = \mu \frac{\partial^2 v}{\partial z^2} \quad (B.3)$$

This equation is immediately recognized as being in the form of the one-dimensional diffusion equation. Donaldson (Reference 31) has demonstrated that solutions of the one-dimensional diffusion equation may be represented using fractional calculus. Of particular interest at this point is the solution to the one-dimensional diffusion equation that occurs when an infinite half-space of such a Newtonian fluid is bounded by a "wetted" planar surface undergoing some known motion.* If the known motion of the bounding surface has a Laplace transform, Laplace transforms may be used to solve the diffusion equation.

*This problem is a generalization of Stokes' second problem in which Stokes assumed the motion of the "wetted" plate to be sinusoidal (Reference 33).

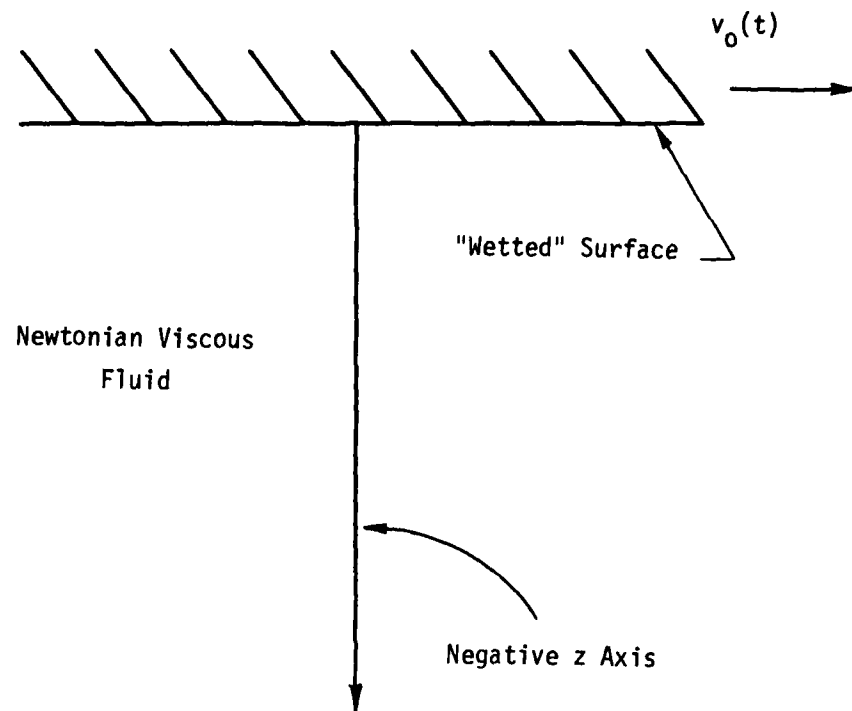


Figure B-1. Schematic of the Half Space of Newtonian Fluid Bounded by a "Wetted" Surface

A derivation of the solution is given here for completeness. Taking the Laplace transform of Equation B.3 results in

$$\rho(sV(s,z) - v(0,z)) = \mu \frac{\partial^2 V}{\partial z^2}(s,z) \quad (B.4)$$

where $V(s,z)$ is the transform of the velocity

$$V(s,z) = \int_0^\infty v(t,z)e^{-st}dt \quad (B.5)$$

Assuming the fluid is initially excited from a state of rest, the initial velocity, $v(0,z)$, is zero and the resulting differential equation is

$$\rho sV(s,z) = \mu \frac{\partial^2 V}{\partial z^2}(s,z) \quad (B.6)$$

The solution of this differential equation is readily seen to be

$$V(s,z) = A(s)e^{+\sqrt{\frac{\rho s}{\mu}}z} + B(s)e^{-\sqrt{\frac{\rho s}{\mu}}z} \quad (B.7)$$

Choosing the coordinate system such that the normal of the bounding surface is parallel to the negative Z axis, one can proceed to determine the functions $A(s)$ and $B(s)$ in terms of the boundary conditions. The first boundary condition to be satisfied is that the magnitude of the velocity of the fluid be bounded for large, negative Z . Consequently, $B(s)$ must be zero. The other boundary condition is that, at the interface of the fluid and the bounding surface, the velocity of the fluid must be equal to the velocity of the bounding surface, $v_0(t)$. To enforce this boundary condition, one first takes the transform of $v_0(t)$

$$V_0(s) = \int_0^t v_0(t)e^{-st}dt \quad (B.8)$$

and the boundary condition is applied in the transform domain as shown

$$V(s,z) = A(s)e^{+\sqrt{\frac{\rho s}{\mu}}z} \quad (B.9)$$

$$V(s,0) = A(s) = V_0(s) \quad (B.10)$$

The resulting expression for the transform of the velocity of the fluid at a distance z below the plate is

$$V(s,z) = V_0(s)e^{+\sqrt{\frac{\rho s}{\mu}}z} \quad (B.11)$$

At this point one wishes to determine the stresses in the fluid according to the Newtonian constitutive relation (Equation B.1). The transform of Equation B.1 is

$$\sigma^*(s,z) = \frac{\partial V(s,z)}{\partial z} \quad (B.12)$$

Substituting Equation B.11 into Equation B.12 for $V(s,z)$ produces

$$\sigma^*(s,z) = \sqrt{\mu\rho} \sqrt{s} V(s,z) \quad (B.14)$$

The transform of the stress may be inverted by observing that the transform is the product of the transforms of two known functions of time.

$$\begin{aligned} \sigma^*(s,z) &= \sqrt{\mu\rho} \frac{1}{\sqrt{s}} \cdot sV(s,z) = \sqrt{\mu\rho} L[(r(\frac{1}{2})t^{\frac{1}{2}})^{-1}] \\ &\quad \cdot L[\dot{v}(t,z)] \end{aligned} \quad (B.15)$$

Thus, the stress is seen to be the convolution of the two functions of time,

$$\sigma(t,z) = \frac{\sqrt{\mu\rho}}{r(\frac{1}{2})} \int_0^t \frac{\dot{v}(t,\tau)}{(t-\tau)^{\frac{1}{2}}} d\tau \quad (B.16)$$

For the zero initial condition on velocity, Equation B.16 is equivalent to

$$\sigma(t,z) = \frac{\sqrt{\mu\rho}}{r(\frac{1}{2})} \frac{d}{dt} \int_0^t \frac{v(t,\tau)}{(t-\tau)^{\frac{1}{2}}} d\tau \quad (B.17)$$

Notice that Equation B.17 states that the stress at any location in the fluid is equal to a constant, $\sqrt{\mu\rho}$, times the generalized derivative of fractional order $\frac{1}{2}$ of the velocity of the fluid at that location.

$$\sigma(t,z) = \sqrt{\mu\rho} D^{\frac{1}{2}} [v(t,z)] \quad (B.18)$$

This stress-velocity relation evaluated over an area A of the "wetted" surface, $z = 0$, produces a force-velocity relation.

$$f(t,0) = A \sqrt{\mu\rho} D^{\frac{1}{2}} [v_0(t)] \quad (B.19)$$

Thus, we see that in this one case, the macroscopic behavior of a Newtonian, viscous fluid is characterized by a generalized derivative of fractional order $\frac{1}{2}$, even though the microscopic behavior is

$$\sigma(t,z) = \mu \dot{\epsilon}(t,z) \quad (B.20)$$

This observation suggests that generalized derivatives may have applications in other situations where a global, or discrete, description is desired of a phenomenon which is locally viscous.

APPENDIX C

RT AND RTG MODELS FOR VISCOELASTIC MATERIALS

Generalized derivative constitutive relations for three viscoelastic materials are presented. The material properties on which the RT and RTG models are based (Reference 34) were determined using the "temperature-frequency superposition" principle (Reference 33).

The RTG model for the shear modulus of the viscoelastic material 3M-467 at 75°F is

$$(1 + b_1 D^{\hat{\beta}_1}) \sigma(t) = (\mu_0 + \mu_1 D^{\hat{\alpha}_1}) \epsilon(t) \quad (C.1)$$

where

$$b_1 = 8 \times 10^{-4} \text{ sec}^{.51} \quad (C.2)$$

$$\mu_0 = 1.0 \text{ lb/in}^2 \quad (C.3)$$

$$\mu_1 = 7.3 \text{ lb-sec}^{.56} / \text{in}^2 \quad (C.4)$$

$$\hat{\beta}_1 = .51 \quad (C.5)$$

and

$$\hat{\alpha}_1 = .56 \quad (C.6)$$

The mechanical properties predicted by the model are compared to the material's properties in Figure C-1. Note the excellent agreement between the model and the material properties over 8 decades of frequency.

The RT model for the viscoelastic Young's modulus of Sylgard 188 at 120°F is

$$\sigma(t) = (E_0 + E_1 D^{\alpha_1}) \epsilon(t) \quad (C.7)$$

where

$$E_0 = 60 \text{ lb/in}^2 \quad (\text{C.8})$$

$$E_1 = 43 \text{ lb-sec}^{.24} / \text{in}^2 \quad (\text{C.9})$$

and

$$\alpha_1 = .24 \quad (\text{C.10})$$

The mechanical properties predicted by the model are compared to the material's properties in Figure C-2.

The RT model for the viscoelastic Young's modulus of BTR at 45°F is

$$\sigma(t) = (E_1 D^{\alpha_1} + E_2 D^{\alpha_2}) \epsilon(t) \quad (\text{C.11})$$

where

$$E_1 = 850 \text{ lb-sec}^{.095} / \text{in}^2 \quad (\text{C.12})$$

$$E_2 = 18 \text{ lb-sec}^{.28} / \text{in}^2 \quad (\text{C.13})$$

$$\alpha_1 = .095 \quad (\text{C.14})$$

and

$$\alpha_2 = .28 \quad (\text{C.15})$$

A comparison of the model and material properties is given in Figure C-3.

Although the agreement between the material properties and their respective models is very good, not all viscoelastic materials lend themselves to characterization by generalized derivatives models. The materials most suited to modeling with generalized derivative

constitutive relations are those that have properties such that the following relation holds in the transition region:

$$\eta \approx \tan \frac{\pi \alpha}{2} \quad (C.16)$$

where η is the loss factor and α is the slope of the plot of the \log_{10} of the real part of the modulus plotted as a function of \log_{10} of the frequency of motion.

In summary, generalized derivative constitutive relations do in fact model the frequency dependent mechanical properties of at least three viscoelastic materials. However, each model is of a different basic form, as can be seen by comparing Equations C.1, C.7, and C.11. Hence, the RT or RTG models are capable of describing viscoelastic materials having distinctly different mechanical properties.

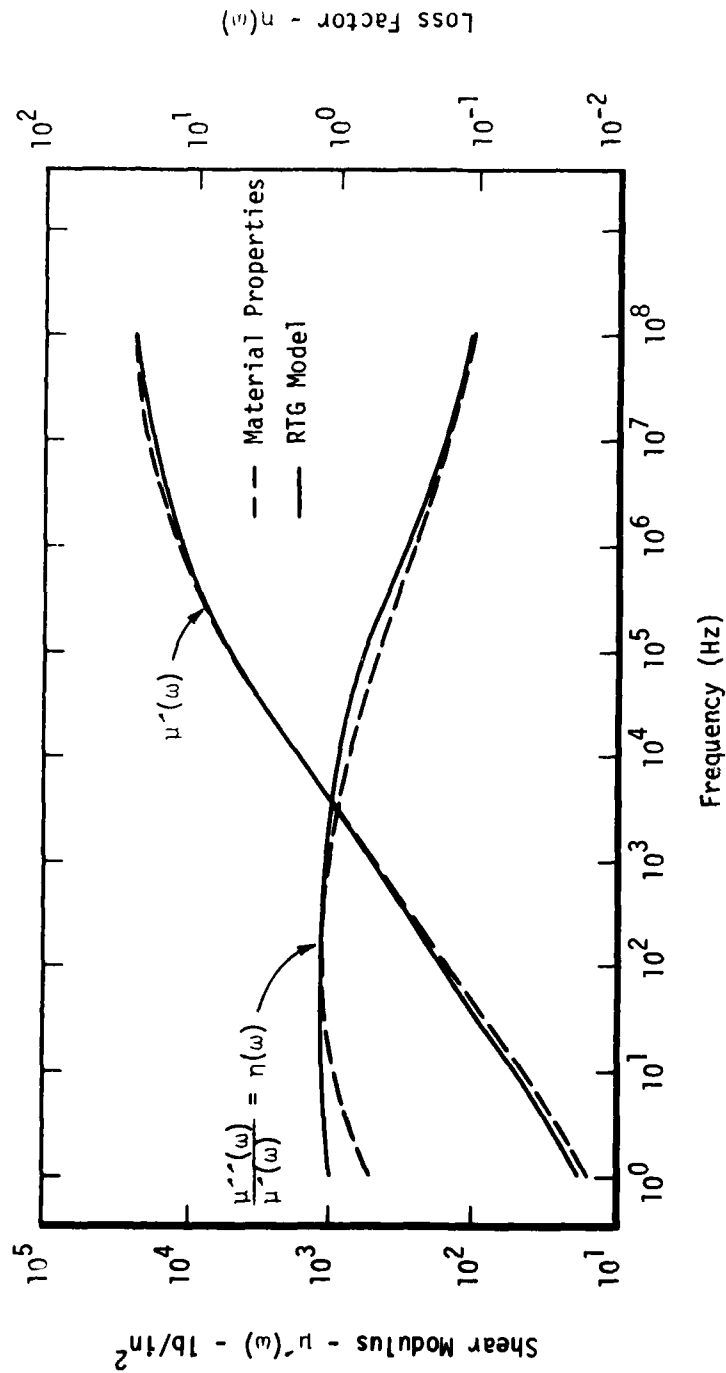


Figure C-1. The Mechanical Properties of 3M-467 Compared to the RTG Model of 3M-467

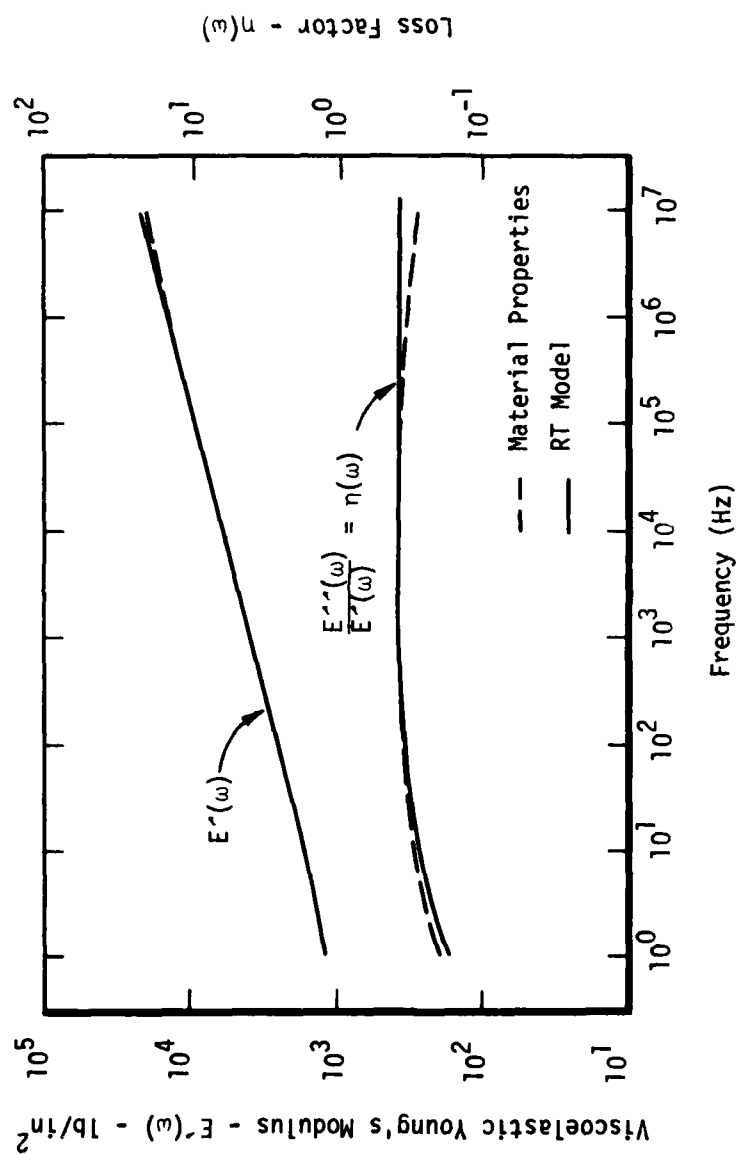


Figure C-2. The Mechanical Properties of Sylgard 188 Compared to the RT Model for Sylgard 188

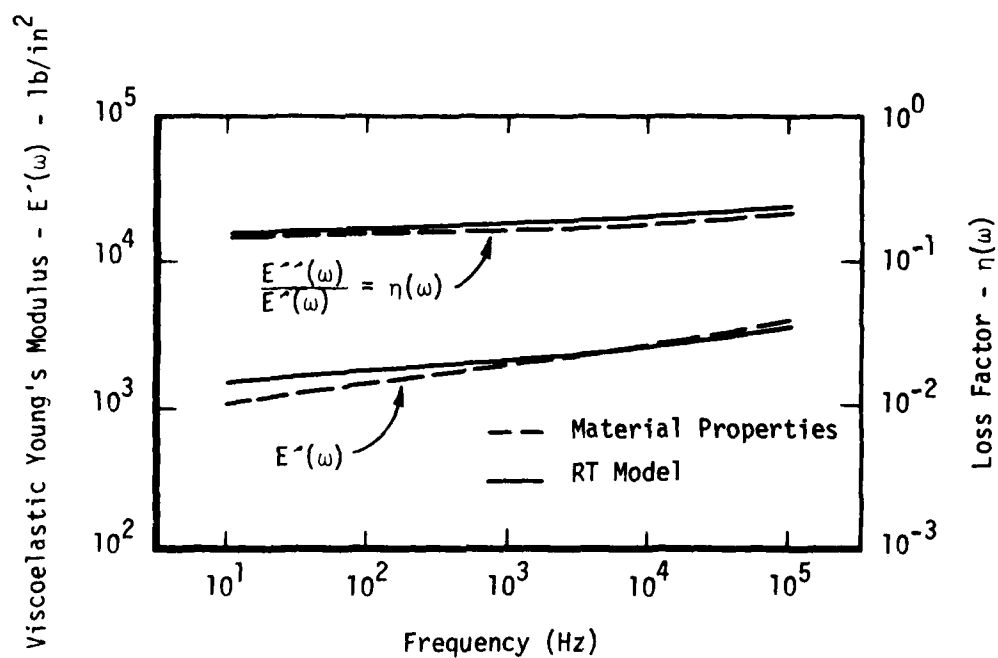


Figure C-3. The Mechanical Properties of BTR Compared to the RT Model of BTR

REFERENCES

1. M. Caputo, "Linear Models of Dissipation Whose Q Is Almost Frequency Independent," Ann. Geofisica, XIX (4): 383-393 (1966).
2. R. M. Christensen, Theory of Viscoelasticity, An Introduction. New York: Academic Press, 1971, p 14.
3. B. Ross, "A Brief History and Exposition of the Fundamental Theory of Fractional Calculus," Lecture Notes in Mathematics, 457: 19. New York: Springer-Verlag, 1975.
4. R. M. Christensen, Theory of Viscoelasticity, An Introduction. New York: Academic Press, 1971, pp 207-218.
5. W. C. Hurty and M. F. Rubenstein. Dynamics of Structures, Prentice-Hall, 1964, p 257.
6. S. H. Crandall, "Dynamic Response of Systems with Structural Damping," Air, Space and Instruments, Draper Anniversary Volume, edited by H. S. Lees. New York: McGraw-Hill, 1963, pp 183-193.
7. R. D. Milne, "A Constructive Theory of Linear Damping," Proceedings of Symposium on Structural Dynamics, c.4.1-c.4.19. Loughborough, England: Loughborough University of Technology, 23-25 March 1970.
8. M. Caputo, "Vibrations of an Infinite Plate with a Frequency Independent Q ," J. Acoust. Soc. Am., 60: 637 (1976).
9. -----, "Linear Models of Dissipation Whose Q is Almost Frequency Independent - II," Geophys. J. R. Astr. Soc., 13: 529-539 (1967).
10. -----, Elasticità e Dissipazione, Bologna: Zanichelli, 1969.
11. M. Caputo and F. Minardi. Pure Appl. Geophys., 91: 134-147 (1971).
12. -----, Riv. Nuovo Cimento, 2: 161-198 (1971).
13. M. Caputo, "Vibrations of an Infinite Viscoelastic Layer with a Dissipative Memory," J. Acoust. Soc. Am., 56 (3): 898 (1971).
14. -----, "Vibrations of an Infinite Viscoelastic Layer with a Dissipative Memory," J. Acoust. Soc. Am., 56 (3): 897-904 (1971).
15. -----, "Vibrations of an Infinite Plate with a Frequency Independent Q ," J. Acoust. Soc. Am., 60: 635-636 (1976).
16. -----, "Vibrations of an Infinite Plate with a Frequency Independent Q ," J. Acoust. Soc. Am., 60: 634 (1976).
17. K. A. Foss, "Co-ordinates Which Uncouple the Equations of Motion of Damped Linear Dynamic Systems," J. Appl. Mech., 25: 361 (1958).

REFERENCES (Cont'd)

18. M. Caputo, "Vibrations of an Infinite Plate with a Frequency Independent Q," J. Acoust. Soc. Am., 60: 902 (1976).
19. B. Ross, "A Brief History and Exposition of the Fundamental Theory of Fractional Calculus," Lecture Notes in Mathematics, 457: 18. New York: Springer-Verlag, 1975.
20. M. Caputo, "Vibrations of an Infinite Plate with a Frequency Independent Q," J. Acoust. Soc. Am., 60: 10 (1976).
21. M. E. Gurtin and E. Sternberg. "On the Linear Theory of Viscoelasticity," Arch. Ration. Mech. Anal. 11: 291 (1962).
22. A. C. Pipkin, "Approximate Constitutive Equations," Modern Developments in the Mechanics of Continua, Proceedings of an International Conference Center on Rheology held at the Pinebrook Conference Center of Syracuse University, Pinebrook, New York, 23-27 August 1965. 95. Edited by S. Eskinazi, New York: Academic Press, 1966.
23. R. M. Christensen, Theory of Viscoelasticity, An Introduction. New York: Academic Press, 1971, p 42.
24. O. C. Zienkiwicz, The Finite Element Method in Structural and Continuum Mechanics. London: McGraw-Hill, 1967, p 220.
25. -----, The Finite Element Method in Structural and Continuum Mechanics. London: McGraw-Hill, 1967, pp 11-12.
26. K. A. Foss, "Co-ordinates Which Uncouple the Equations of Motion of Damped Linear Dynamic Systems," J. Appl. Mech., 25: 361 (1958).
27. R. L. Bisplinghoff, et al. Aeroelasticity. Reading, Massachusetts: Addison-Wesley, 1955, p 168.
28. R. V. Churchill, Book of Operational Mathematics, Second Edition, McGraw Hill, Page 178, 1958.
29. C. Truesdell, "Thermodynamics of Deformations," Modern Developments in the Mechanics of Continua, Proceedings of an International Conference Center on Rheology held at the Pinebrook Conference Center of Syracuse University, Pinebrook, New York, 23-27 August 1965. 1. Edited by S. Eskinazi, New York: Academic Press, 1966.
30. B. D. Coleman, Arch. Rational Mech. Anal., 17: 1 (1964 a).
31. J. A. Donaldson, "A Family of Integral Representations for the Solution of the Diffusion Equation," Lecture Notes in Mathematics, 457: 146. New York: Springer-Verlag, 1975.

REFERENCES (Cont'd)

32. B. D. Coleman, Arch. Rational Mech. Anal., 17: 230 (1964 b).
33. H. Schlichting, Boundary Layer Theory. New York: McGraw-Hill, 1968, p 85.
34. D. I. G. Jones, "Temperature-Frequency Dependence of Dynamic Properties of Damping Materials," Journal of Sound and Vibration, 33 (4): 451-470 (1974).
35. R. M. Christensen, Theory of Viscoelasticity, An Introduction. New York: Academic Press, 1971, pp 96-98.